PERFORMANCE ANALYSIS OF 8 X 8 MIMO-OFDM SYSTEM USING QOSTBC UNDER DIFFERENT FADING CHANNELS FOR HIGHER ORDER MODULATIONS

A Thesis submitted in partial fulfillment of the

Requirements for the award of the Degree of

MASTER OF ENGINEERING

IN

ELECTRONICS AND COMMUNICATION ENGINEERING

Submitted By:-

LAVISH KANSAL

Roll No. 800961025

Under the guidance of:-

Mr. ANKUSH KANSAL
Assistant Professor , ECED

Dr. KULBIR SINGH
Assistant Professor, ECED

DEPARTMENT OF ELECTRONICS AND COMMUNICATION ENGINEERING,

THAPAR UNIVERSITY

PATIALA-147001, PUNJAB, INDIA

JUNE, 2011

CERTIFICATE

I, Lavish Kansal hereby certify that the work which is being presented in this thesis entitled **"Performance Analysis of 8 X 8 MIMO-OFDM System Using QOSTBC Under different Fading Channels For Higher Order Modulations"** by me in partial fulfillment of the requirements for the award of degree of Masters of Engineering in Electronics and Communication Engineering from Thapar University, Patiala is an authentic record of my own work carried under the supervision of Dr. Kulbir Singh and Mr. Ankush Kansal and referred other researcher's work which are duly listed in the reference section.

The matter presented in this report has not been submitted in any University/Institute for the award of Masters of Engineering.

(Lavish Kansal) Date:- 10/6/11

Signature of Student

This is certified that the above statement made by the candidate is correct to best of my knowledge.

Mr. Ankush Kansal

(Supervisor)

Date :- 13/6/11

(Dr. Kulbir Singh)

(Supervisor)

Date :- 13/6/11

(Dr. A.K. Chaterjee) 14.6.11

Head of Department

ECED, T.U. Patiala

(Dr. S.K. Mohapatra)

Dean of Academic Affairs

T.U. Patiala

ACKNOWLEDGEMENT

This thesis is completed with prayer of many and love of my family and friends. However, there are few people that I would like to specially acknowledge and extend my heartfelt gratitude who have made the completion of this thesis possible. With the biggest contribution to this thesis; I would like to thank **Dr. Kulbir Singh** had given me his full support in guiding me with stimulating suggestions and encouragement to go ahead in all the time of the thesis. I would also like to thank **Mr. Ankush Kansal** for his kind support during this work.

I am also thankful to **Dr. A. K. Chatterjee,** Head, Electronics and Communication Engineering Department, for providing us with the adequate infrastructure in carrying the work.

I am also thankful to **Dr. Alpana Agarwal**, P.G. Coordinator, Electronics and Communication Engineering department, for the motivation and inspiration that triggered me for the thesis.

At last but not the least my gratitude towards my parents, I would also like to thank God for not letting me down at a time of crisis and showing me the silver lining in the dark clouds.

LAVISH KANSAL

ABSTRACT

With the evolution of the wireless system the demand for high speed data services have been increasing day by day, which is impossible to be achieve by the conventional serial data transmission system without trade-off between high speed data services and QOS without increasing the band width of the system. Here both the options are inconvenient, as one never demands the degradation of the service quality (because if we increase data rate in serial data transmission ISI will gradually increase which make the extraction of actual information at receiver nearly impossible) and secondly the need for extra spectrum in a limited spectrum scenario. In order to overcome this problem new parallel data transmission system was proposed, which is known as OFDM system. The performance of OFDM system can further be improved by using multiple antennas at transmitting and receiving side to provide spatial diversity. Multiple antennas can be used at the transmitter and receiver, an arrangement called a MIMO system. A MIMO system takes advantage of the spatial diversity that is obtained by spatially separated antennas in a dense multipath scattering environment. Recently, there have been a lot of interests in combining the OFDM systems with the multiple-input multiple-output (MIMO) technique. These systems are known as MIMO-OFDM systems. MIMO-OFDM system has been currently recognized as one of the most competitive technology for 4G mobile wireless systems. MIMO system can provide the spatial diversity with the help of Space Time Coding when no channel side information is available at the transmitter side. There are different types of Space Time Coding techniques likely Alamouti Space Time Coding, Orthogonal Space Time Coding, Quasi Orthogonal Space Time Coding, etc. Quasi Orthogonal Space Time Coding technique is more preferable over other techniques because it provides more code rate than other Space Time Coding techniques for same no. of transmitting and receiving antennas.

In this thesis, a general Quasi orthogonal space time block code (QOSTBC) structure is proposed for multiple-input multiple-output–orthogonal frequency-division multiplexing (MIMO-OFDM) systems for 8 X 8 antenna configuration. The signal detection technology used in this work for MIMO-OFDM system is Zero-Forcing Equalization (linear detection technique). In the present work the analysis of high level of modulations (i.e. M-QAM and M-PSK for different values of M) on MIMO-OFDM system is presented. Here AWGN, Rayleigh and Rician channels have

been used for analysis purpose and their effect on BER and Spectral Efficiency for high data rates have been presented. The proposed system has better performance than the other systems in terms of SNR improvement of 3-5 dB and spectral efficiency.

The methodology described above is also used to evaluate the performance of the MIMO-OFDM systems using WiMAX Protocols. Here Alamouti 2 X N_R Space Time Coding is used for analysis purpose. It is shown that the using multiple antennas at transmitter or receiver side provides significant gains of approximately 2 dB over single transmit single receive antenna (SISO) systems.

TABLE OF CONTENT

LIST OF FIGURES

LIST OF TABLES

LIST OF ABREVATIONS

2G	2nd Generation
3GPP	3rd Generation Partnership Project
4G	4th Generation
ADC	Analog to Digital Conversion
ADSL	Asymmetric Digital Subscriber Line
AMC	Adaptive Modulation and Coding
ATM	Asynchronous Transfer Mode
AWGN	Additive White Gaussian Noise
BER	Bit Error Rate
BPSK	Binary Phase Shift Keying
BRAN	Broadcast Radio Access Network
QPSK	Quardrature Phase Shift Keying
BS	Base Station
CDMA	Code Division Multiple Access
COFDM	Coded Orthogonal Frequency Division Multiplexing
CP	Cyclic Prefix
CSI	Channel State Information
DAC	Digital to Analog Conversion
DFT	Discrete Fourier Transform
DPSK	Differential Phase Shift Keying
DQPSK	Differential Quadrature PhaseShift keying
DSL	Digital Subscriber Line
DTFT	Discrete-Time Fourier Transforms
ETSI	European Telecommunications Standards Institute
FDD	Frequency Division Duplexing
FDM	Frequency Division Multiplexing
FEC	Forward Error Correction
FFT	Fast Fourier Transform
GMSK	Gaussian Minimum Shift Keying

ICI	InterCarrier Interference
IDFT	Inverse Discrete Fourier Transform
IEEE	Institute of Electrical and Electronics Engineers
ISI	InterSymbol Interference
LAN	Local Area Network
LOS	Line of Sight
LTE	Long Term Evolution
MAC	Medium Access Control
MAN	Metropolitan Area Network
MCM	Multi Carrier Modulation
MIMO	Multiple Input Multiple Output
ML	Maximum Likelihood
MMSE	Minimum Mean Square Error
MRC	Maximum Ratio Combining
M-PSK	M ary Phase Shift Keying
M-QAM	M ary Quadrature Amplitude Modulation
NLOS	Non Line of Sight
OFDM	Orthogonal Frequency Division Multiplexing
OFDMA	Orthogonal Frequency Division Multiple Access
OSTBC	Orthogonal Space Time Block Code
QAM	Quadrature Amplitude Modulation
QOS	Quality of Service
QPSK	Quadrature PhaseShift keying
QOSTBC	Quasi Orthogonal Space Time Block Code
SDM	Spatial Division Multiplexing
SISO	Single Input Single Output
SNR	Signal to Noise Ratio
SS	Subscriber Stations
STBC	Space Time Block Code
STD	Spatial Transmit Diversity
STTC	Space Time Trellis Coding

SVD	Singular Value Decomposition
TCM	Trellis Coded Modulation
TDD	Time Division Duplexing
TDM	Time Division Multiplexing
TDMA	Time Division Multiple Access
VLSI	Very Large Scale Integration
V-BLAST	Vertical-Bell Laboratories Layered Space-Time
WAN	Wide Area Network
WiMAX	Worldwide Interoperability for Microwave Access
ZF	Zero Forcing

CHAPTER 1: INTRODUCTION

1.1 Preamble

Wireless communication is one of the most vivacious areas in the communication field now a day. Although the development in this area was started way back in 1960s, but a lot of research is done in this area in last decade. The reason for this is due to a variety of factors discussed below:

- The demand for seem-less connectivity has risen manifolds, mainly due to cellular telephony but expected to be soon eclipsed by wireless data applications.
- The sophisticated signal processing algorithms can be implemented with the advent of VLSI technology. Due to the success of 2G wireless standards especially CDMA it has been shown that communication ideas can be implemented in practice. The research push in the past decade has led to a much better-off set of perspectives and tools on how to communicate over wireless channels, and the scenario is still very much in the emerging stages.

There are two fundamental aspects of wireless communication that make the problem demanding and motivating as compared to wire line communication.

- First is the phenomenon of fading: the time variation of the channel strengths due to the small-scale effect of multipath fading, as well as larger-scale effects such as path loss via distance attenuation and shadowing by obstacles.
- Second, unlike in the wired world where each transmitter–receiver pair can often be thought of as an isolated point-to-point link, wireless users communicate over the air and there is significant interference between them. The interference can be between transmitters communicating with a common receiver (e.g., uplink of a cellular system), between signals from a single transmitter to multiple receivers (e.g., downlink of a cellular system), or between different transmitter–receiver pairs (e.g., interference between users in different cells).

1.2 OFDM

OFDM has become a popular technique for transmission of signals over wireless channels [1]. OFDM has been adopted in several wireless standards such as digital audio broadcasting (DAB), digital video broadcasting (DVB-T), the IEEE 802.11a [2] LAN standard and the IEEE 802.16a [3] MAN standard. OFDM is also being pursued for dedicated short-range communications (DSRC) for road side to vehicle communications and as a potential candidate for fourth-generation (4G) mobile wireless systems.

OFDM converts a frequency-selective channel into a parallel collection of frequency flat subchannels. The subcarriers have the minimum frequency separation required to maintain orthogonality of their corresponding time domain waveforms, yet the signal spectra corresponding to the different subcarriers overlap in frequency. Hence, the available bandwidth is used very efficiently. If knowledge of the channel is available at the transmitter, then the OFDM transmitter can adapt its signaling strategy to match the channel. Due to the fact that OFDM uses a large collection of narrowly spaced subchannels, these adaptive strategies can approach the ideal water pouring capacity of a frequency-selective channel. In practice this is achieved by using adaptive bit loading techniques, where different sized signal constellations are transmitted on the subcarriers.

OFDM is a block modulation scheme where a block of N information symbols is transmitted in parallel on N subcarriers. The time duration of an OFDM symbol is N times larger than that of a single-carrier system. An OFDM modulator can be implemented as an IDFT on a block of N information symbols followed by an ADC. To mitigate the effects of ISI caused by channel time spread, each block of IDFT coefficients is typically preceded by a CP or a guard interval consisting of G samples, such that the length of the CP is at least equal to the channel length. Under this condition, a linear convolution of the transmitted sequence and the channel is converted to a circular convolution. As a result, the effects of the ISI are easily and completely eliminated. Moreover, the approach enables the receiver to use fast signal processing transforms such as a fast FFT for OFDM implementation [1]. Similar techniques can be employed in single-carrier systems as well, by preceding each transmitted data block of length N by a CP of length, while using frequency-domain equalization at the receiver.

OFDM systems are attractive for the way they handle ISI, which is usually introduced by frequency selective multipath fading in a wireless environment. Each sub-carrier is modulated at a very low symbol rate, making the symbols much longer than the channel impulse response. In this way, ISI is diminished. Moreover, if a guard interval between consecutive OFDM symbols is inserted, the effects of ISI can completely vanish. This guard interval must be longer than the multipath delay. Although each sub-carrier operates at a low data rate, a total high data rate can be achieved by using a large number of sub-carriers. ISI has very small or no effect on the OFDM systems hence an equalizer is not needed at the receiver side.

OFDM has many advantages compared with other transmission techniques. One of such advantages is high spectral efficiency (measured in bits/sec/Hz). The orthogonal in OFDM implies a precise mathematical relationship between the frequencies of the subchannels that use in the OFDM system. Each one of the frequencies is an integer multiple of a fundamental frequency. This ensures that a sunchannel does not interfere with other subchannels even though the subchannels overlap. This results in high spectral efficiency.

OFDM has been adopted in the IEEE802.11a LAN and IEEE802.16a LAN/MAN standards. OFDM is also being considered in IEEE802.20a, a standard in the making for maintaining high-bandwidth connections to users moving at speeds up to 60 mph. The IEEE802.11a LAN standard operates at raw data rates up to 54 Mb/s (channel conditions permitting) with a 20-MHz channel spacing, thus yielding a bandwidth efficiency of 2.7 b/s/Hz. The actual throughput is highly dependent on the MAC protocol. Likewise, IEEE802.16a operates in many modes depending on channel conditions with a data rate ranging from 4.20 to 22.91 Mb/s in a typical bandwidth of 6 MHz, translating into a bandwidth efficiency of 0.7 to 3.82 bits/s/Hz.

1.3 MIMO

Multiple antennas can be used at the transmitter and receiver, an arrangement called a MIMO system. A MIMO system takes advantage of the spatial diversity that is obtained by spatially separated antennas in a dense multipath scattering environment. MIMO systems may be implemented in a number of different ways to obtain either a diversity gain to combat signal fading or to obtain a capacity gain. Generally, there are three categories of MIMO techniques. The first aims to improve the power efficiency by maximizing spatial diversity. Such techniques

include delay diversity, STBC [4], [5] and STTC [6]. The second class uses a layered approach to increase capacity. One popular example of such a system is V-BLAST suggested by Foschini et al. [7] where full spatial diversity is usually not achieved. Finally, the third type exploits the knowledge of channel at the transmitter. It decomposes the channel coefficient matrix using SVD and uses these decomposed unitary matrices as pre- and post-filters at the transmitter and the receiver to achieve near capacity [8].

1.4 MIMO-OFDM

Spatially multiplexed MIMO is known to boost the throughput, on the other hand, when much higher throughputs are aimed at, the multipath character of the environment causes the MIMO channel to be frequency-selective. OFDM can transform such a frequency-selective MIMO channel into a set of parallel frequency-flat MIMO channels and also increase the frequency efficiency. Therefore, MIMO-OFDM [9] technology has been researched as the infrastructure for next generation wireless networks.

Therefore, MIMO-OFDM, produced by employing multiple transmit and receive antennas in an OFDM system has becoming a practical alternative to single carrier and SISO transmission [10]. However, channel estimation becomes computationally more complex compared to the SISO systems due to the increased number of channels to be estimated. This complexity problem is further compounded when the channel from the i_{th} transmit antenna to the m_{th} receive antenna is frequency-selective. Using OFDM, information symbols are transmitted over several parallel independent sub-carriers using the computationally efficient IFFT/FFT modulation/demodulation vectors. [11]

These MIMO wireless systems, combined with OFDM, have allowed for the easy transmission of symbols in time, space and frequency. In order to extract diversity from the channel, different coding schemes have been developed. The seminal example is the Alamouti Space Time Block code [4] which could extract spatial and temporal diversity. Many other codes have also been proposed [5] which have been able to achieve some or all of the available diversity in the channel at various transmission rates.

In open-loop schemes, there are generally two approaches to implement MIMO systems. One is to increase the STD by means of space-time coding and space-frequency coding. Another

is to raise the channel capacity by employing SDM that simultaneously transmits independent data symbols through multiple transmit antennas. STD mitigates impairments of channel fading and noise, whereas SDM increases the spectral efficiency. [12]

1.5 Objective of Thesis

1. The objective of the thesis is to analyze the MIMO-OFDM system using QOSTBC 8 X 8 code structure (i.e. 8 Transmitting antennas and 8 Receiving antennas). For this two sub-objective have been taken first is BER analysis and the second is Spectral efficiency analysis.

2. Second step towards objective is to implement the most ideal channel (AWGN) for our model, for different modulation techniques and for different antenna configurations using QOSTBC code structure.

3. Third step is to test the system under practical fading channels like Rayleigh channel and finally Rician channel. Whole process has been repeated for different antenna configuration and different modulation techniques.

4. The last objective is to analyze the performance of MIMO-OFDM system with WiMAX Protocol under different environments.

1.6 Organization of Thesis

This thesis consists of total five chapters which are organized as below:

Chapter 1: Introduction, it is consisting of introduction to OFDM system and its application, then a brief introduction to the MIMO system is provided.

Chapter 2: Literature Review, vigorous study of research papers of related field in sequence has been discussed.

Chapter 3: MIMO-OFDM System, in this chapter theory of MIMO-OFDM system along with mathematical expressions for all modulation techniques and Space Time Coding Techniques under consideration has been discussed in detail. Also the detection techniques for MIMO-OFDM system have been discussed in brief.

Chapter 4: MIMO-OFDM with WiMAX Protocol, in this chapter a basic idea about the WiMAX Protocol is given along with its specifications for physical layer. Then the mathematical frame work for implementing MIMO-OFDM with WiMAX Protocol using Alamouti 2 X N_R Space Time Coding is presented.

Chapter 5: Results and Discussions, in this chapter all the results simulated in MATLAB-2009a has been discussed along with comparison tables, starting with AWGN channel, Rayleigh channel and Rician channel for our model, for different modulation techniques and different antenna configurations. A complete analysis of BER and Spectral efficiency is presented. Then the BER vs SNR graphs for MIMO-OFDM with WiMAX Protocol using Alamouti 2 X N_R Space Time Coding are presented for AWGN and Rayleigh fading channel.

Chapter 6: Conclusion, in this chapter whole work has been concluded, on the basis of results and also future scope has been discussed.

CHAPTER 2: LITERATURE REVIEW

MIMO antenna system with OFDMA is the most promising combination of technologies for high data-rate services in next generation wireless networks. Nowadays, different commercial solutions employing the OFDMA technology are under development, such as the IEEE WiMAX and 3GPP. These high data-rate systems are expected to operate in heterogeneous environments. Interference mitigation and channel-aware scheduling algorithms are crucial to maximally exploit their capacity. The work carried out till date on the said field is reported here forth.

2.1 OFDM

P. S. Mundra et.al [13] describes the emerging modulation technologies in the family of linear modulation and constant envelope techniques of digital modulation. Both of these techniques have been used extensively in mobile communication systems. The selection of one over the other depends on the priorities set in the system requirements. If most efficient bandwidth utilization and moderate hardware complexity is the key note – QPSK (π/4 QPSK) will be a better choice. Whereas continuous phase modulation schemes offer constant envelope, narrow power spectra, good error rate performance, etc. GMSK is the solution when out of band signal power, tolerance against filter parameter and non-linear power amplifiers are important features and compromise in channel separation is permissible and higher circuit complexity is of less consideration. Spectral efficiency can be further improved by using suitable coding techniques.

Higher modulation schemes with COFDM for a Rician fading channel with two frequency bands are considered by W.A.C. Fernando [14]. Rectangular QAM and 8-PSK constellation modulation schemes are considered with convolutional coding and TCM. Coding gain is considered at two different values of BER. It has been shown that there is no significant difference of BER performance between two frequency bands considered. BER slope is high for CC-OFDM for high SNR values whereas, TCM-OFDM performance seems to be better compared to CC-OFDM by considering the fact that TCM code has a lower trellis size.

Exact analytical calculation has been described by A. Maraz et.al [15], which is appropriate to determine the symbol error probability of MPSK and M-QAM modulation schemes. Results

could be utilized in advanced wireless networks (e.g. 3GPP LTE and WiMAX) to predict symbol error rate, or even channel capacity. Transmission happens in the presence of additive white Gaussian noise, different types of fading channels have effect on analyzed signal, and arbitrary number interference sources are modeled. M-QAM and M-PSK symbol error rate results are extended for OFDMA transmission with equally spaced subcarriers of interferers. Proposed method is capable for analyzing a composite OFDMA transmission system model with various fading and interference scenarios, which could be hereby a substantial component of an accurate physical layer scheduling algorithm in mentioned wireless systems.

2.2 MIMO-OFDM

OFDM for MIMO channels (MIMO-OFDM) is considered by Y. Li et.al [16] for wideband transmission to mitigate intersymbol interference and enhance system capacity. The MIMO-OFDM system uses two independent space-time codes for two sets of two transmit antennas. At the receiver, the independent space-time codes are decoded using pre-whitening followed by ML decoding based on successive interference cancellation. Using these techniques in a 4-input 4-output OFDM system, the net data transmission rate can reach 4 Mbits/sec over a 1.25 MHz wireless channel, with a 10-11 dB SNR required for a 10% SER, depending on the radio environment and signal detection technique for word lengths up to 500 bits.

S. Moghe et.al [17] introduced a new generation of IEEE 802.11n wireless network standard. The objective is to obtain numerical values for various measures of networking performance of IEEE 802.11n. The initial approach was to investigate the abilities of IEEE 802.11n standard to model a transmitter and receiver that communicated over a user defined channel. Simulation of single OFDM symbol SISO system followed by MIMO is presented. Also, the performance of the system using Matlab's built in BER tool in both SISO and MIMO Techniques is tested. Different Variation in BER on varying Parameters like Delay and K factor are carried out in the work.

Y. Wu et.al [18] gives an idea about the theoretical framework for the analysis of code diversity. It can be applied to an arbitrary space–time code, but the value of code diversity will depend on the particular choice of code. It is also shown that it not only improves the diversity and coding advantages for general space time codes but also enables optimal decoding performance with

low complexity decoding and only a small number of feedback bits. The method of code diversity also reduces the capacity loss associated with some forms of space–time coding. The code diversity scheme presented here is more robust than other low-rate feedback schemes such as transmit antenna selection and its variations. A new family of full-rate circulant codes are introduced and the advantage of suboptimal linear decoding in combination with code diversity is also demonstrated.

A bit and power allocation strategy for AMC based spatial multiplexing MIMO-OFDMA systems is studied by M. S. Al-Janabi et.al [19]. This strategy aims to maximize the average system throughput by allocating the available resources optimally among the utilized bands depending on the corresponding channel conditions and the total transmission power constraints. The average system throughput is represented as a trade-off criterion between the spectral efficiency and BER. The considered AMC technique utilizes distinct modulation and coding scheme (MCS) options rather than adopting fixed or uncoded approaches. The transmitter divides the OFDMA frame at each transmit antenna into bands depending on the number of active users in an assigned base station (BS). The simulation results show superior performance of the MIMO-AMC-OFDMA system, which adopts the proposed strategy, over other conventional schemes.

A channel estimation method for STBC - OFDM is investigated by F. Delestre et.al [20] for Mobile WiMax systems. A new channel estimation approach is proposed using the dedicated pilot subcarriers defined at constant intervals by the WiMax standard. The estimation method has low computation as only linear operations are needed due to orthogonal pilot coding. The performances of the proposed method have been demonstrated by extensive computer simulations. For the OFDM system with two transmit antennas and one to four receive antennas and using QPSK modulation, the simulated results under different Stanford University Interim (SUI) channels show that the proposed method has only a 4dB loss compared to the ideal case where the channel is known at the receiver.

S. Ajey et.al [21] focuses on the performance of a LTE system with two transmit antennas and two receive antennas in a frequency selective fading environment. 4G wireless systems predominately employ MIMO with an OFDM system. Like other 4G systems LTE also employs MIMO-OFDM physical layer. MIMO helps in increasing the throughput whereas OFDM

converts a frequency selective fading channel to multiple flat fading sub-channels facilitating easy equalization. It is proposed that LTE system should mandatorily support 2x2 MIMO setup. The performance of the MIMO system is better than that of a single antenna based system either in terms of performance (diversity) or throughput as in the case of transmit diversity or spatial multiplexing respectively.

A novel analytical method for BER and FER estimation of bit-loaded coded MIMO-OFDM systems operating over frequency-selective quasi-static channels with nonideal interleaving is developed by M. M. Avval et.al [22]. The presented numerical results illustrate that the proposed analysis technique provides an accurate estimation of the BER of loaded BICM-MIMO-OFDM systems. This allows the system performance analysis without resorting to lengthy simulations. In the case of bit loading, the relative performance of bit-loading algorithms for coded OFDM is system dependent, and thus, some care should be given to the selection of loading algorithms for coded OFDM systems. The proposed SL (Selected Loading) algorithm guarantees the best performance, at a cost of somewhat higher complexity, when performing loading. Adaptive interleaving has been confirmed to be an interesting alternative and addition to bit loading in coded OFDM.

An analytical framework for the performance assessment of bit-interleaved coded multi-antenna OFDMA systems over space-frequency selective fading channels with application to practical 4G broadband wireless standards is given by D. Molteni et.al [23]. A multicell scenario has been considered for inter-cell interference based on either coordinated or randomized multi-user access. The analytical formulation accounts for the spatial-frequency selectivity of the fading channel and possible non-stationary interference due to subcarrier randomization. Both beamforming and diversity schemes have been considered as multi-antenna systems. The analysis has been carried out for convolutionally coded BICM systems with BPSK modulation, then extended to higher order modulations. Two practical standards have been used as benchmark for the analytical analysis, 3GPP LTE and WiMAX IEEE 802.16d-e.

2.3 Beamforming in MIMO Systems

A nonlinear interpolation and a modified clustering based transmit beamforming schemes are investigated by J. Huang et.al [24] to reduce the feedback information and improve performance

for a MIMO-OFDM system. In the first approach, the indices of both beamforming vectors of the pilot subcarriers and phase parameters are feedback to the transmitter. Then the beamforming vectors for the non-pilot subcarriers in each cluster are constructed via beamforming vectors of the pilot subcarriers using nonlinear interpolation, which fully exploits the correlation between beamforming vectors and outperforms the existing linear interpolation. In the second scheme, only the indice of the beamforming vector in each cluster is conveyed back to the transmitter and the beamforming vector is reused for the whole subcarriers in that cluster.

An exact BER analysis for MIMO-OFDM systems with transmit beamforming and MRC reception in multipath Rayleigh fading channels, under channel prediction and interpolation errors, was presented by F. J. L. Martinez et.al [25]. The resulting exact closed form expression was composed by a finite sum of elementary functions. This expression was used to evaluate the system performance under different channel configurations and number of antennas, with Wiener and sinc filter schemes for both channel prediction and interpolation. Although Wiener filtering outperforms sinc-type filtering, the latter is shown to be a reasonable approach for implementation in a real system, since it offers a good trade-off between performance and complexity.

K. Yi et.al [26] investigated the interference cancellation algorithms for the downlink multi-user MIMO systems. Combined the conventional SLNR (signal-to-leakage and noise ratio) criterion with codebook selection mechanism, a new beamforming algorithm is proposed. Instead of using the channel matrix decomposition as the BD (Block Diagonalization) algorithm, the CSBF (codebook selection for beamforming algorithm) algorithm selects sub codebook from the corresponding codebook for each user and transmits their indices to the users. Consequently, it not only improves the system performance, but also reduces the computational complexity compared with the conventional BD beamforming algorithm. However, the channel state information must be known at transmitter.

A beamforming scheme combined with QOSTBC is demonstrated by Q. Tao et.al [27]. At the transmitter, quasi-orthogonal space-time block coded signals is transmitted by using four independent transmit beams. As the receiver, a pairwise decoding algorithm is employed. A flat Rayleigh fading channel model is used in the simulations to compare performance of the proposed scheme with the traditional quasi-orthogonal space-time block codes approach where

four independent transmit antennas are used. It is shown that the best rotation for rotate BPSK-QOSTBC is $\pi/2$. In spite of the contradictive requirement of antenna element spacing, the results show that the performance of the beams-based transmit diversity is superior to the classic transmit diversity with four independent transmit antennas.

An ICI/ISI-aware beamforming algorithm is devised by X. Sun et.al [28] to cope with large delay spread environments. They constructed an optimization problem and solved it with either an optimal or a suboptimal solution, depending on the antenna configuration. For the optimal solution, the best steering vector achieves the maximum SINR for all subcarriers. For the suboptimal solution, the steering vectors are selected to reduce the ICI/ISI crosstalk among subcarriers. Simulation of the proposed algorithm is also presented and compared it with MRC and beamforming. The results show that, although the ICI/ISI cannot be completely removed, but ICI/ISI aware beamforming can significantly improve the performance of MIMO-OFDM systems in which delay spread is significant.

A new user scheduling strategy is proposed by S. Rahima et.al [29] for multiuser MIMO-OFDM system with a low complexity generalized beamforming (GBF) scheme. In GBF, user antenna outputs are linearly combined with the receive GBF vector to construct an equivalent MISO downlink channel for each subcarrier. The scheduler located at the base station allocates data streams to users based on the subchannel gains of their subcarriers on each spatial channel. The user with maximum variance of subchannel gains is allowed to select his best subcarrier on his best spatial channel in order to maximize the system weighted sum-rate and fairness among users. The system power is simply uniformly allocated to all the subchannels.

2.4 MIMO-OFDM Systems using STBC

V. Tarokh et.al [30] designs a channel codes for improving the data rate and the reliability of communications over fading channels using multiple transmit antennas. The data is encoded by a channel code and the encoded data is split into multiple streams that are simultaneously transmitted using multiple transmit antennas. The received signal at each receive antenna is a linear superposition of the different transmitted signals. The performance criteria for designing channel codes under the assumption that the fading is slow and frequency non-selective is also

derived. Performance is shown to be determined by diversity gain quantified by ranks and coding gain quantified by determinants of certain matrices that are constructed from the code sequences.

Improved MIMO-OFDM techniques were studied by Y. Li et.al [31] for wireless systems using QPSK modulation for four transmit and four receive antennas (4 X 4). A system employing two 16-states, 2-antenna space–time codes with successive interference cancellation and channel estimation was considered, which was previously proposed to reduce the complexity of a 4-antenna space–time code system. The results depicts that recently proposed space–time code has a 2-dB improvement over a previously published code at 5-Hz fading. Furthermore, a 4-antenna, 16-state code that achieves an additional 2-dB improvement with lower complexity and a 256-state code that achieves an additional 2-dB gain were also proposed. The 256-state code performed within 3 dB of outage capacity (and within 2 dB with perfect channel estimation).

S. Suthaharan et.al [32] presents a space time block coded multiple-input multiple-output orthogonal frequency division multiplexing (MIMO-OFDM) scheme over frequency selective fading channels. The system provides spectrally efficient transmissions to increase system capacity or system throughput for individual users. The proposed technique utilizes OFDM to transform frequency selective fading channels into multiple flat fading sub channels on which space-time block coding is applied. A multi-user environment with multiple synchronous co-channel users, each equipped with n transmit antennas is considered. The receiver is equipped with multiple receive antennas. At the receiver signals from different users are decoded using minimum mean squared error (MMSE) interference cancellation followed by maximum likelihood (ML) decoding. It is shown that the proposed scheme, with two co-channel terminals, doubles the data rate while maintaining the frame error rate (FER) performance similar to a single user scheme with some additional decoding complexity.

The performance of a wireless communication system is analyzed by A. K. M. N. lslam et.al [33] considering multi-carrier OFDM with MIMO wireless channel and STBC. BER expression for MIMO-OFDM system without and with STBC is presented considering fading and timing jitter with QPSK, DPSK and DQPSK modulation schemes. The performance results are evaluated without and with rate ½ convolution coding with hard decision decoding. The results are presented in terms of BER, power penalty due to fading and coding gain due to error correction coding. It is noticed that there is significant power penalty due to fading and can be reduced by

increasing the number of receiving antennas. Among the different modulation schemes QPSK is found to provide the best performance.

Y. Huang et.al [34] gives the system model and the STBC encoding and decoding schemes in MIMO-OFDM system according to STBC coding theories. It focuses on researching and simulating the MIMO-OFDM system's performances, which had added STBC. A detailed analytical behavior and simulated BER performance of the system with different number of transceiver antennas is given. At the same time, BER performance of the system with different modulation modes such as QPSK, 8-PSK, and 16-QAM is also analyzed and simulated. Simulation results show that the system's performance in multipath environment is improved when MIMO-OFDM system has added STBC. Decoding at the receiver is simple linear processing, to keep the decoding complexity as low as possible.

2.5 MIMO-OFDM Systems using QOSTBC

H. Jafarkhani [35] says that quasi orthogonal codes are designed which provide full transmission rate. The quasi orthogonal codes are those in which transmission metric column are divided into groups the column within each group are not orthogonal instead different groups are orthogonal to each other. As compared to full diversity orthogonal code quasi orthogonal codes have better performance (lower BER) at low SNR's whereas their performance is degrading at higher SNR's.

N. Sharma et.al [36] discuss that a significant improvement in the performance of Quasi orthogonal ST codes is achieved if we phase shift or rotate the constellations of the codes symbols. The basis of constellation rotation is that it increase the minimum distance between the ST code words thus improving performance. Particularly at low BER's performance gain of 6 db and 4 db have been obtained for QPSK & 8PSK respectively as compared to no rotation.

J. Hou et.al [37] analyzed the transmission matrices of QOSTBC's and also proposes some new patterns for the matrices. The main aim of new designs is to reduce the interference of adjacent symbols. The purposed new codes NPI &NP2 performs better as compared to Jafarkhani & TBM codes. The new codes are designed by changing the distribution of conjugates in transmission matrices.

The QOSTBC are designed properly to ensure good performance ever at high SNR. The thing is to choose half of the symbols in quasi orthogonal design from signal constellation set A & other half from rotated constellation C & A. The resulting codes out perform the orthogonal codes in items of diversity decoding & SNR as given by S. Weifeng et.al [38].

B. Badic et.al [39] studies antenna selection for QOSTBC at the transmitter & receiver. A optimum selection criteria for choosing the best antenna subset is proposed for achieving high diversity & SNR. A simple zero forcing receiver is considered and it is assumed that at the transmitter $N \geq 4$ antennas are available and at receiver only $n_r=1$ antenna is used.

The concept of transmit beam forming is considered & a beam forming matrix is constituted for STBC. The concept of beam forming is extended by L Liu et.al [40] for QSTBC by which has not been implemented yet. The resulting QSTBC beam forming has high rate and degree of spatial diversity.

C. Toker [41] explores 2 feed back methods for QO STBC for achieving full diversity and code rate. The first method purposes rotation of signals by phasors according to feed back from receiver. The second method is based on antenna weighting/selection. The performance gap between the uncoded QO STBC and the four antenna transmit beamformer is reduced to 2.5db using feedback. The proposed scheme is more robust to dynamics in mobile environment & when combined with turbo codes 2.75 db performance gain is obtained.

In the paper given by H. Jafarkhani et.al [42] a family of QOSTBC are considered as building block for QOS ST Trellis codes. The QOSTBC are designed by combining set portioning and a super set of QO STBC & provide full rate diversity & high coding gain.

J. Klutto et al. [43] propose channel orthogonalised space-time block codes (C-STBC) for five & six transmit antennas which are closed loop (feedback) & have rate 3/4 1-5 db gain in obtained as compared to open loop scheme. A closed form expression for evaluating feedback angle is also given.

The scheme of existing complex orthogonal STBC for 7 transmitting antennas is extended for 8 transmitting antennas by X.B. Liang [44] which achieves same rate & decoding delay. This is

done by padding a transmission to vector of the 8th transmit antenna to the transmission matrix of the existing complex OSTBC for 7 transmit antennas.

Analyzing the structure and character of several issues of the quasi-orthogonal space–time block code (QOSTBC) X. Wu et.al [45] proposes two novel quasi-orthogonal space–time block codes for four antennas. The novel codes are enriched the family of QOSTBC. Experiment results indicate that these two codes have good performance as Jafarkhani scheme, while the decoding complexity is the same as other quasi-orthogonal codes. The performance of these two schemes is compared when using the ML, MMSE, QR decomposition and ZF algorithm. The decoding algorithm is simplified to decoding of four independent single symbols, so that the complexity of decoding is decreased. By using zero-forcing decoding algorithm for novel codes, simulation results show that zero-forcing algorithm has better bit error rate performance as compared to the existing typical codes and can reduce the computation complexity at receiver.

J. S. Jeong et.al [46] invented a new decoding scheme for reducing complexity at the decoder. By using Quasi-ZF based on the traditional Zero Forcing technique and Quasi-MMSE based on the traditional MMSE technique, we can have channel interference parameter be zero. As a result, only diagonal components remain. Eventually, we can detect the transmitted symbols easily with single ML detector. The proposed schemes can be applied to QOSTBC where channel interference parameters are pure imaginary values. The existing QOSTBC using the pairs of transmitted symbols can be decoded with two parallel ML detectors. Therefore, QOSTBC has higher complexity than OSTBC at the decoder.

S. Cho et.al [47] introduces a new computationally efficient MIMO OFDM transmitter using QO-STBC schemes. Straightforward implementation of these systems requires separate IFFT processing blocks for each of the transmit antennas. In the proposed scheme symmetry properties of Fourier transform are used, which results in good reduction in computational burden. Usually, four transmit antennas need a four IFFT converters. But, using the two kinds of the properties, transmission characteristics of QOSTBC and symmetry of Fourier transform, the Common denominator of signal can be found. As a result, if four antennas have a IFFT converter, calculation of the other values can be done easily. If the number of conversion of IFFT is minimized, computation efficient MIMO OFDM transmitter using QOSTBC schemes can be realized.

2.6 Signal Detection in MIMO-OFDM Systems

M. B. Breinholt et.al [48] developed a equalization techniques that facilitate aggressive frequency reuse in cellular OFDM system. The initial focus is on the case of a single strong interfering base at the mobile. The interfering base is asynchronous, because its cyclic prefix is not time-aligned with the desired base's cyclic prefix. Various methods for combating the asynchronous, interfering base are developed based on channel shortening ideas. The most promising method works to align the cyclic prefix while holding all channel lengths equal to the cyclic prefix length or less. For the case of two receive antennas at the mobile, two sets of space time filters are designed so that the respective channels at either output for either base are time-aligned with length no greater than the cyclic prefix length. As a result, standard frequency-domain equalization/interference suppression techniques (e.g., MMSE combining) can be applied to the outputs of the space-time filters on a per frequency bin basis to obtain symbol estimates for the desired base. Simulations are presented comparing the BER performance of the candidate techniques.

The signal detection technology of MIMO-OFDM system is described by X. Zhang et.al [49]. The signal detection technology of MIMO-OFDM system involves linear detection method of ZF detection and the MMSE detection, as well as the non-linear detection method of V-BLAST detection, those detection algorithms are simulated based on matlab in different modulation for searching which is the optimal detection algorithm for particular channel. Non-linear detection algorithm is superior to the linear detection algorithm in four different modulation modes by the comparison of the simulation results. For non-linear detection algorithm for V-BLAST, the BER between the line ZF and MMSE detection algorithms are relatively low in high SNR conditions. And a further comparison between the two types of non-linear detection algorithms concludes that MMSE-SIC algorithm is better than ZF-SIC.

A new group iterative linear ZF receiver for a MIMO-OFDM system is analyzed by Z. wang et.al [50]. The signals of all layers are firstly grouped and the signals in every group are detected by linear ZF detection method. The successive interference cancellation detection is applied between the different groups. Computer simulation results state the proposed algorithm achieves marked performance improvement compared to standard linear MIMO ZF detection algorithms. When convolutional encoding is applied, the proposed scheme may almost obtain the same

performance of conventional ZF-VBLAST while the complexity of proposed algorithm is reduced by about 25%.

Improved Decoder Schemes for QOSTBCs Based on Single-Symbol Decoding are explored by P. V. Bien et.al [51]. The decoder schemes presented in the work can fully eliminate channel interference parameters in detection matrix. As a result, only diagonal components remain and we can detect the transmitted symbols easily with single-symbol ML detector. The proposed schemes can be used for all known QOSTBCs in four transmit antennas systems and can be extended for systems with number of transmit antennas greater than four. The two improved decoder schemes named Modified-ZF and Modified-MMSE are used to reduce decoding complexity of QOSTBCs at the expense of slight SNR lose.

CHAPTER 3: MIMO-OFDM SYSTEM

3.1 Introduction

Multicarrier transmission, also known as OFDM is a technique with a long history back to 1960 that has recently seen rising popularity in wireless and wire line applications. The recent interest in this technique is mainly due to the recent advances in digital signal processing technology. International standards making use of OFDM for high-speed wireless communications are already established or being established by IEEE 802.11, IEEE, 802.16, IEEE 802.20 and ETSI BRAN committees. For wireless applications, an OFDM-based system can be of interest because it provides greater immunity to multipath fading and impulse noise, and eliminates the need for equalizers, while efficient hardware implementation can be realized using FFT techniques [52].

OFDM is a multi-carrier modulation technique where data symbols modulate a parallel collection of regularly spaced sub-carriers. The sub-carriers have the minimum frequency separation required to maintain orthogonality of their corresponding time domain waveforms, yet the signal spectra corresponding to the different sub-carriers overlap in frequency. The spectral overlap results in a waveform that uses the available bandwidth with a very high bandwidth efficiency.

OFDM is simple to use on channels that exhibit time delay spread or, equivalently, frequency selectivity. Frequency selective channels are characterized by either their delay spread or their channel coherence bandwidth which measures the channel decorrelation in frequency. The coherence bandwidth is inversely proportional to the root-mean-square (rms) delay spread.

By choosing the sub-carrier spacing properly in relation to the channel coherence bandwidth, OFDM can be used to convert a frequency selective channel into a parallel collection of frequency flat subchannels. Techniques that are appropriate for flat fading channels can then be applied in a straight forward fashion. The frequency domain of an OFDM and FDM system is represented in the diagram below for ten channels.

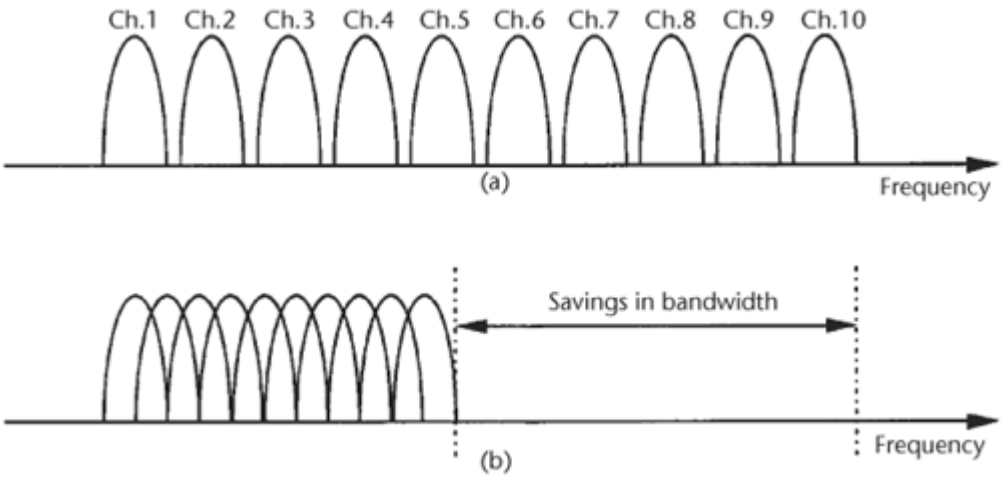

Figure 3.1: Concept of the OFDM signal (a) conventional multicarrier technique and (b) orthogonal multicarrier modulation technique

If one observe the Figure 3.1 given above, one can easily notice that the bandwidth taken by the convectional parlor system (FDM) is far higher then that of OFDM system for the same number of channel. Thus one can easily sense the advantage of OFDM system over ordinary FDM system.

OFDM is similar to FDM technique except that the *'N'* sub-carriers are made orthogonal to each other over the OFDM symbol (frame) duration T_s. By orthogonality of the carriers, we mean that the carrier frequencies satisfy the following requirement –

$$f_k = f_0 + \frac{k}{T_s}, k = 1,2,\ldots\ldots\ldots,N\text{-}1 \quad (3.1)$$

T_s = OFDM symbol duration

K = an integer

f_k = frequency of k^{th} carrier

f_0 = fundamental frequency

Key advantages of OFDM Transmission:

• OFDM is an efficient way to deal with multipath; for a given delay spread, the implementation complexity is significantly lower than that of a single-carrier system with an equalizer.

• In relatively slow time-varying channels, it is possible to enhance capacity significantly by adapting the data rate per SC according to the signal-to-noise ratio (SNR) of that particular SC.

• OFDM is robust against narrowband interference because such interference affects only a small percentage of the SCs.

• OFDM makes single-frequency networks possible, which is especially attractive for broadcasting applications.

Disadvantages of OFDM Transmission:

• OFDM is more sensitive to frequency offset and phase noise.

• OFDM has a relatively large peak-to-average-power ratio, which tends to reduce the power efficiency of the radio frequency (RF) amplifier.

Application of OFDM

During the past decade, OFDM has been adopted in many wireless communication standards, including European digital audio broadcasting, terrestrial digital video broadcasting, and satellite terrestrial interactive multiservice infrastructure in China. In addition, OFDM has been considered or approved by many IEEE standard working groups, such as IEEE 802.11a/g/n, IEEE 802.15.3a, and IEEE 802.16d/e.

The applications include wireless personal area networks, wireless local area networks, and wireless metropolitan networks. Currently, OFDMA is being investigated as one of the most promising radio transmission techniques for LTE of the 3rd Generation Partnership Project (3GPP), International Mobile Telecommunications-Advanced Systems.

3.2 OFDM Signal Model

Figure 3.2 shows the block diagram of a OFDM system with SISO configuration. Denote $X_l\ (\ l = 0,1,2,\ldots,N\ -1)$ as the modulated symbols on the l_{th} transmitting subcarrier of OFDM symbol at transmitter, which are assumed independent, zero-mean random variables, with average power σ_X^2.The complex baseband OFDM signal at output of the IFFT can be written as:

$$x_n = \frac{1}{\sqrt{N}} \sum_{l=0}^{N-1} X_l e^{j\frac{2\pi}{N}nl} \tag{3.2}$$

where N is the total number of subcarriers and the OFDM symbol duration is T seconds.

At the receiver, the received OFDM signal is mixed with local oscillator signal, with the frequency offset deviated from Δf the carrier frequency of the received signal owing to frequency estimation error or Doppler velocity, the received signal is given by:

$$\hat{x}_n = (x_n \otimes h_n)\ e^{j\frac{2\pi}{N}n\Delta fT} + z_n \tag{3.3}$$

where h_n, $e^{j\frac{2\pi}{N}n\Delta fT}$, and z_n represent the channel impulse response, the corresponding frequency offset of received signal at the sampling instants: $\Delta f\ T$ is the frequency offset to subcarrier frequency spacing ratio, and the AWGN respectively, while $\otimes$ denotes the circular convolution. Assuming that a cyclic prefix is employed; the receiver have perfect time synchronization. Note that a discrete Fourier transform (DFT) of the convolution of two signals in time domain is equivalent to the multiplication of the corresponding signals in the frequency domain. Then the output of the FFT in frequency domain signal on the k_{th} receiving subcarrier becomes:

$$\hat{X}_k = \sum_{l=0}^{N-1} X_l H_l Y_{l-k} + Z_k, \qquad k=0,\ldots,N-1$$

$$= X_k H_k U_0 + \sum_{l=0,l\neq k}^{N-1} X_l H_l Y_{l-k} + Z_k \tag{3.4}$$

The first term of Equation (3.4) is a desired transmitted data symbol X_k. The second term represents the ICI from the undesired data symbols on other subcarriers in OFDM symbol. H_k is the channel frequency response and Z_k denotes the frequency domain of z_n. The term Y_{l-k} is the coefficient of *FFT* (*IFFT*), is given by:

$$Y_{l-k} = \frac{1}{N}\sum_{n=0}^{N-1} e^{j\frac{2\pi}{N}n(l-k+\Delta fT)} \tag{3.5}$$

when the channel is flat, Y_{l-k} can be considered as a complex weighting function of the transmitted data symbols in frequency domain [53].

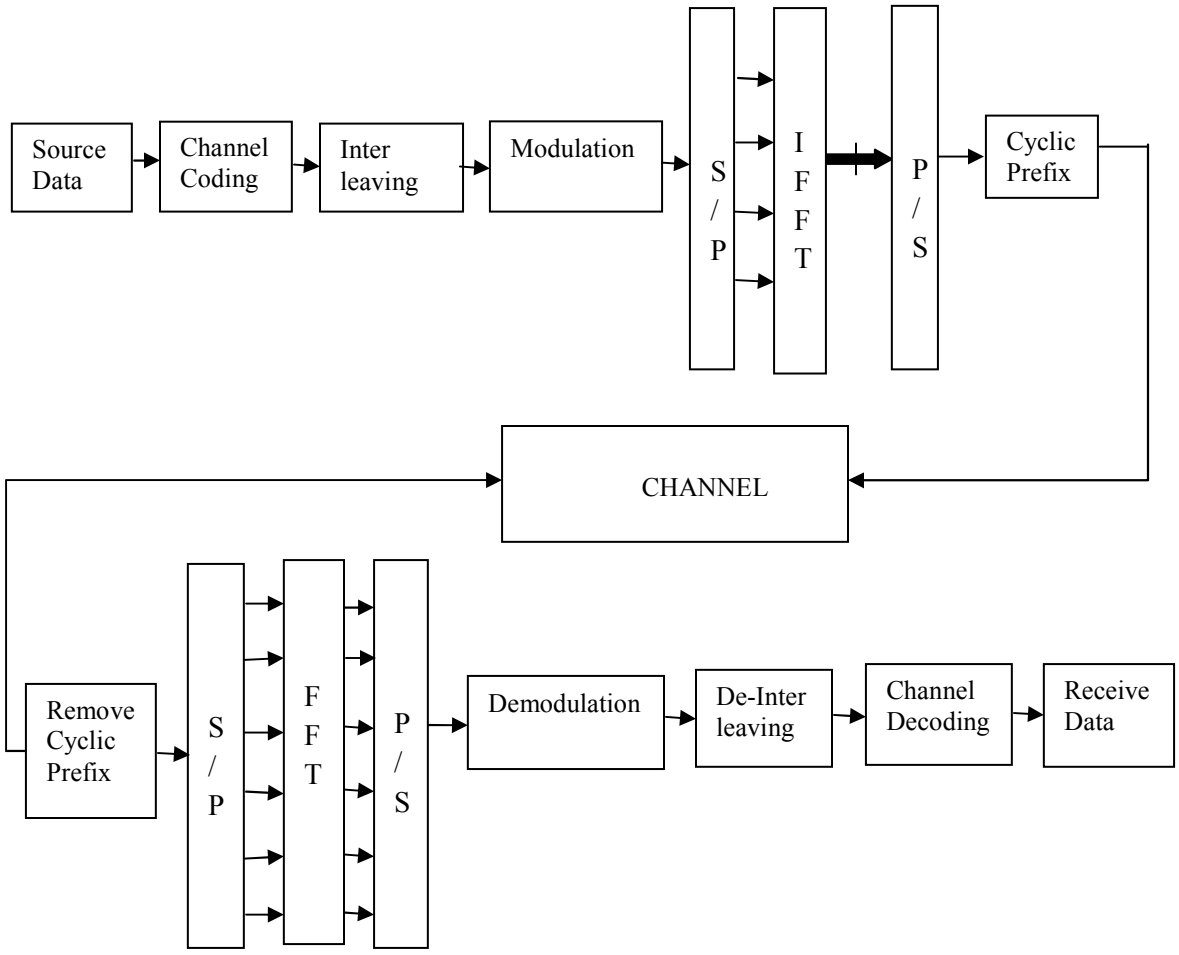

Figure 3.2: Block Diagram of OFDM system

In the above figure we can see the block diagram of the basis OFDM system; now in the following subsection we will investigate the operation and the importance of each block in brief.

Source coding entails the efficient representation of information sources. For both discrete and continuous sources, the correlations between samples are exploited to produce an efficient representation of the information. The aim of source coding is either to improve the SNR for a given bit rate or to reduce the bit rate for a given SNR. An obvious benefit of the latter is a reduction in the necessary system resource of bandwidth and/or energy per bit to transmit the information source.

A discussion on source coding requires the definition of a quantity, which measures the average self information in each discrete alphabet, termed source entropy [54.

The self-information $I(x_j)$ for discrete symbol or alphabet x_j is defined as:-

$$I(x_j) = -\log_2(p_j) \tag{3.6}$$

where p_j is the probability of occurrence for x_j. The source entropy $H(x_j)$ is found by taking the statistical expectation of the self-information, i.e.,

$$H(x_j) = E\{I(x_j)\} = -\sum_{j=1}^{M} p_j \log_2(p_j) \tag{3.7}$$

where M is the cardinality of the discrete alphabet set and the units of measure for $H(x_j)$ are bits/symbol. The source entropy can also be thought of as the average amount of uncertainty contained in the alphabet x_j. Therefore, the source entropy is the average amount of information that must be communicated across the channel per symbol. It can be easily shown that $H(x_j)$ is bounded by the following expression

$$0 \leq H(x_j) \leq \log_2 M \tag{3.8}$$

In other words, the source entropy is bounded below by zero if there is no uncertainty, and above by $\log_2 M$ if there is maximum uncertainty. As an example, consider a binary source x_j that generates independent symbols 0 and 1 with respective probabilities of p_0 and p_1. The source entropy is given by

$$H(x_j) = -[\, p_1 \log_2(p_1) + p_0 \log_2(p_0) \,] \tag{3.9}$$

Proper coding design is extremely important for a digital communication link. A designer should take several design factors into account. Those include required coding gain for intended link budget, channel characteristics, source coding requirements, modulation, etc. Coding in OFDM systems has an additional dimension. It can be implemented in time and frequency domain such that both dimensions are utilized to achieve better immunity against frequency and time selective fading [55].

Convolutional codes are commonly specified by three parameters n, k, m. Where n is the number of output bits, k is the number of input bits and m is the number of memory registers. Encoder for a convolutional code accepts k-bit blocks of information sequence and produces an encoded

sequence (codeword) of n-bit blocks. However, each encoded block depends not only on the corresponding k-bit message block at the same time unit, but also on M previous blocks. Hence, the encoder has a memory length of m. Encoder operates on the incoming message sequence continuously in a serial manner.

The quantity k/n called the code rate, is a measure of code's efficiency. Other important parameter of convolutional code is the constraint length of the code and is defined by L=k (m− 1). The constraint length L represents the number of bits in the encoder memory that affect the generation of the n output bits. The error correction capacity is related with this value. The number of bits' combinations in the registers is called the states of the code and are defined by number of states Ns = 2L, where L is the constraint length of the code.

The convolutional code structure is easy to draw from its parameters. First draw m boxes representing the memory registers. Then n modulo-2 adders to represent the n output bits. Now connect the memory registers to the adders using the polynomial generator. The selection of which bits are going to be added to produce the output bit is called the polynomial generator g for that output bit. For instance, in Figure 3.3 is presented a small convolutional coder with code rate k/n = 1/2 and two memory elements. The Output 0 has a generator polynomial g0 = (111) and the Output 1 has a generator polynomial g1 = (101). The number of memory's registers determines the gain that the convolution code can achieve [56].

However, the number of registers is limited by the decoding complexity of Viterbi algorithm because, its complexity grows exponentially with the number of memory elements. IEEE 802.11a limited the number of elements to 6. The basic measure of channel coding performance is coding gain, which is usually measured in dB s as the reduction of required Signal to Noise Relation SNR to achieve a certain bit error rate (BER) in AWGN channel. The minimum free distance of the code determines the performance of the convolutional code. The coding gain is:

$$C_{gain} = 10log_{10}(CR_{dfree}) \quad (3.10)$$

where CR is the coding rate and dfree is the free distance defined as the minimum Hamming distance between two different code words.

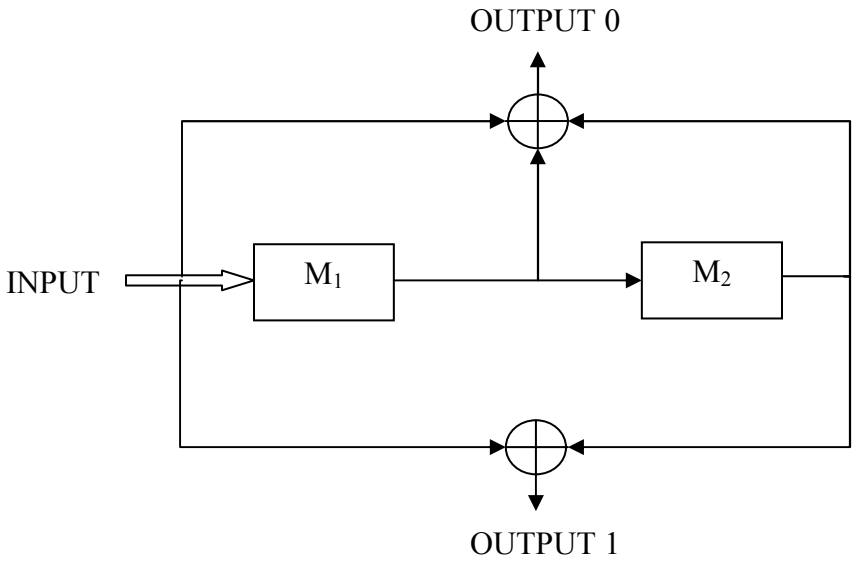

Figure 3.3: Block Diagram of Convolutional Encoder k/n = 1/2 , m=2

Unlike a block code that has a fixed word length n, a convolution code has no particular size. However, convolution codes are often forced into a block structure by periodic truncation. This requires a number of zero bits to be appended to the end of input data sequence, for the purpose of clearing of flushing the encoding shift register of the data bits. Since the added zeros carry no information, the effective code rate falls below k/n. To keep the code rate close to k/n, the truncation period is generally made as long as practical.

Modulation and channel coding are fundamental components of a digital communication system. Modulation is the process of mapping the digital information to analog form so it can be transmitted over the channel. Consequently every digital communication system has a *modulator* that performs this task. Closely related to modulation is the inverse process, called *demodulation,* done by the receiver to recover the transmitted digital information [13]. The design of optimal demodulators is called *detection* theory. An OFDM system performs modulation and demodulation for each subcarrier separately, although usually in a serial fashion, to reduce complexity [14].

- Phase-shift keying (M-PSK) for which the signal set is:

$$X_i(t) = \sqrt{2E_s/T_s}\ \cos(2\pi * f_{c\tau} + 2(i-1)/M) \quad i=1,2,.....M \ \&\ 0 < t < T_s \qquad (3.11)$$

Where E_s the signal energy per symbol T_s is the symbol duration, and $f_{c\tau}$ is the carrier frequency. This phase of the carrier takes on one of the M possible values, namely

$$\theta_i = 2(i-1)^{\Pi/M} \qquad \text{where } i=1,2,...,M$$

An example of signal-space diagram for 8-PSK

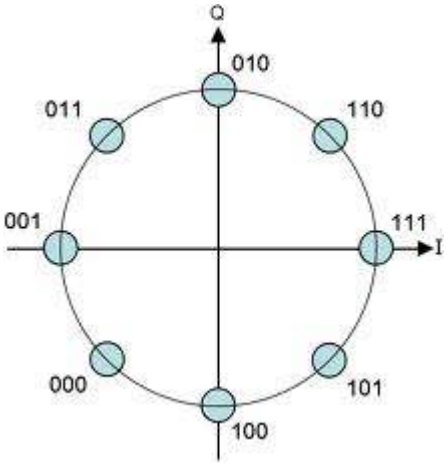

Figure 3.4: Signal-space diagram for 8-PSK

- In M-ary PSK modulation, the amplitude of the transmitted signals was constrained to remain constant, thereby yielding a circular constellation [15]. By allowing the amplitude to also vary with the phase, a new modulation scheme called quadrature amplitude modulation (QAM) is obtained.

The transmitted M-aray QAM symbol I can be expressed as

$$X_i(t)=\sqrt{2}/T_s\, a_n\cos(2\pi^* f_{c\tau})-\sqrt{2}/T_s b_n \cos(2\pi^* f_{c\tau})\ i=1,2,.....M\ \&\ 0<t<T_s \qquad (3.12)$$

Where a_n and b_n are amplitudes taking on the values and

$$a_n\,,\ b_n = \pm a, \pm 3a, ... \pm(\log_2 * M-1)a \qquad (3.13)$$

Where M is assumed to be a power of 4.

The parameter a can be related to the average signal energy (E_s) by

$$a = \sqrt{3E_s/2(M-1)}$$

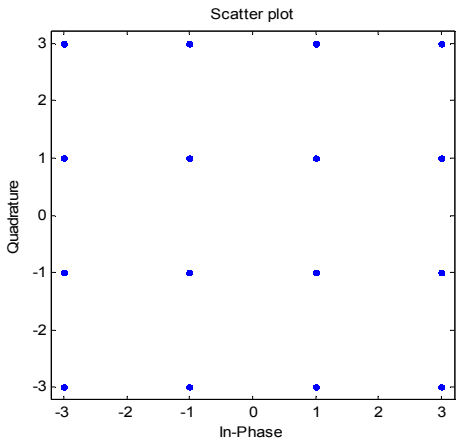

Figure 3.5: QAM Constelations for 16-QAM

Interleaving aims to distribute transmitted bits in time or frequency or both to achieve desirable bit error distribution after demodulation. What constitutes a desirable error distribution depends on the used FEC code. What kind of interleaving pattern is needed depends on the channel characteristics. If the system operates in purely AWGN environment, no interleaving is needed, because the error distribution cannot be changed by relocating the bits. Communication channels are divided into *fast* and *slow* fading channels. A channel is fast fading if the impulse response changes approximately at the symbol rate of the communication system, whereas a slow fading channel stays unchanged for several symbols [56].

- Block interleaving operates on one block of bits at a time. The number of bits in the block is called *interleaving depth,* which defines the delay introduced by interleaving. A block interleaver can be described as a matrix to which data is written in columns and read in rows, or vice versa. For example, Figure 3.6 shows a 8x6 block interleaver, hence interleaving depth is 48. The input bits are written in columns as [*b*0, *b*1, *b*2, *b*3,…] and the interleaved bits are read by rows as [*b*0, *b*8, *b*16, *b*24,…] .Block interleaver is simple to implement using random access memory (RAM) on current digital circuits.

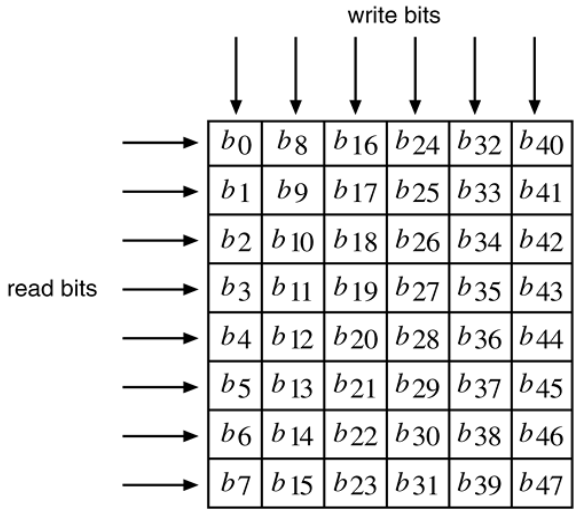

Figure 3.6: Bit write and read structure of 8×6 Block Interleaver

- A convolutional interleaver is another possible interleaving solution that is most suitable for systems that operate on continuous stream of bits. This interleaver structure was published by Ramsey.

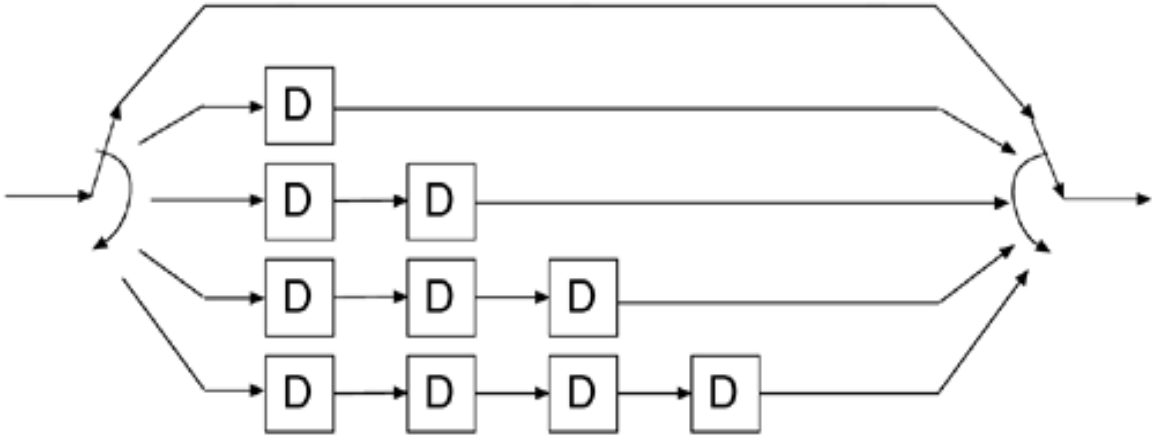

Figure 3.7: Basic structure of Convolutinal Interleaver

Figure 3.7 shows the basic structure of a convolutional interleaver. The interleaver operates by writing the bits into the commutator on the left, and reading bits out from the commutator on the right. The delay elements *D* are clocked after each cycle of the commutators is completed; that is, after the last delay line has been written and read. The main benefit of a convolutional interleaver is that it requires approximately half of the

memory required by a block interleaver to achieve the same interleaving depth. This saving can be significant for long interleaver depths.

In an OFDM system, each channel can be broken into various sub-carriers. The use of sub-carriers makes optimal use out of the frequency spectrum but also requires additional processing by the transmitter and receiver. This additional processing is necessary to convert a serial bit stream into several parallel bit streams to be divided among the individual carriers. Once the bit stream has been divided among the individual sub-carriers, each sub-carrier is modulated as if it was an individual channel before all channels are combined back together and transmitted as a whole. The receiver performs the reverse process to divide the incoming signal into appropriate sub-carriers and then demodulating these individually before reconstructing the original bit stream.

The DFT is, arguably, the most widely used design and analysis tool in electrical engineering. For many situations, frequency-domain analysis of discrete-time signals and systems provide insights into their characteristics that are not easily ascertainable in the time-domain. The DFT is a discrete version of the DTFT); that is, the DTFT is a function of a continuous frequency variable, whereas the DFT is a function of a discrete frequency variable [57]. The DFT is useful because it is more amenable to digital implementations. A general N-to-N point linear transformation requires N^2 multiplications and additions. This would be true of the DFT and IDFT if each output symbol were calculated separately. However, by calculating the outputs simultaneously and taking advantage of the cyclic properties of the multipliers $e^{\pm j2\pi kn/N}$ FFT techniques reduce the number of computations to the order of $N \log N$. The FFT is most efficient when N is a power of two. Several variations of the FFT exist, with different ordering of the inputs and outputs, and different use of temporary memory.

FFT can be implemented in two ways i.e. DIT and DIF. Two main differences between decimation in time (DIT) and decimation in frequency (DIF) are noted [58]. First, for DIT, the input is bit-reversed and output is in natural order, while in DIF, the reverse is true. Secondly, for DIT complex multiplication is performed before the add-subtract operation, while in DIF the order is reversed. While complexity of the two structures is similar in typical DFT, this is not the

case for partial FFT. The reason is that in the DIT version of partial FFT, a sign change (multiplication by 1 and -1) occurs at the first stages, but in the DIF version it occurs in later stages. One variation, decimation in time, is shown in Figure 3.8.

Inverse DFT and DFT are critical in the implementation of an OFDM system.

$$IDFT\, x(n) = \frac{1}{N}\sum_{k=0}^{N-1} X(k) e^{j\frac{2\pi}{N}kn} \tag{3.14}$$

$$DFT\, X(k) = \sum_{n=0}^{N-1} x(n) e^{-j\frac{2\pi}{N}kn} \tag{3.15}$$

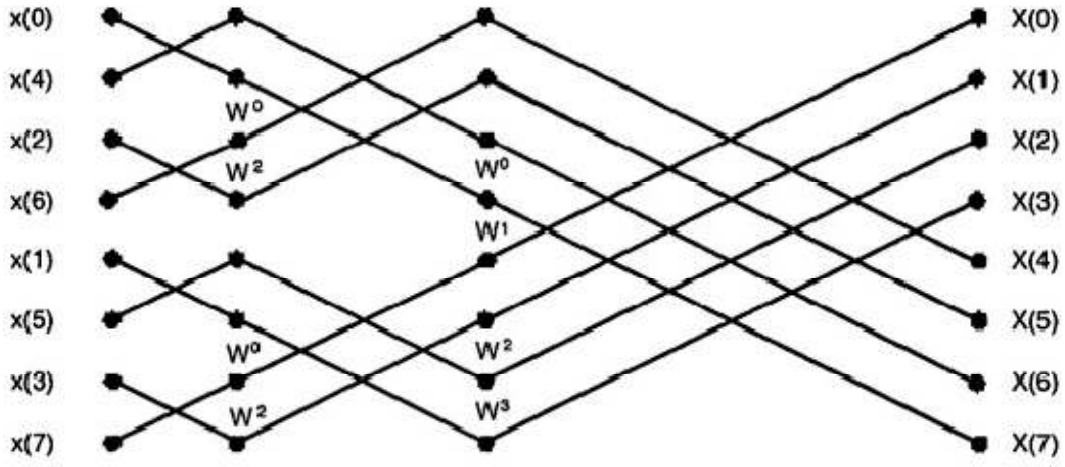

Figure 3.8: An FFT Implementation (Decimation In Time)

❖ The orthogonality of sub channels in OFDM can be maintained and individual sub channels can be completely separated by the FW at the receiver when there are no ISI and ICI introduced by transmission channel distortion. In practice these conditions cannot be obtained. Since the spectra of an OFDM signal is not strictly band limited (sinc(f) function), linear distortions such as multipath cause each subchannel to spread energy into the adjacent channels and consequently cause ISI. A simple solution is to increase the symbol duration or the number of carriers so that the distortion becomes insignificant [59]. However, this method may be difficult to implement in terms of carrier stability, Doppler shift, FFT size and latency.

One way to prevent IS1 is to create a cyclically extended guard interval, where each OFDM symbol is preceded by a periodic extension of the signal itself. Considering the discrete time implementation of the Multi Carrier system, sampling the transmitted Multi Carrier signal at a

rate equal to the data rate one obtains a frame structure composed of the IDFT of the data symbols and of a cyclic prefix, as shown in Figure 3.9, and where the OFDM frame will contain $N_{total} = L + N$ samples. Here L is the number of samples copied from the end of N sample IDFT frame and glued at the start of each IDFT frame. At the receiver, removing the guard interval becomes equivalent to removing the cyclic prefix, while the effect of the channel transforms into the periodic convolution of the discrete time channel with the IDFT of the data symbols. Performing a DFT on the received samples after the cyclic prefix is discarded, the periodic convolution is transformed into multiplication, as it was the case for the analog Multi Carrier receiver. Therefore, a discrete time implementation of the Multi Carrier transmitter will use a cyclic prefix to emulate the guard interval from the analog transmission [60].

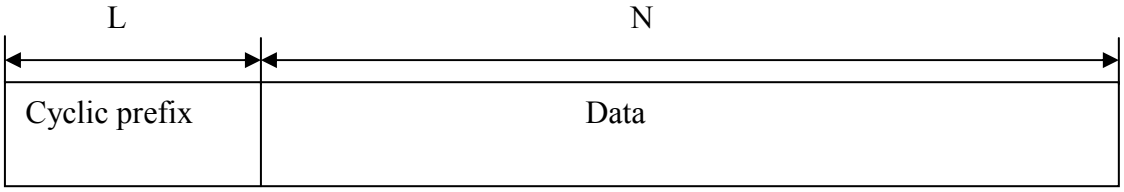

Figure 3.9: Cyclic Prefix in OFDM Transmission

When the guard interval is longer than the channel impulse response, or the multipath delay, the IS1 can be eliminated. However, the ICI, or in-band fading, still exists. The ratio of the guard interval to useful symbol duration is application-dependent. Since the insertion of guard interval will reduce data throughput L is usually less than N/4.

❖ Wireless transmission uses air or space for its transmission medium. The radio propagation is not as smooth as in wire transmission since the received signal is not only coming directly from the transmitter, but the combination of reflected, diffracted, and scattered copies of the transmitted signal.

Reflection occurs when the signal hits a surface where partial energy is reflected and the remaining is transmitted into the surface. Reflection coefficient, the coefficient that determines the ratio of reflection and transmission, depends on the material properties. Diffraction occurs when the signal is obstructed by a sharp object which derives secondary waves. Scattering occurs

when the signal impinges upon rough surfaces, or small objects. Received signal is sometimes stronger than the reflected and diffracted signal since scattering spreads out the energy in all directions and consequently provides additional energy for the receiver which can receive more than one copies of the signal in multiple paths with different phases and powers. Figure 3.10 illustrates the propagation mechanisms [61].

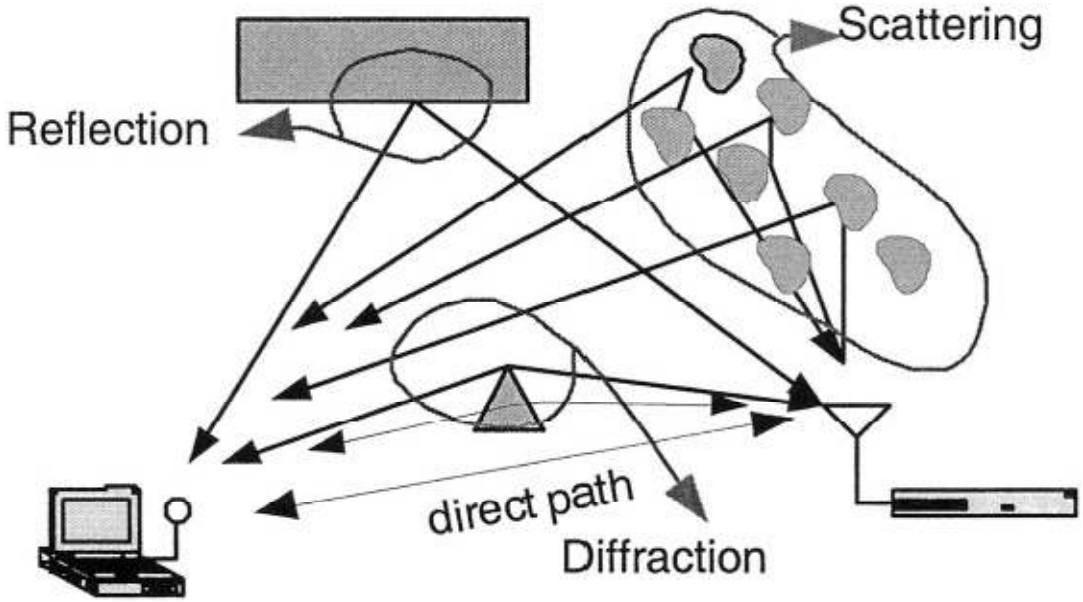

Figure 3.10: Wireless Propagation

- AWGN channel is a universal channel model for analyzing modulation schemes. In this model, the channel does nothing but add a white Gaussian noise to the signal passing through it. This implies that the channel's amplitude frequency response is flat (thus with unlimited or infinite bandwidth) and phase frequency response is linear for all frequencies so that modulated signals pass through it without any amplitude loss and phase distortion of frequency components. Fading does not exist. The only distortion is introduced by the AWGN. The received signal is simplified to

$$r(t) = x(t) + n(t) \tag{3.16}$$

where n(t) is the additive white Gaussian noise.

The whiteness of n(t) implies that it is a stationary random process with a flat power spectral density (PSD) for all frequencies. It is a convention to assume its PSD as

$$N(f) = No/2, \qquad -\infty < f < \infty \tag{3.17}$$

This implies that a white process has infinite power. This of course is a mathematical idealization. According to the Wiener-Khinchine theorem, the autocorrelation function of the AWGN is

$$R(\tau) = No/2\,\delta(\tau) \tag{3.18}$$

where $\delta(\tau)$ is the Dirac delta function.

- Fading is a phenomenon that occurs when the amplitude and phase of a radio signal change rapidly over a short period of time or travel distance. Fading is caused by interference between two or more versions of the transmitted signal which arrive at the receiver at slightly different times. These waves, called multipath waves, combine at the receiver antenna to give a resultant signal which can vary widely in amplitude and phase. If the delays of the multipath signals are longer than a symbol period, these multipath signals must be considered as different signals. In this case, we have individual multipath signals [62].

- Constructive and destructive nature of multipath components in flat fading channels can be approximated by Rayleigh distribution if there is no line of sight which means when there is no direct path between transmitter and receiver. The Rayleigh distribution is basically the magnitude of the sum of two equal independent orthogonal Gaussian random variables and the probability density function (pdf) is given by:

$$p(r) = \frac{r}{\sigma^2} e^{-\frac{r^2}{2\sigma^2}} \quad 0 \le r \le \infty \tag{3.19}$$

where σ^2 is the time-average power of the received signal

- When there is line of sight, direct path is normally the strongest component goes into deeper fade compared to the multipath components. This kind of signal is approximated by Ricean distribution. As the dominating component run into more fade the signal characteristic goes from Ricean to Rayleigh distribution.

The Ricean distribution is given by:

$$p(r) = \frac{r}{\sigma^2} e^{-\frac{(r^2+A^2)}{2\sigma^2}} I_o\left(\frac{A\,r}{\sigma^2}\right) \; for\,(A \geq 0, r \geq 0) \tag{3.20}$$

where A denotes the peak amplitude of the dominant signal and $I_0[.]$ is the modified Bessel function of the first kind and zero-order [63].

3.3 MIMO System Model

Multi-antenna systems can be classified into three main categories. Multiple antennas at the transmitter side are usually applicable for beam forming purposes. Transmitter or receiver side multiple antennas for realizing different (frequency, space) diversity schemes. The third class includes systems with multiple transmitter and receiver antennas realizing spatial multiplexing (often referred as MIMO by itself).

In radio communications MIMO means multiple antennas both on transmitter and receiver side of a specific radio link. In case of spatial multiplexing different data symbols are transmitted on the radio link by different antennas on the same frequency within the same time interval. Multipath propagation is assumed in order to ensure the correct operation of spatial multiplexing, since MIMO is performing better in terms of channel capacity in a rich scatter multipath environment than in case of environment with LOS . This fact was spectacularly shown in [64].

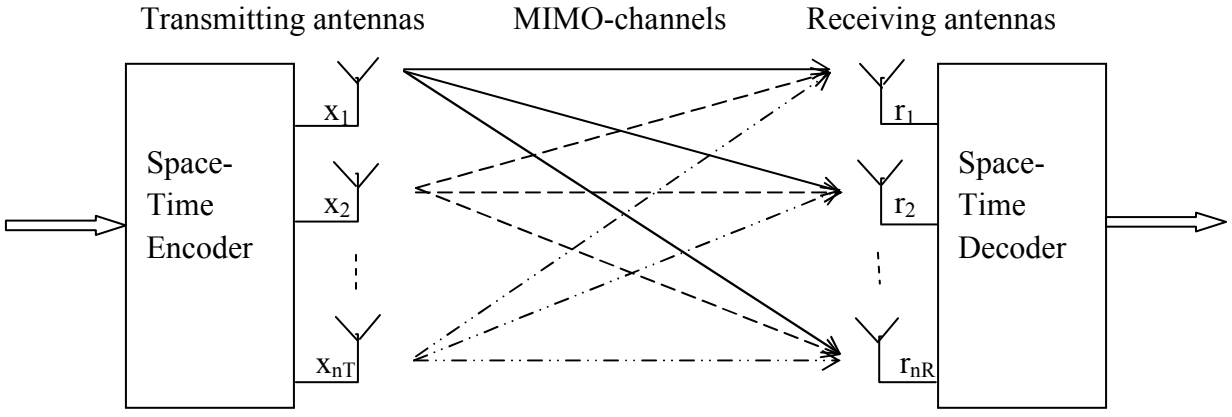

Figure 3.11: Block Diagram of a generic MIMO system with n_T transmitters and n_R receivers

Let us consider a single point-to-point MIMO system with arrays of n_T transmit and n_R receive antennas. We focus on a complex baseband linear system model described in discrete time. The system block diagram is shown in Figure 3.11. The transmitted signals in each symbol period are represented by an $n_T \times 1$ column matrix x, where the ith component x_i, refers to the transmitted signal from antenna i. We consider a Gaussian channel, for which, according to information theory [65], the optimum distribution of transmitted signals is also Gaussian. Thus, the elements of x are considered to be zero mean independent identically distributed (i.i.d.) Gaussian variables. The covariance matrix of the transmitted signal is given by

$$R_{xx} = E\{xx^H\} \tag{3.21}$$

where $E\{\cdot\}$ denotes the expectation and the operator A^H denotes the Hermitian of matrix A, which means the transpose and component-wise complex conjugate of A. The total transmitted power is constrained to P, regardless of the number of transmit antennas n_T. It can be represented as :

$$P = tr(R_{xx}) \tag{3.22}$$

where $tr(A)$ denotes the trace of matrix A, obtained as the sum of the diagonal elements of A. If the channel is unknown at the transmitter, we assume that the signals transmitted from individual antenna elements have equal powers of P / n_T. The covariance matrix of the transmitted signal is given by:

$$R_{xx} = \frac{P}{n_T} I_{nT} \tag{3.23}$$

where I_{nT} is the $n_T \times n_T$ identity matrix. The transmitted signal bandwidth is narrow enough, so its frequency response can be considered as flat. In other words, we assume that the channel is memoryless.

The channel is described by an $n_R \times n_T$ complex matrix, denoted by H. The i, j^{th} component of the matrix H, denoted by h_{ij}, represents the channel fading coefficient from the jth transmit to the ith receive antenna. For normalization purposes we assume that the received power for each of n_R receive branches is equal to the total transmitted power. Physically, it means that we ignore signal attenuations and amplifications in the propagation process, including shadowing,

antenna gains etc. Thus we obtain the normalization constraint for the elements of H, on a channel with fixed coefficients, as

$$\sum_{j=1}^{nT} |h_{ij}|^2 = n_T, \qquad i = 1,2,.....,n_R \tag{3.24}$$

When the channel matrix elements are random variables, the normalization will apply to the expected value of the above expression. We assume that the channel matrix is known to the receiver, but not always at the transmitter. The channel matrix can be estimated at the receiver by transmitting a training sequence. The estimated CSI can be communicated to the transmitter via a reliable feedback channel. The elements of the channel matrix H can be either deterministic or random. We will focus on examples relevant to wireless communications, which involve the Rayleigh and Rician distributions of the channel matrix elements. In most situations we consider the Rayleigh distribution, as it is most representative for NLOS radio propagation.

The noise at the receiver is described by an $n_R \times 1$ column matrix, denoted by n. Its components are statistically independent complex zero-mean Gaussian variables, with independent and equal variance real and imaginary parts. The covariance matrix of the receiver noise is given by:

$$R_{nn} = E[nn^H] \tag{3.25}$$

there is no correlation between components of n, the covariance matrix is obtained as:

$$R_{nn} = \sigma^2 I_{nn} \tag{3.26}$$

Each of n_R receive branches has identical noise power of σ^2.

The receiver is based on a maximum likelihood principle operating jointly over n_R receive antennas. The received signals are represented by an $n_R \times 1$ column matrix, denoted by r, where each complex component refers to a receive antenna. We denote the average power at the output of each receive antenna by P_r. The average SNR at each receive antenna is defined as:

$$\gamma = \frac{P_r}{\sigma^2} \tag{3.27}$$

As we assumed that the total received power per antenna is equal to the total transmitted power, the SNR is equal to the ratio of the total transmitted power and the noise power per receive antenna and it is independent of n_T. Thus it can be written as:

$$\gamma = \frac{P}{\sigma^2} \tag{3.28}$$

By using the linear model the received vector can be represented as:

$$r = Hx + n \tag{3.29}$$

The received signal covariance matrix, defined as $E\{rr^H\}$, by using Equation (3.29), is given by

$$R_{rr} = HR_{xx}H^H \tag{3.30}$$

while the total received signal power can be expressed as $tr(R_{rr})$.

MIMO transmission can be characterized by the time variant channel matrix:

$$H(\tau, T) = \begin{pmatrix} h_{1,1}(\tau,t) & h_{1,2}(\tau,t) & \dots & h_{1,n_R}(\tau,t) \\ h_{2,1}(\tau,t) & \ddots & \ddots & \vdots \\ \vdots & \ddots & \ddots & \vdots \\ h_{n_T,1}(\tau,t) & \dots & \dots & h_{n,n_R}(\tau,t) \end{pmatrix} \tag{3.31}$$

Where the general element, $h_{nT,nR}(\tau, t)$ represents the complex time-variant channel transfer function at the path between the $n_{T\text{-}th}$ transmitter antenna and the $n_{R\text{-}th}$ receiver antenna. n_T and n_R represent the number of transmitter and receiver antennas respectively.

Derived from Shannon's law, for the capacity of MIMO channel the following expression was proven in [64]:

$$C = \max_{tr(R_{xx}) \le p} log_2 (det(I + H R_{xx} H^H)) \tag{3.32}$$

where H denotes the channel matrix and H^H its transpose conjugate, I represents the identity matrix and R_{xx} the covariance matrix of the transmitted signal x.

Benefits of MIMO technology-

Array gain

Array gain is the average increase in the SNR at the receiver that arises from the coherent combining effect of multiple antennas at the receiver or transmitter or both. If the channel is known to the multiple antenna transmitters, the transmitter will weigh the transmission with weights, depending on the channel coefficients, so that there is coherent combining at the single antenna receiver (MISO case). The array gain in this case is called transmitter array gain. Alternately, if we have only one antenna at the transmitter and no knowledge of the channel and a multiple antenna receiver, which has perfect knowledge of the channel, then the receiver can suitably weight the incoming signals so that they coherently add up at the output (combining), thereby enhancing the signal. This is the SIMO case. This is called receiver array gain. Basically, multiple antenna systems require perfect channel knowledge either at the transmitter or receiver or both to achieve this array gain.

Interference reduction and avoidance

Interference in wireless networks results from multiple users sharing time and frequency resources. Interference may be mitigated in MIMO systems by exploiting the spatial dimension to increase the separation between users. For instance, in the presence of interference, array gain increases the tolerance to noise as well as the interference power, hence improving the signal-to-noise-plus-interference ratio (SINR). Additionally, the spatial dimension may be leveraged for the purposes of interference avoidance, i.e., directing signal energy towards the intended user and minimizing interference to other users. Interference reduction and avoidance improve the coverage and range of a wireless network.

Diversity gain

Multipath fading is a significant problem in communications. In a fading channel, signal experiences fades (i.e they fluctuate in their strength). When the signal power drops significantly, the channel is said to be in deep fade. This gives rise to high BER. We resort to diversity to combat fading. This involves providing replicas of the transmitted signal over time, frequency, or space

Spatial multiplexing

Spatial multiplexing offers a linear (in the number of transmit-receive antenna pairs or min (*MR*, *MT*) increase in the transmission rate (or capacity) for the same bandwidth and with no additional power expenditure. It is only possible in MIMO channels. Consider the cases of two transmit and two receive antennas. This can be extended to more general MIMO channels. The bit stream is split into two half-rate bit streams, modulated and transmitted simultaneously from both the antennas. The receiver, having complete knowledge of the channel, recovers these individual bit streams and combines them so as to recover the original bit stream. Since the receiver has knowledge of the channel it provides receive diversity, but the system has no transmit diversity since the bit streams are completely different from each other in that they carry totally different data. Thus spatial multiplexing increases the transmission rates proportionally with the number of transmit-receive antenna pairs.

3.4 Classifications of MIMO Techniques

MIMO techniques can be classified with respect to the quality of channel knowledge at the transmitter.

3.4.1 MIMO with Perfect Transmit Channel Knowledge

Analogous to the previous sections, let us first focus on maximizing the diversity gain of a $n_R \times n_T$ MIMO system. Intuitively, this can be done through transmitting the same signal from all transmit antennas after weighting by a $n_T \times 1$ vector w_t. At the receive array, the antenna outputs are combined into a scalar signal z through a weighted summation according to a $n_R \times 1$ vector w_r Subsequently, the transmission is described by

$$y = \sqrt{E_s}\, H\, w_t\, c + n \tag{3.33}$$

$$r = w_r^H y$$

$$= \sqrt{E_s}\, w_r^H H w_t c + w_r^H n \tag{3.34}$$

Maximizing the receive SNR comes to maximizing $\|w_r^H H w_t\|_F^2 / \|w_r\|_F^2$. To solve this problem, we need to use the singular value decomposition (SVD) of H as

$$H = U_H \sum_H V_H^H \tag{3.35}$$

Where U_H and V_H are n_R *x r(H)* and n_T *x r(H)* unitary matrices, *r(H)* being the rank of H and

$$\sum_H = diag\{\sigma_1, \sigma_2, \dots\dots, \sigma_{r(H)}\} \tag{3.36}$$

is the diagonal matrix containing the singular values of H. Using this particular decomposition of the channel matrix, it is easily shown in [66] that the receive SNR is maximized when w_t and w_r are the transmit and receive singular vectors corresponding to the maximum singular value of *H,* $\sigma_{max} = = max \{\sigma_1, \sigma_2, \dots\dots, \sigma_{r(H)}\}$. This technique is known as the dominant eigenmode transmission, and Equation (3.34) may be rewritten as:

$$z = \sqrt{E_s}\, \sigma_{max} c + \hat{n} \tag{3.37}$$

where $\hat{n} = w_r^H\ n$ has a variance equal to σ_n^2.

From Equation (3.37), it is easily observed that the array gain is equal to $\varepsilon\{\sigma_{\max}^2\} = \varepsilon\{\lambda_{\max}\}$, where $\lambda_{\max}$ is the largest eigenvalue of HH^H . The array gain for i.i.d. Rayleigh channels is thus bounded as follows:

$$max\{n_t, n_r\} \leq g_a \leq n_T\, n_R \tag{3.38}$$

In the i.i.d. Rayleigh case, the asymptotic array gain of a dominant eigenmode transmission (i.e., for large n_T, n_R) is given by:

$$g_a = (\sqrt{n_T} + \sqrt{n_R})^2 \tag{3.39}$$

Finally, the diversity gain is obtained by upper and lower-bounding the error rate at high SNR (assuming that the Chernoff bound is a good approximation of the SER at high SNR)

$$\overline{N}_\varepsilon \left(\frac{\rho d_{min}^2}{4\, min\{n_T, n_R\}}\right)^{-n_t n_r} \geq \tilde{P} \geq \overline{N}_\varepsilon \left(\frac{\rho d_{min}^2}{4}\right)^{-n_T n_R} \tag{3.40}$$

The above equation implies that the error rate maintains a slope of $n_T n_R$ as a function of the SNR: the dominant eigenmode transmission extracts a full diversity gain of $n_T n_R$.

3.4.2 MIMO with Partial Transmit Channel Knowledge

The exploitation of the array gain may also be possible if the transmitter has only a partial channel knowledge. Perfect channel knowledge at the transmitter has been covered in previous section, but requires a high rate feedback link between the receiver and the transmitter to keep the latter continuously informed about the channel state. By contrast, exploiting only the channel statistics or a quantized version of the channel at the transmitter requires a much lower rate feedback link.

Precoding techniques generally consist in combining a multi-mode beamformer spreading the codewords in orthogonal directions related to the channel distribution with a constellation shaper, or more simply, a power allocation scheme. There are naturally many similarities with the various eigenmode transmissions of previous section, the difference being that the eigenbeams are now based on the statistics of H rather than on the instantaneous value of H [67].

Similarly, antenna selection techniques may rely only on partial channel knowledge, choosing transmit or receive antennas based on the first and second-order statistics of H. Intuitively, this comes to choose the antenna pairs with the lowest correlation. Naturally, such a technique does not minimize the instantaneous error performance, but only the average error rate. As a result, it leads mostly to a coding gain and small diversity advantage.

A generalization of antenna selection consists of exploiting a limited amount of feedback at the transmitter through quantized precoding. This technique relies on a codebook of precoding matrices, i.e. a finite set of precoders, designed off-line and known to both the transmitter and receiver. The receiver estimates the best precoder as a function of the current channel and then feeds back the index of the best precoder in the codebook.

3.4.3 MIMO without Transmit Channel Knowledge

When the transmitter has no channel knowledge, the presence of multiple antennas at both sides may allow extracting diversity and increasing the capacity. This is achieved through the use of so-called space–time codes, which expand symbols over the antennas (i.e. over space) and over time. STBCs are the simplest type of spatial temporal codes that exploit the diversity offered in systems with several transmit antennas. In 1998, Alamouti designed a simple transmission diversity technique for systems having two transmit antennas [4]. This method provides full

diversity and requires simple linear operations at both transmission and reception side. The encoding and decoding processes are performed with blocks of transmission symbols. Alamouti's simple transmit diversity scheme was extended in [5] and [6] thanks to the theory of orthogonal designs for larger numbers of transmit antennas. These codes are referred to in the literature as OSTBCs.

3.5 MIMO with Alamouti Space Time Coding

Historically, the transmit diversity technique proposed by Alamouti was the first STBC. The encoding and decoding operation is carried out in sets of two modulated symbols. Hence, the information data bits are first modulated and mapped into their corresponding constellation points. Therefore, let us denote by x_1 and x_2 the two modulated symbols that enter the space–time encoder. Usually, in systems with only one transmit antenna, these two symbols are transmitted at two consecutive time instances t_1 and t_2. The times t_1 and t_2 are separated by a constant time duration T. Then, the encoder takes a block of two modulated symbols x_1 and x_2 in each encoding operation and maps them to the transmit antennas according to a code matrix given by

$$X = \begin{bmatrix} x_1 & -x_2^* \\ x_2 & x_1^* \end{bmatrix} \tag{3.41}$$

The encoder outputs are transmitted in two consecutive transmission periods from two transmit antennas. During the first transmission period, two signals $x1$ and $x2$ are transmitted simultaneously from antenna one and antenna two, respectively. In the second transmission period, signal $-x_2^*$ is transmitted from transmit antenna one and signal x_1^* from transmit antenna two, where x_1^* is the complex conjugate of x_1 [4].

It is clear that the encoding is done in both the space and time domains. Let us denote the transmit sequence from antennas one and two by x^1 and x^2, respectively.

$$x^{t1} = [x_1, -x_2^*]$$

$$x^{t2} = [x_2, x_1^*]$$

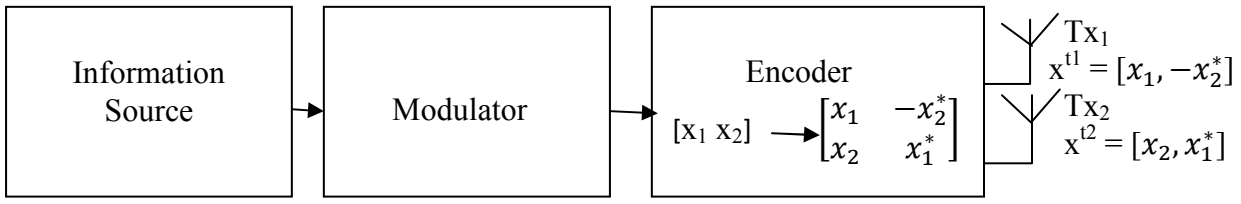

Figure 3.12: A Block Diagram of Alamouti Space-time Encoder

The key feature of the Alamouti scheme is that the transmit sequences from the two transmit antennas are orthogonal, since the inner product of the sequences x^1 and x^2 is zero, i.e.

$$x^{t1} . \ x^{t2} = x_1 x_2^* - x_2^* x_1 \tag{3.42}$$

The code matrix has the following property:

$$X. X^H = \begin{bmatrix} |x_1|^2 + |x_2|^2 & 0 \\ 0 & |x_1|^2 + |x_2|^2 \end{bmatrix}$$

$$= (|x_1|^2 + |x_2|^2) I_2 \tag{3.43}$$

where I_2 is a 2 X 2 identity matrix

At the receive antenna, the received signals over two consecutive symbol periods, denoted by r_1 and r_2 for time t and $t + T$, respectively, can be expressed as

$$r_1 = h_1 x_1 + h_2 x_2 + n_1$$

$$r_2 = -h_1 x_2^* + h_2 x_1^* + n_2 \tag{3.44}$$

where n_1 and n_2 are independent complex variables with zero mean and power spectral density $N_0/2$ per dimension, representing additive white Gaussian noise samples at time t and t + T , respectively.

3.6 MIMO with Orthogonal Space Time Block Coding

The transmit diversity scheme designed by Alamouti can be used only in a system with two transmit antennas. It turns out that this technique belongs to a general class of codes named

Space–Time Block Codes or, more precisely, Orthogonal STBCs, since they are based on the theory of orthogonal designs. The authors of [5] introduced the theory of generalized orthogonal designs in order to create codes for an arbitrary number of transmit antennas.

The general idea behind STBCs construction is based on finding coding matrices X that can satisfy the following condition:

$$X.X^H = p.(\sum_{i=1}^{n}|x_i|^2)\ .\ I_{nT} \tag{3.45}$$

In this equation, X^H is the Hermitian of X, p is a constant, I_{nT} is the identity matrix of size $n_T \times n_T$, n_T represents the number of transmit antennas, and n is the number of symbols x_i transmitted per transmission block in X. The generalized theory of orthogonal design is exploited to provide codes that satisfy Equation 3.45.

The orthgonality property of STBCs is reflected in the fact that all rows of X are orthogonal to each other. In other words, the sequences transmitted from two different antenna elements are orthogonal to each other for each transmission block. For real signal, it is possible to reach full rate. However, it has been proven in [5] that this statement is false for two-dimensional constellations, i.e., complex signals. The encoding and decoding approaches follow the pattern described in Alamouti's scheme.

For complex signals, the theory of orthogonal designs can be used to generate coding matrices that achieve a transmission rate of 1/2 for the cases of 3 and 4 transmission antennas:

$$X_{1/2} = \begin{bmatrix} x_1 & -x_2 & -x_3 & -x_4 & x_1^* & -x_2^* & x_3^* & -x_4^* \\ x_2 & x_1 & x_4 & -x_3 & x_2^* & x_1^* & x_4^* & -x_3^* \\ x_3 & -x_4 & x_1 & x_2 & x_3^* & -x_4^* & x_1^* & x_2^* \end{bmatrix}$$

$$X_{1/2} = \begin{bmatrix} x_1 & -x_2 & -x_3 & -x_4 & x_1^* & -x_2^* & -x_3^* & -x_4^* \\ x_2 & x_1 & x_4 & -x_3 & x_2^* & x_1^* & x_4^* & -x_3^* \\ x_3 & -x_4 & x_1 & x_2 & x_3^* & -x_4^* & x_1^* & x_2^* \\ x_4 & x_3 & -x_2 & x_1 & x_4^* & x_3^* & -x_2^* & x_1^* \end{bmatrix} \tag{3.46}$$

Using the theory of orthogonal design to construct STBCs is not necessarily the optimal approach. There exist some sporadic STBCs mentioned in the literature, [6] [31], that can provide a transmission rate of 3/4 for schemes of either 3 or 4 transmit antennas.

$$X_{3/4} = \begin{bmatrix} x_1 & -x_2^* & x_3^* & 0 \\ x_2 & x_1^* & 0 & -x_3^* \\ x_3 & 0 & -x_1^* & x_2^* \end{bmatrix}$$

$$X_{3/4} = \begin{bmatrix} x_1 & 0 & x_2 & -x_3 \\ 0 & x_1 & x_3^* & x_2^* \\ -x_2^* & -x_3 & x_1^* & 0 \\ x_3^* & -x_2 & 0 & x_1^* \end{bmatrix} \quad (3.47)$$

It is important to notice that the channel coefficients must remain constant during the transmission of a block of coded symbols *X*.

The decoding of the STBCs described above can be easily deduced from the encoding matrix. Let us assume that we wish to estimate symbols x_p and that we have defined by r_j^k the received signal from antenna *j* at time instance *k*. The values to be added at the linear combiner are:

- $+ (h_{j,i}).\, r_j^k$ if we have x_p at column *k* and line (transmit antenna) *i* of *X*.
- $- (h_{j,i}).\, r_j^k$ if we have $-x_p$ at column *k* and line (transmit antenna) *i* of *X*.
- $+ (h_{j,i}).\, (r_j^k)^*$ if we have $(x_p)^*$ at column *k* and line (transmit antenna) *i* of *X*.
- $- (h_{j,i}).\, (r_j^k)^*$ if we have $-(x_p)^*$ at column *k* and line (transmit antenna) *i* of *X*.

The linear combiner sum is realized for all receive antennas *j*.

It is important to remember that STBCs based on orthogonal design do not achieve a rate of 1 for complex signal constellations. In [8], it has been shown for 3 and 4 transmit antennas the maximum possible rate is 3/4 with 4 delays. For 5 to 8 transmit antennas, the achievable rate is 1/2 with 8 delays, and for the 9 to 16 case, the rate becomes 5/16 in 16 time instances. In order to achieve the rate of a SISO system, the orthogonal property of STBCs must be broken as described in [68].

3.7 MIMO with Quasi Orthogonal Space Time Block Coding (QOSTBC)

MIMO systems with O-STBC [35] are particularly attractive due to the fact that they require a relatively simple linear decoding scheme while still providing full diversity gain. Unfortunately, they suffer from a lower code rate when a complex signal constellation and the complexity that more than two transmit antennas are used. To overcome the disadvantages of O-STBC, QO-

STBC was proposed in the literature [41]-[42] and the existing works have shown that QO-STBC offers a higher data rate and partial diversity gain.

To design a QO-STBC with full diversity gain, an improved QO-STBC through constellation rotation was proposed in [42] and [43].Maximum-likelihood (ML) decoding in QO-STBC works with pairs of transmitted symbols, leading to an increase in decoding complexity with modulation level M2. This subsequently increases transmission delay when a high-level modulation scheme or multiple antennas are employed [69]. Sung et al. [70] proposed a method to improve the QO-STBC performance with iterative decoding, which of course achieves higher reliability but increases decoding complexity [70]. In [71], some new decoding methods were proposed to reduce the computational complexity.

Consider a system with 8 transmit antennas (i.e. n_T = 8) and 8 receive antennas (i.e. n_R =8). In what follows, assume that perfect CSI is available at the receiver but unavailable at the transmitter. Also assume that the channel is quasi-static, i.e. the channel coefficients are constant within one block of code transmission and independently realized from block to block.

Let us consider the generator matrix for Alamouti codes as in [4]

$$A_{12} = \begin{bmatrix} x_1 & x_2 \\ -x_2^* & x_1^* \end{bmatrix} \text{ and } A_{34} = \begin{bmatrix} x_3 & x_4 \\ -x_4^* & x_3^* \end{bmatrix}$$

Here the subscript 12 and 34 are used to represent the indeterminate x_1, x_2, x_3 and x_4 in the transmission matrix. The main properties of an orthogonal design are simple separate decoding and full diversity. To design full-rate codes, we relax the simple separate decoding property. In this discussion, we consider codes for which decoding pairs of symbols independently is possible. We call this class of codes QOSTBCs. Now consider the space time block code for n_T and n_R equals to 4 according the method given in [35], the matrix for 4 X 4 antenna configuration can also be constructed as follows :

$$B = \begin{bmatrix} A_{12} & A_{34} \\ -A_{34}^* & A_{12}^* \end{bmatrix} = \begin{bmatrix} x_1 & x_2 & x_3 & x_4 \\ -x_2^* & x_1^* & -x_4^* & x_3^* \\ -x_3^* & -x_4^* & x_1^* & x_2^* \\ x_4 & -x_3 & -x_2 & x_1 \end{bmatrix} \quad (3.48)$$

Note that it has been proven in [30] maximum diversity of the order of $4*n_R$ for a rate one code is impossible in this case. Now, suppose $V_i,\ i = 1, 2\ldots..,\ 4$ as the i_{th} column of B, it is easy to see that

$$\langle V_1, V_2\rangle = \langle V_1, V_3\rangle = \langle V_2, V_4\rangle = \langle V_3, V_4\rangle = 0, \tag{3.49}$$

Where $\langle V_i, V_j\rangle$ is the inner product of the vectors V_i and V_j. Therefore, the subspace created by V_1 and V_4 is orthogonal to the subspace created by V_2 and V_3. This is the rationale behind the name "Quasi-Orthogonal" for the code. The diversity of the code is two, which is less than the maximum possible diversity of four.

The main idea behind the structure of the generator matrices for QOSTBCs in Equation (3.48), and other similar structures, is to build a 4 × 4 matrix from two 2 × 2 matrices to keep the transmission rate fixed. A similar idea can be used to combine any two $N \times N$ orthogonal STBCs to build a $2N \times 2N$ QOSTBC with the same rate [35]. One can even combine two non-square orthogonal STBCs to build a non-square QOSTBC. Now, we consider the following QOSTBC for eight transmit antennas:

$$G = \begin{bmatrix} x_1 & x_2 & x_3 & 0 & x_4 & x_5 & x_6 & 0 \\ -x_2^* & x_1^* & 0 & -x_3 & x_5^* & -x_4^* & 0 & x_6 \\ x_3^* & 0 & -x_1^* & -x_2 & -x_6^* & 0 & x_4^* & x_5 \\ 0 & -x_3^* & x_2^* & -x_1 & 0 & x_6^* & -x_5^* & x_4 \\ -x_4 & -x_5 & -x_6 & 0 & x_1 & x_2 & x_3 & 0 \\ -x_5^* & x_4^* & 0 & x_6 & -x_2^* & x_1^* & 0 & x_3 \\ -x_6^* & 0 & -x_4^* & x_5 & -x_3^* & 0 & -x_1^* & x_2 \\ 0 & x_6^* & -x_5^* & -x_4 & 0 & x_3^* & -x_2^* & -x_1 \end{bmatrix} \tag{3.50}$$

The QOSTBC in Equation (3.50) provides a rate $R = 3/4$ by transmitting six symbols in eight time slots. We denote the i^{th} column of G as V_i. Then, for any indeterminate variables $x_1,\ x_2,\ x_3,\ x_4, x_5, x_6$, we have

$$\begin{aligned} \langle V_1,\ V_i\rangle &= 0,\ i \neq 5 & \langle V_5,\ V_i\rangle &= 0,\ i \neq 1 \\ \langle V_2,\ V_i\rangle &= 0,\ i \neq 6 & \langle V_6,\ V_i\rangle &= 0,\ i \neq 2 \\ \langle V_3,\ V_i\rangle &= 0,\ i \neq 7 & \langle V_7,\ V_i\rangle &= 0,\ i \neq 3 \\ \langle V_4,\ V_i\rangle &= 0,\ i \neq 8 & \langle V_8,\ V_i\rangle &= 0,\ i \neq 4 \end{aligned} \tag{3.51}$$

Where $\langle V_i,\ V_j\rangle = \sum_{l=1}^{8}(V_i)_l\ \ (V_j)_l^*$ is the inner product of vectors V_i and V_j. Therefore, the subspace created by V_1 and V_4 is orthogonal to the subspace created by V_2 and V_5, and similar is true for other columns as given by Equation (3.50). The diversity of these codes are four if we pick all symbols ($x_1, x_2, x_3, x_4, x_5, x_6$) from the same constellation

3.8 Signal Detection of MIMO-OFDM System

Signal detection of MIMO-OFDM system can be carried out by various sub-carrier channel signal detection. Although the whole channel is a frequency-selective fading, but various sub-carriers channel divided can be regarded as flat fading, so the flat fading MIMO signal detection algorithm for MIMO-OFDM system can be directly into the detection of all sub-channels, and signal detection algorithm of the corresponding MIMO-OFDM system can be obtained. Similarly, the other optimization algorithms used in flat fading MIMO signal detection can also be leaded into the MIMO-OFDM system. MIMO-OFDM detection methods consist of linear and nonlinear detection test [49].

3.8.1 Zero Forcing Algorithm

Zero Forcing algorithm is regard the signal of each transmitting antenna output as the desired signal, and regard the remaining part as a disturbance, so the mutual interference between the various transmitting antennas can be completely neglected. The specific algorithm is as follows:

For $k = 0, 1, 2, \ldots\ldots\ldots\ldots, K\text{-}1$, so that,

$$R(k) = [R_1(k), R_2(k), \ldots\ldots\ldots\ldots\ldots, R\,\mathrm{n_R}\ (k)]^T \tag{3.52}$$

$$X(k) = [X_1(k), X_2(k), \ldots\ldots\ldots\ldots\ldots, X\,\mathrm{n_T}\ (k)]^T \tag{3.53}$$

$$N(k) = [N_1(k), N_2(k), \ldots\ldots\ldots\ldots\ldots, N\,\mathrm{n_R}\ (k)]^T \tag{3.54}$$

$$H(k) = \begin{bmatrix} H(k)_{11} & H(k)_{12} & \ldots & H(k)_{1\mathrm{nT}} \\ H(k)_{21} & H(k)_{22} & \ldots & H(k)_{2\mathrm{nT}} \\ \vdots & \vdots & \ddots & \vdots \\ H(k)_{\mathrm{nR1}} & H(k)_{\mathrm{nR2}} & \ldots & H(k)_{\mathrm{nRnT}} \end{bmatrix} \tag{3.55}$$

Here $R(k),\ X(k),\ N(k)$ respectively express output signal, the input signal and noise vector of the k sub-channels in MIMO-OFDM system, for n_T transmitting antennas and n_R receiving antennas,

H(k) expresses channel matrix of the k sub-channels, mathematical expression of sub-channel in the MIMO-OFDM system is as follows:

$$R(k) = H(k)X(k) + N(k) \tag{3.56}$$

There is a linear relationship between input signal X(k) and output signal R(k), that is similar to the flat fading channel for each subcarrier channel in MIMO-OFDM system. Its equivalent block diagram is shown in Figure 3.13. Therefore, signal detection can be transformed into K sub-channels in their signal detection to complete in MIMO-OFDM system and each sub-channel detection of the above can be used flat fading MIMO channel to achieve the detection algorithm.

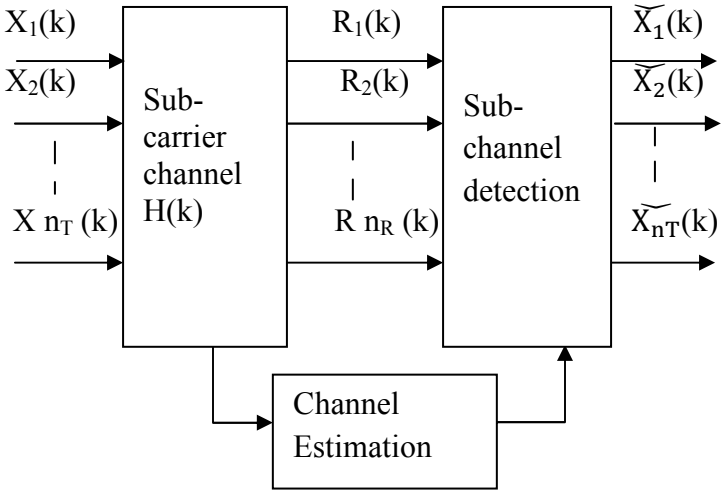

Figure 3.13: Baseband block diagram of k subcarrier channel in MIMO-OFDM system

Zero-forcing (ZF) detection algorithm for MIMO detection algorithm is the most simple and basic algorithms, and the basic idea of zero forcing algorithm is get rid of MIMO-channel interference by multiplying received signal and the inverse matrix of channel matrix. Zero-Forcing solution of MIMO-OFDM system is as follows:

$$X_{ZF} = H^{-1} R = X + H^{-1} N \tag{3.57}$$

In which H^{-1} is the channel matrix for the generalized inverse matrix, the type is obtained for hard-decision demodulation after that to be the source signal estimates:

$$\hat{X}_{ZF} = E(X_{ZF}) \tag{3.58}$$

3.8.2 Minimum Mean Square Error (MMSE) Algorithm

MMSE algorithm is a commonly used MIMO detection algorithm in low SNR environment and has a good bit error rate performance, complexity is also relatively low. MMSE detection solution of MIMO-OFDM Systems is as follows:

$$S_{MMSE} = \left(\Omega^H \Omega + \frac{\sigma^2 N}{\varepsilon_s}\right)^{-1} \Omega^H R \tag{3.59}$$

Here, $E\,[\,|X_i|^2] = \varepsilon_s$, $E\,[\,|E_i|^2] = \sigma_N^2$, $E[.]$, mean the statistical average of random variable demand.

ZF detection completely offset the interference between different antennas (MSI), and separate different data streams by the expense of an increase in noise. While the MMSE regard the minimum mean-square error as the criterion, and the mean square error between the actual symbols sent and detector output is minimum, namely:

$$G_{MMSE} = arg\,min_G \; |Gr-s|^2 \tag{3.60}$$

Orthogonality principle can be used:

$$E\{(G_{MMSE}\, r - s)\, r^H\} = 0 \tag{3.61}$$

Simplification to be:

$$G_{MMSE} = H^H (HH^H + \sigma^2 I_n)^{-1} = H^H (H^H H + \sigma^2 I_n)^{-1} \tag{3.62}$$

Therefore, the output signal of filtering is estimated as follows:

$$\hat{S}_{MMSE} = G_{MMSE}\, r = H^H r(H^H H + \sigma^2 I_n)^{-1} \tag{3.63}$$

Estimated covariance matrix is written as follow:

$$\varphi_{MMSE} = E\{(\hat{x} - x)(\hat{x} - x)\} = \sigma^2 (H^H H + \sigma^2 I_n)^{-1} \tag{3.64}$$

At high SNR, MMSE detection performance converges to ZF detection.

The expansion of the channel matrix $\overline{H}$ and the expansion of the received signal vector $\bar{r}$ are introducted as follows:

$$\bar{H} = \begin{bmatrix} H \\ \sigma I_n \end{bmatrix} \quad , \quad \bar{r} = \begin{bmatrix} r \\ o_{n,1} \end{bmatrix} \tag{3.65}$$

The type vector of $\hat{S}_{MMSE} = G_{MMSE}\, r = H^H\, r\, (H^H H + \sigma^2 I_n)^{-1}$ can be written as :

$$\widehat{S}_{MMSE} = \bar{H} + \bar{r} = (\bar{H}^H H)^{-1} \bar{H}^H \bar{r} \tag{3.66}$$

At this point the covariance matrix becomes:

$$\varphi_{MMSE} = \sigma^2\ (\bar{H}^H H)^{-1} = \sigma^2 \bar{H}^+ \bar{H}^{+H} \tag{3.67}$$

ZF and MMSE linear detection of the linear expressions are similar by comparing the above two type and ZF expressions after the introduction of extended matrix, and H, r respectively transform into $\bar{H}, \bar{r}$ in the ZF expression.

CHAPTER 4: MIMO-OFDM with WiMAX Protocol

4.1 WiMAX Standard

Broadband Wireless Access (BWA) has emerged as a promising solution for last mile access technology to provide high speed internet access in the residential as well as small and medium sized enterprise sectors. As discussed above section, cable and digital subscriber line (DSL) technologies are providing broadband service. But due to the practical difficulties many urban and suburban locations may not be served by DSL connectivity as it can only reach about three miles from the central office switch [72]. On Broadband wireless Access, because of its wireless nature, it can be faster to deploy, easier to scale and more flexible, thereby giving it the potential to serve customers not served or not satisfied by their wired broadband alternatives. IEEE 802.16 standard for BWA and its associated industry consortium, Worldwide Interoperability for Microwave Access (WiMAX) forum promise to offer high data rate over large areas to a large number of users where broadband is unavailable.

This is the first industry wide standard that can be used for fixed wireless access with substantially higher bandwidth than most cellular networks. Wireless broadband systems have been in use for many years, but the development of this standard enables economy of scale that can bring down the cost of equipment, ensure interoperability, and reduce investment risk for operators. The first version of the IEEE 802.16 standard operates in the 10–66GHz frequency band and requires line-of-sight (LOS) towers. Later the standard extended its operation through different PHY specification 2-11 GHz frequency band enabling non line of sight (NLOS) connections, which require techniques that efficiently mitigate the impairment of fading and multipath [73]. Taking the advantage of OFDM technique the PHY is able to provide robust broadband service in hostile wireless channel. The OFDM based physical layer of the IEEE 802.16 standard has been standardized in close cooperation with the European Telecommunications Standards Institute (ETSI) High Performance Metropolitan Area Network (HiperMAN) [18]. Thus, the HiperMAN standard and the OFDM based physical layer of IEEE 802.16 are nearly identical. Both OFDM based physical layers shall comply with each other and a global OFDM system should emerge [73]. The WiMAX forum certified products for BWA comply with the both standards. Communications with direct visibility in the frequency band

from 10 to 66 GHz, were dealt by IEEE 802.16 standard, the amendment IEEE 802.16a specifies working in a lower frequency band 2- 11 GHz. IEEE 802.16d a variation of IEEE 802.16a was basically about optimizing the power consumption of mobile device. IEEE 802.16e is an amendment to IEEE 802.16-2004 and added portability and is oriented to both stationary and mobile deployments. WiMAX standards based projects can work equally well with both the above IEEE standards.

4.2 WiMAX Applications

WiMAX is a WMAN technology, which fits between WLANs and wireless wide area networks (WANs). It has been developed to provide cost effective, high-quality, and flexible BWA solutions using certified, compatible and interoperable equipments from different vendors. WiMAX can provide broadband services to people who could not afford wired broadband services before and cover areas where broadband services have not been available before. Compared to wired broadband technologies, WiMAX has the following advantages: cheaper implementation costs, less monthly ongoing maintenance costs, quicker and easier setup/deployment/reconfiguration/disassembly, less impact on environment, more scalability for future network expanding, and more flexibility. The distance of a WiMAX connection can be up to 30 miles (50 km) at data rates up to 75 Mbps using both the unlicensed and licensed spectrums. WiMAX has a wide range of applications, from large area coverage to last-mile access and backhauling. In the following sections, we will introduce some of them.

4.3 WiMAX Model for Physical Layer

The block diagram for Wi-MAX system (standard: 802.16e) is shown in figure 4.1 [74]. Now we will take each block one by one in detail and in present paper simulation has been done for each block separately.

- Randomization is the first process carried out in layer after the data packet is received from the higher layers each burst in Downlink and Uplink is randomized. It is basically scrambling of data to generate random sequence to improve coding performance.

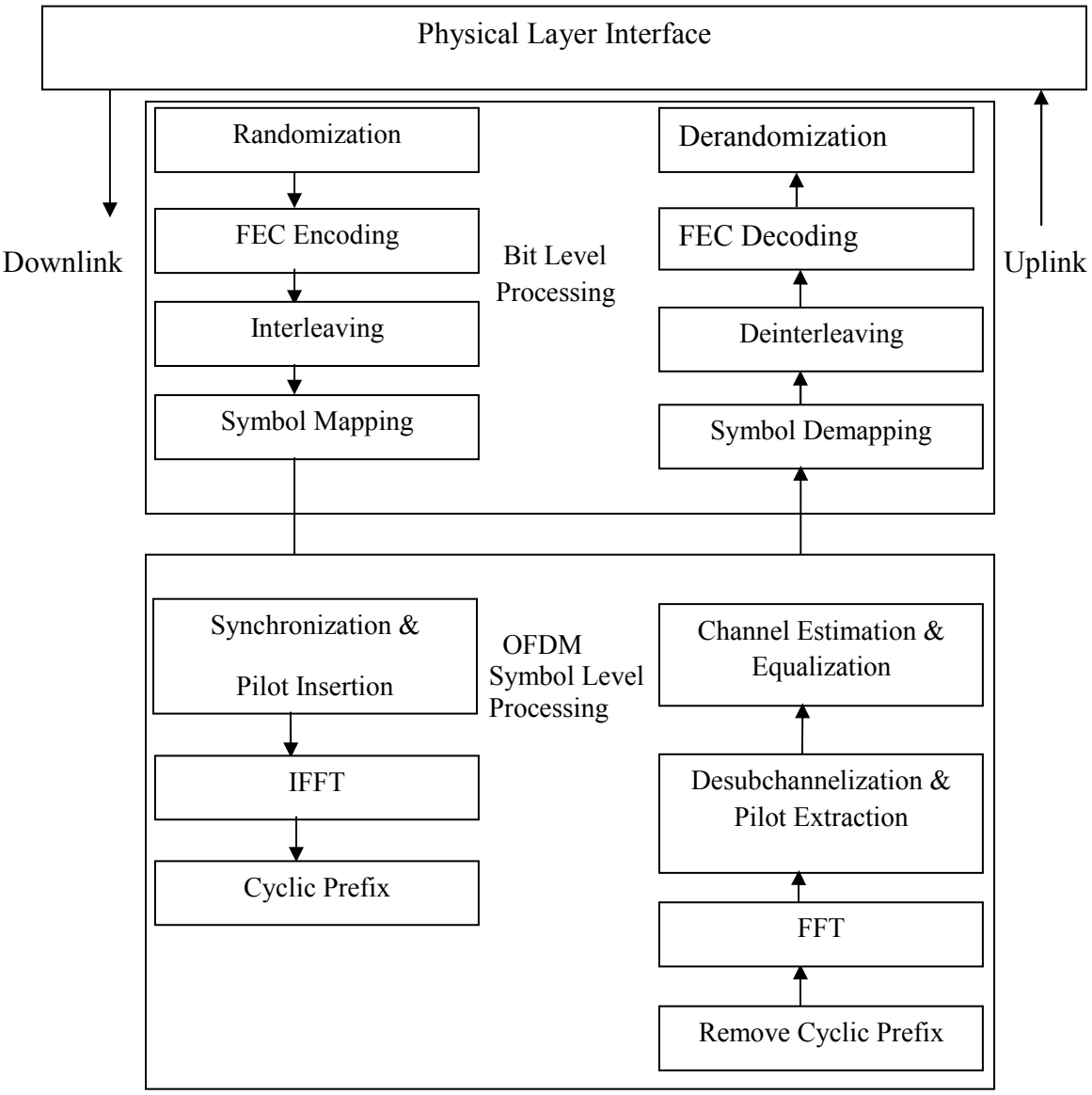

Figure 4.1: WiMAX Model for Physical layer (802.16)

➢ In Forward Error Correction (FEC) there are number of coding system like RS codes, convolution codes Turbo codes etc. But in the present paper only RS codes and convolution codes has been taken for simulation.

RS codes basically add redundancy to the data .this redundancy improves Blocks error. RS-encoder is based on Galois field computation to add the redundancy bits. WiMAX is based on GF (2^8) that corresponds to as RS (N = 255, K = 239, T =8)

where:

N = Number of Bytes after encoding

K = Data Bytes before encoding

T - Number of bytes that can be corrected

In this coding two polynomials are required namely code generator polynomial g(x) and field generator polynomial p(x). Code generator polynomial is given as:

$$G(x) = (x + k^0)(x + k^1)(x + k^2) \ldots\ldots (x + k^{2T-1}) \quad (4.1)$$

Field generator polynomial

$$P(x) = x^8 + x^4 + x^3 + x^2 + 1 \quad (4.2)$$

convolution code introduces redundant bits into the data stream through the use of linear shift register. The information bits are input into shift register and the output encoded bits are obtained by modulo-2 addition of the input information bits and the contents of the shift register 802.11a physical layer uses Convolution code as the mandatory FEC. The convolutional encoder shall use the industry standard generator polynomials, g0 = 1338 and g1 = 1718, of rate R = 1/2. Higher rates like 2/3 and 3/4, are derived from it by employing "puncturing." Puncturing is a procedure for omitting some of the encoded bits in the transmitter (thus reducing the number of transmitted bits and increasing the coding rate) and inserting a dummy "zero" metric into the convolutional decoder on the receive side in place of the omitted bits.

For Decoding the Viterbi algorithm is used. To describe a convolution code, one needs to characterize the encoding function (m), so that given an input sequence m, one can readily compute the output sequence U. Several methods are used for representing a convolutional encoder, the most popular being the connection pictorial, connection vectors and polynomials, the state diagram, the tree diagram.

- Interleaving aims to distribute transmitted bits in time or frequency or both to achieve desirable bit error distribution after demodulation. What constitutes a desirable error distribution depends on the used FEC code. What kind of interleaving pattern is needed depends on the channel characteristics. If the system operates in purely AWGN environment, no interleaving is needed, because the error distribution cannot be changed by relocating the bits.

- Communication channels are divided into *fast* and *slow* fading channels. A channel is fast fading if the impulse response changes approximately at the symbol rate of the communication system, whereas a slow fading channel stays unchanged for several symbols.

- Modulation and channel coding are fundamental components of a digital communication system. Modulation is the process of mapping the digital information to analog form so it can be transmitted over the channel. Consequently every digital communication system has a modulator that performs this task. Closely related to modulation is the inverse process, called demodulation, done by the receiver to recover the transmitted digital information. The design of optimal demodulators is called detection theory. Different coherent mapping used are BPSK, QPSK and M-QAM .However there is trade-off between, different Mapping tech and spectral efficiency. In present paper all mappings are used for simulation purpose.

- Pilot insertion is used for channel estimation & synchronization purpose.

- An inverse Fourier transform converts the frequency domain data input to time domain representing OFDM Subcarrier. IFFT is useful for OFDM because it generates samples of a waveform with frequency component satisfying orthogonality condition. It also removes the need of oscillator. A general *N*-to-*N* point linear transformation requires N^2 multiplications and additions. This would be true of the DFT and IDFT if each output symbol were calculated separately.

However, by calculating the outputs simultaneously and taking advantage of the cyclic properties of the multipliers $e^{\pm j2\pi kn/N}$ Fast Fourier Transform (FFT) techniques reduce the number of computations to the order of *N* log *N*. The FFT is most efficient when *N* is a power of two. Several variations of the FFT exist, with different ordering of the inputs and outputs, and different use of temporary memory.

- One way to prevent IS1 is to create a cyclically extended guard interval, where each OFDM symbol is preceded by a periodic extension of the signal itself. Considering the discrete time implementation of the Multi Carrier system, sampling the transmitted Multi Carrier signal at a rate equal to the data rate one obtains a frame structure composed of the IDFT of the data

symbols and of a cyclic prefix and where the OFDM frame will contain $N_{total} = L + N$ samples. Here L is the number of samples copied from the end of N sample IDFT frame and glued at the start of each IDFT frame.

At the receiver, removing the guard interval becomes equivalent to removing the cyclic prefix, while the effect of the channel transforms into the periodic convolution of the discrete time channel with the IDFT of the data symbols. Performing a DFT on the received samples after the cyclic prefix is discarded, the periodic convolution is transformed into multiplication, as it was the case for the analog Multi Carrier receiver.1/2 or 1/4 or1/8 or 1/16 or 1/32 times of data symbol is added at beginning of the OFDM. MIMO-OFDM system can be implemented according to WiMAX Specifications.

These Specifications are given in table 4.1.

Table 4.1: WiMAX Specifications

PARAMETERS	VALUES
N_{FFT}	256
Nominal channel B.W.	2.5MHz.
No. of used sub-carriers	192
Sub carrier spacing (Δf)	11.2
Upper guard	28
Lower guard	27
N_{DC}	1(prefix 128)
$F_{S(\text{sampling frequency})}$	2.86MHz
T_b	89 micro sec.
$T_g = G.T_b$	Variable.
$T_{symbols} = T_b + T_g$	Variable.
Ratio guard time to symbol time(G)	Variable (1/4,1/8,1/16,132)

4.4 MIMO-OFDM with WiMAX Protocol using Alamouti 2 X n_R Space Time Coding

In this case, there are two antennas at the transmitter side and n_R receiving antennas at the receiver side [75]. First, consider the signal model received at a receiver side with a single receive antenna, i.e. $n_R = 1$. In this case, the received signal can be represented in the following form

$$\tilde{r} = \sqrt{\frac{P_o}{2}}\,\overline{H^{(0)}}\,x_0 + \sum_{k=1}^{K}\sqrt{\frac{P_k}{2}}\,\overline{H^{(k)}}\,x_k + n \tag{4.3}$$

where x, r and n are transmit, receive and noise vectors respectively (with zero mean and variance σ_n^2, circularly symmetric normal distributed entries), and H_k is the $n_T \; X \; n_R$ channel matrix, K is the number of interferers and P_k is the received power from the K_{th} receiver and is given by:

$$P_k = P_T\, G_K \frac{10^{\,X_k/10}}{L(d_k)} \tag{4.4}$$

here P_T is the transmit power, X_k is the log normal shadowing, $L(d_k)$ is the path loss at the distance d_k, and G_k is the aggregate antenna gain. $\overline{H^{(k)}}$ is an equivalent channel matrix given by

$$\overline{H^{(k)}} = \begin{bmatrix} h_{0,0}^{(k)} & h_{0,1}^{(k)} \\ h_{0,1}^{(k)*} & -h_{0,0}^{(k)*} \end{bmatrix} \tag{4.5}$$

We then premultiply the received vector with the transpose conjugate of the equivalent channel matrix for an MRC receiver, i.e., $w = \overline{H^{(0)}}$. Thus, we have that

$$z = w^* \tilde{y}$$

$$= \sqrt{\frac{P_o}{2}}\,\overline{H^{(0)H}}\;\overline{H^{(0)}}\,x_0 + \sum_{k=1}^{K}\sqrt{\frac{P_k}{2}}\,\overline{H^{(0)H}}\;\overline{H^{(k)}}\,x_k + \overline{H^{(0)H}}\;n \tag{4.6}$$

The SINR on the stream is given as follows

$$\gamma_s = \frac{\frac{1}{2} P_o \, (\overline{H^{(0)H}} \; \overline{H^{(0)}})ss}{\frac{1}{2} \sum_{k=1}^{K} P_k \frac{(\overline{\overline{H^{(k)}} \, \overline{H^{(0)}} H^{(0)H}} \; \overline{H^{(k)}})ss}{(\overline{H^{(0)H}} \; \overline{H^{(0)}})ss} + \sigma_n^2} \tag{4.7}$$

where $(.)ss$ denotes the s^{th} row and s^{th} column element of the matrix within the braces. Note the transmit power is shared between two antennas and hence the power is scaled by 2. The signal power and interference power are given as

$$f(.) = \frac{1}{2} (\overline{H^{(0)H}} \; \overline{H^{(0)}})ss \tag{4.8}$$

and $$g(.) = \frac{1}{2} \frac{(\overline{\overline{H^{(k)}} \, \overline{H^{(0)}} H^{(0)H}} \; \overline{H^{(k)}})ss}{(\overline{H^{(0)H}} \; \overline{H^{(0)}})ss} \tag{4.9}$$

Next the STC Alamouti scheme can be extended to any number of receive antennas, $n_R \geq 2$, by row appending (stacking) channel matrix from each receiver. Hence, now the equivalent matrix would be

$$\overline{H^{(0)}} = [\overline{H_1^{(0)}} \;\; \overline{H_2^{(0)}} \;\; \ldots\ldots \;\; \overline{H_{N_r}^{(0)}}]^T \tag{4.10}$$

Where $\overline{H_{nR}^{(0)}}$ is the equivalent Alamouti matrix to the n_r^{th} antenna.

CHAPTER 5: RESULTS AND DISCUSSIONS

In this report behavior of the MIMO-OFDM system under different environments is studied and the effects of increasing the order of the modulation on the BER performance of the system are presented. The system discussed above has been designed using the QOSTBC code structure for MIMO-OFDM system. Coherent Zero Forcing equalization is used to decode the QOSTBC coded data symbols at the receiver side. Results are shown in the form of SNR vs BER plot for different modulations and different channels. Here different antenna configurations such as 1 X 1, 2 X 2, 4 X 4, 6 X 6 and proposed 8 X 8 are used to show the advantage in term of SNR of using 8 X 8 antenna configurations over the other configurations. The analysis has been done for different wireless fading channels namely AWGN, Rayleigh and Rician channel. Results have been presented for different antenna configurations over different fading channels using different modulation levels.

The performance of MIMO-OFDM system is analyzed using two criterions namely

1. BER Analysis
2. Spectral Efficiency Analysis

5.1 BER Analysis of MIMO-OFDM system

In this section BER analysis of MIMO-OFDM system using QOSTBC code structure is done for higher order Modulations over different fading channels. First, the analysis of MIMO-OFDM system using M-PSK is presented over different fading channels and then same procedure is done for M-QAM. The fading channels used for this purpose are AWGN, Rayleigh and Rician channels.

5.1.1 M-PSK over different Fading channels

In this section the BER performance of MIMO-OFDM system is analyzed using M-PSK over different fading channels.

5.1.1.1 M-PSK over AWGN channel

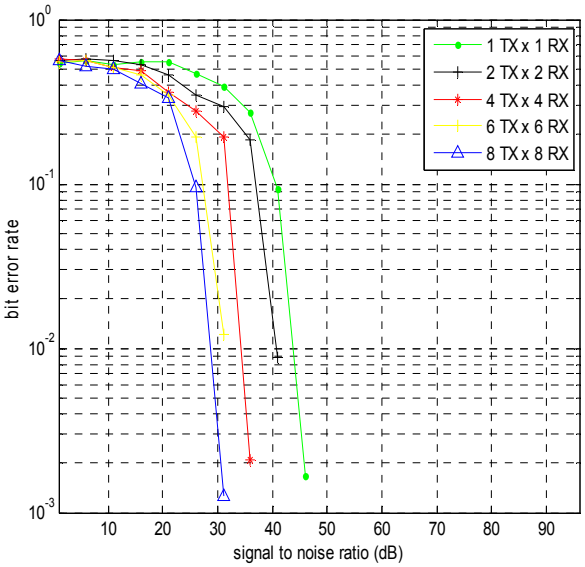

(a) 32-PSK

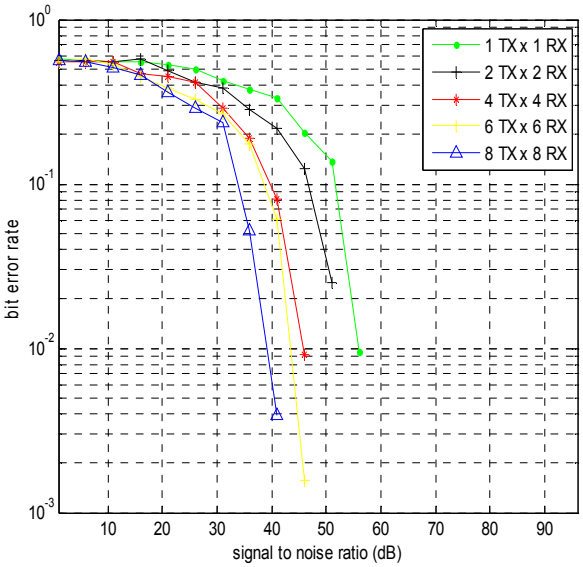

(c) 128-PSK

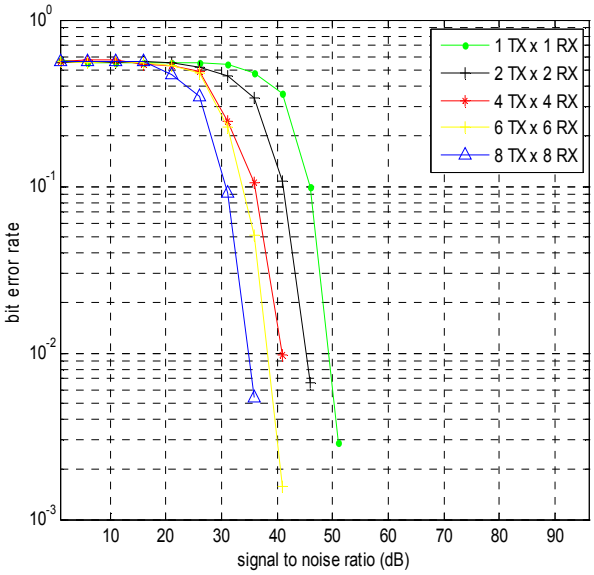

(b) 64-PSK

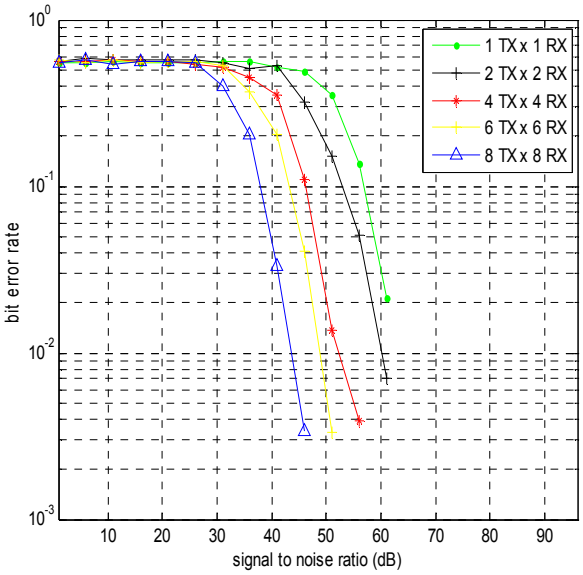

(d) 256-PSK

Figure 5.1: SNR vs BER plots for M-PSK over AWGN channel a) 32-PSK b) 64-PSK c) 128-PSK d) 256-PSK e) 512-PSK f) 1024-PSK

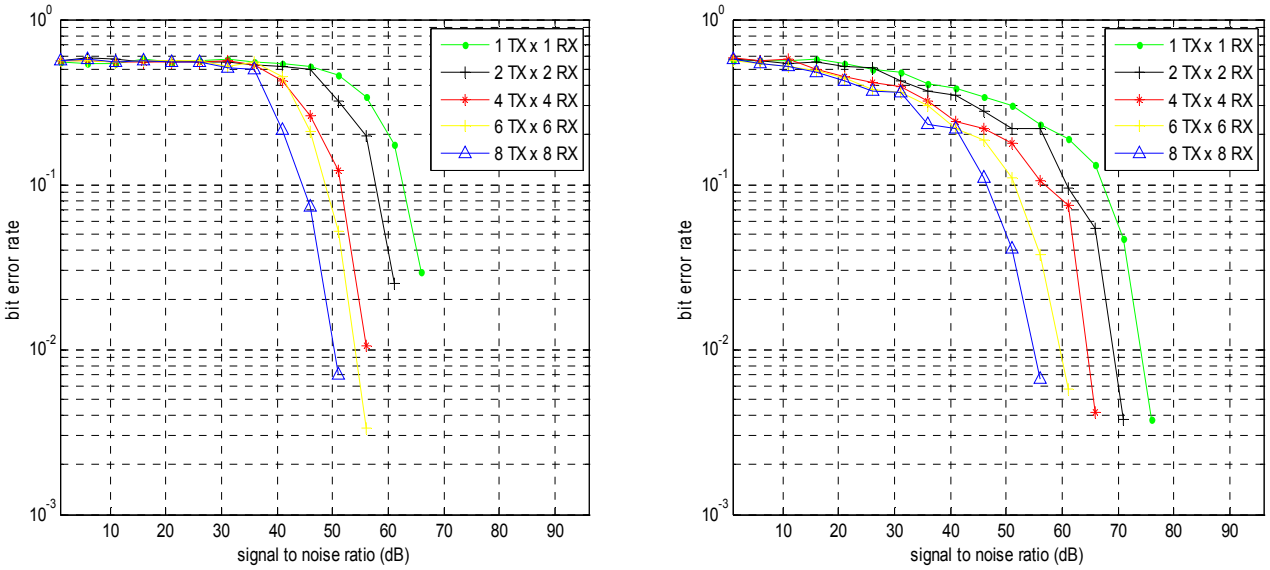

(e) 512-PSK **(f)** 1024-PSK

Figure 5.1: SNR vs BER plots for M-PSK over AWGN channel a) 32-PSK b) 64-PSK c) 128-PSK d) 256-PSK e) 512-PSK f) 1024-PSK

SNR vs BER plots for M-PSK over AWGN channel for MIMO-OFDM system employing different antenna configurations have been presented in Figure 5.1 (a) – (f). Here the graph depicts that in MIMO-OFDM system as we goes on increasing the no. of Transmitting and Receiving antennas, the BER keeps on decreasing due to space diversity and the proposed system provide better BER performance as compared to the other antenna configurations.

Table 5.1: SNR improvement for M-PSK in AWGN channel by using 8 X 8 antenna configuration over 6 X 6 antenna configuration

Different Modulation levels	SNR improvement for AWGN Channel (db)
32-PSK	2 dB
64-PSK	4 dB
128-PSK	3.5 dB
256-PSK	5 dB
512-PSK	4 dB
1024-PSK	5 dB

In table 5.1 the advantage of using higher order (8 X 8) antenna configuration over lower order (6 X 6) antenna configuration is shown in the form of SNR gain in dB for M-PSK. As, we goes

on to higher order antenna configuration the BER will keeps on decreasing. For M-PSK, with the increase in the level of the modulation the BER will also increase. In order to mitigate that effect we have to increase the SNR values for higher level modulation.

5.1.1.2 M-PSK over Rayleigh channel

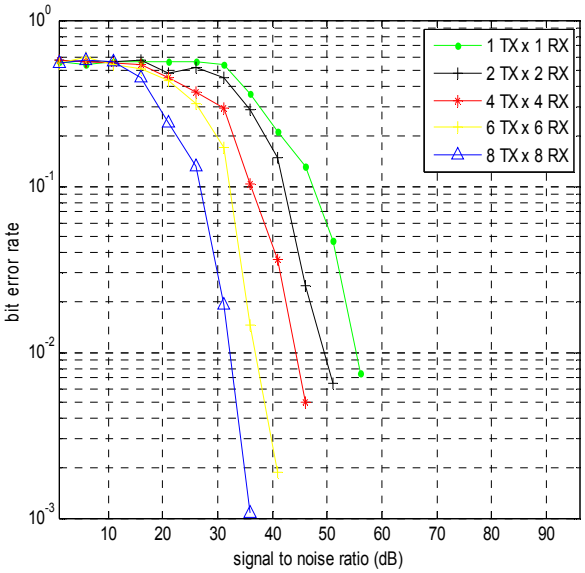

(a) 32-PSK

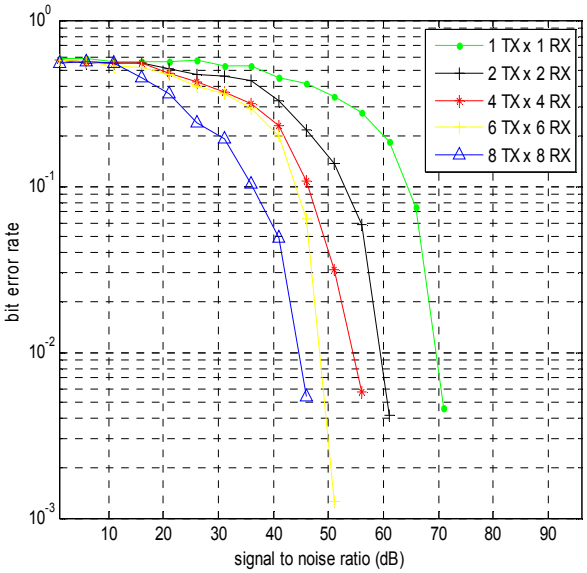

(c) 128-PSK

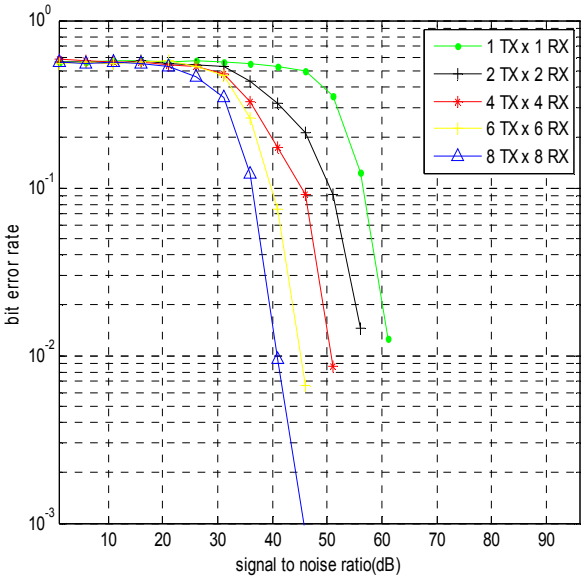

(b) 64- PSK

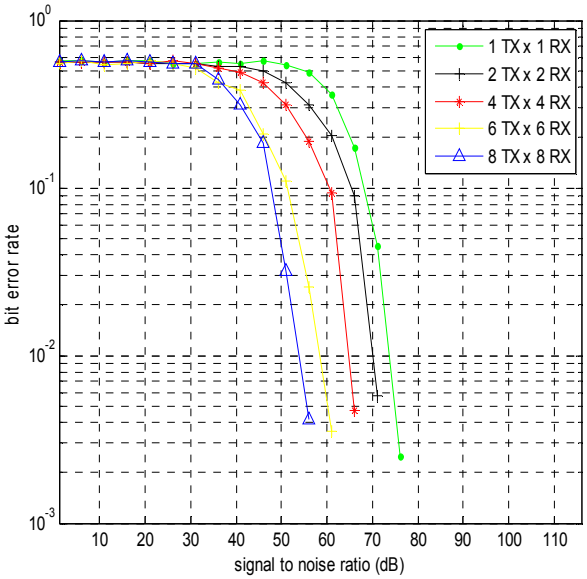

(d) 256-PSK

Figure 5.2: SNR vs BER plots for M-PSK over Rayleigh channel a) 32-PSK b) 64-PSK c) 128-PSK d) 256-PSK e) 512-PSK f) 1024-PSK

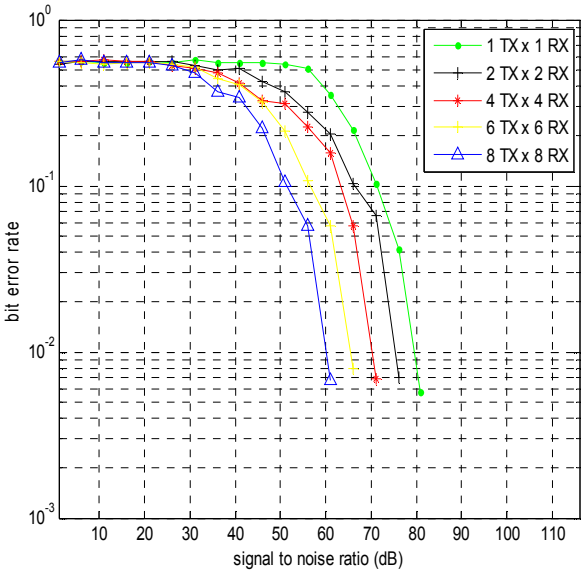

(e) 512-PSK

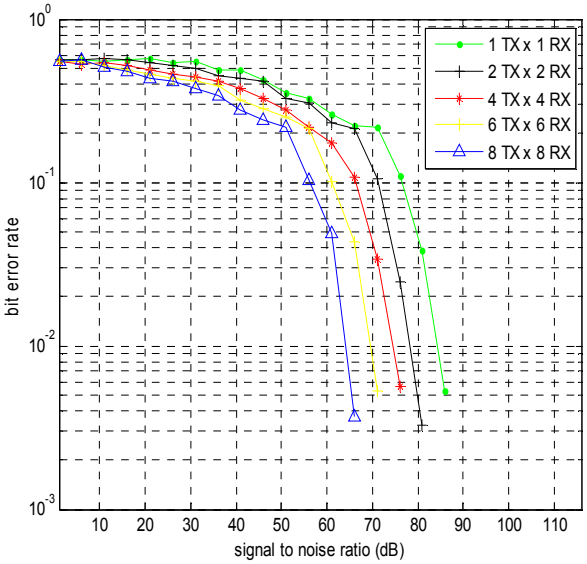

(f) 1024-PSK

Figure 5.2: SNR vs BER plots for M-PSK over Rayleigh channel a) 32-PSK b) 64-PSK c) 128-PSK d) 256-PSK e) 512-PSK f) 1024-PSK

In Figure 5.2 (a) – (f) SNR vs BER plots for M-PSK over Rayleigh channel for MIMO-OFDM system employing different antenna configurations are presented. It can be concluded from the graphs that in MIMO-OFDM system as we goes on increasing the no. of Transmitting and Receiving antennas the BER keeps on decreasing due to space diversity and the proposed system provide better BER performance as compared to the other antenna configurations. But here BER is greater than the AWGN channel.

Table 5.2: SNR improvement for M-PSK in Rayleigh channel by using 8 X 8 antenna configuration over 6 X 6 antenna configuration

Different Modulation levels	SNR improvement for Rayleigh Channel (db)
32-PSK	4.5 dB
64-PSK	4 dB
128-PSK	3.5 dB
256-PSK	4 dB
512-PSK	4.5 dB
1024-PSK	5.5 dB

The superiority of using higher order (8 X 8) antenna configuration over lower order (6 X 6) antenna configuration is shown in the form of SNR gain in dB for M-PSK over Rayleigh channel

in table 5.2. As, we goes on to higher order antenna configuration the BER will keeps on decreasing. The SNR gain varies from one modulation level to another due to random noise and fading effect.

5.1.1.3 M-PSK over Rician channel

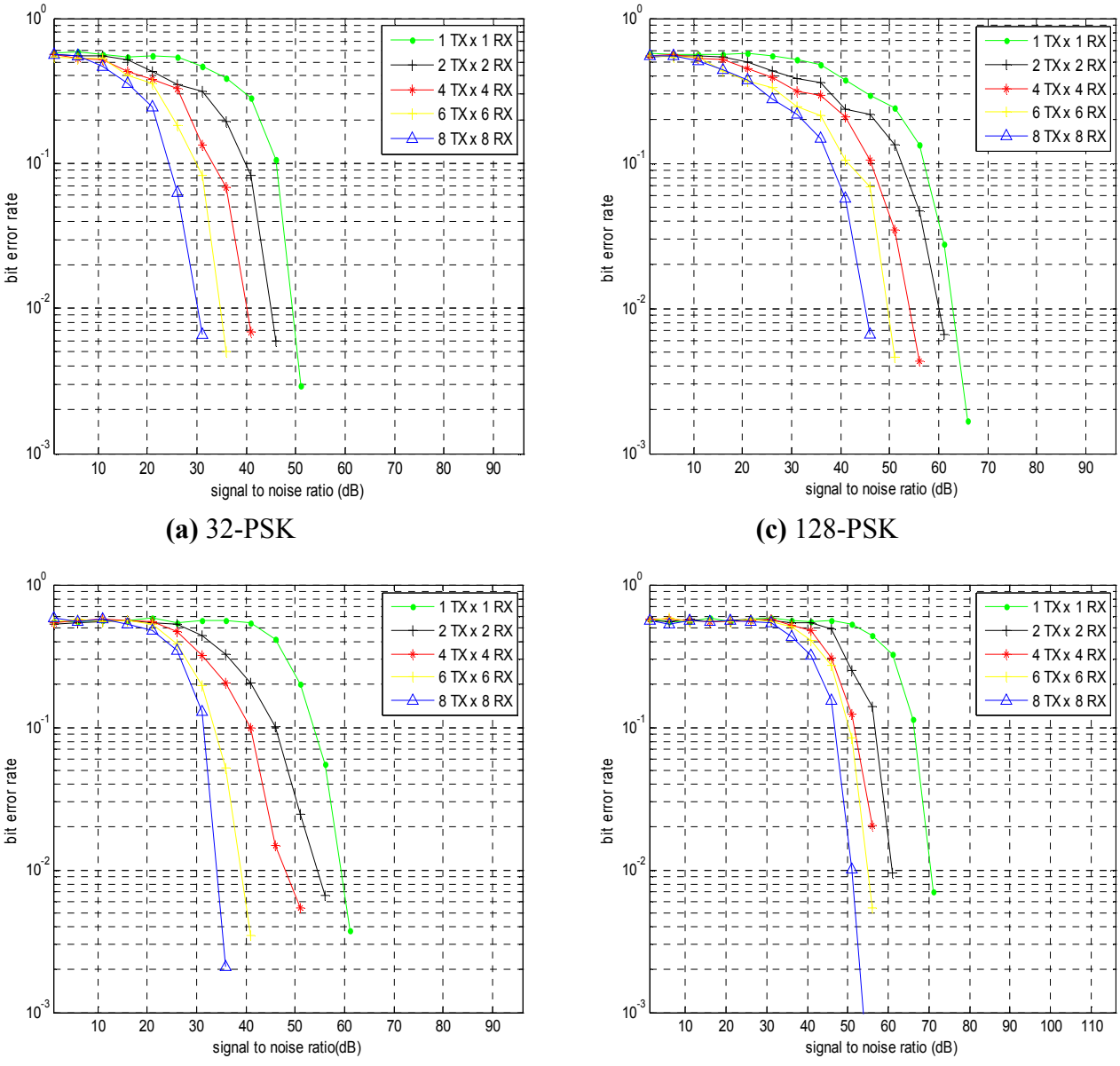

(a) 32-PSK

(c) 128-PSK

(b) 64-PSK

(d) 256-PSK

Figure 5.3: SNR vs BER plots for M-PSK over Rician channel a) 32-PSK b) 64-PSK c) 128-PSK d) 256-PSK e) 512-PSK f) 1024-PSK

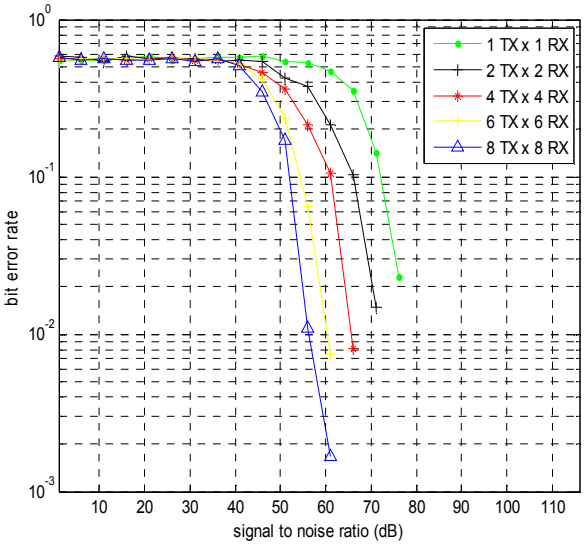

(e) 512-PSK

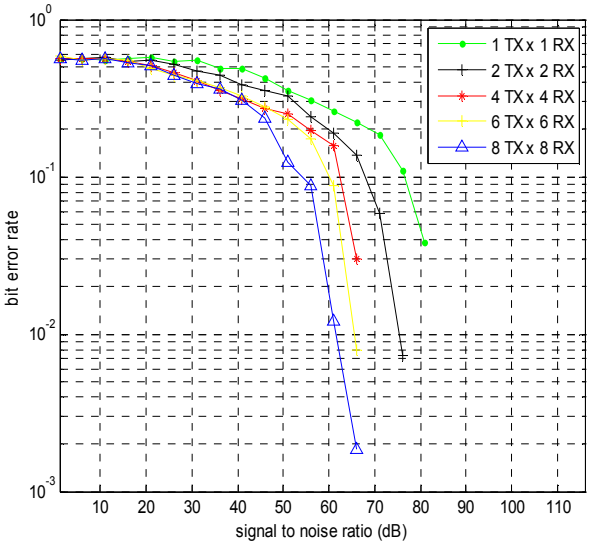

(f) 1024-PSK

Figure 5.3: SNR vs BER plots for M-PSK over Rician channel a) 32-PSK b) 64-PSK c) 128-PSK d) 256-PSK e) 512-PSK f) 1024-PSK

The performance in the form of SNR vs BER plots for M-PSK over Rician channel for MIMO-OFDM system employing different antenna configurations have been presented in Figure 5.3 (a) – (f). The graphs clearly point out the dependency of the MIMO-OFDM system on the no. of Transmitting and Receiving antennas. Here the BER keeps on decreasing due to space diversity as we goes on increasing the no. of Transmitting and Receiving antennas and the proposed system provide better BER performance as compared to the other antenna configurations.

Table 5.3: SNR improvement for M-PSK in Rician channel by using 8 X 8 antenna configuration over 6 X 6 antenna configuration

Different Modulation levels	SNR improvement for Rician Channel (db)
32-PSK	4 dB
64-PSK	4.5 dB
128-PSK	5 dB
256-PSK	3 dB
512-PSK	3.5 dB
1024-PSK	4 dB

As, we goes on to higher order antenna configuration the BER will keeps on decreasing. The SNR gain varies from one modulation level to another due to random noise and fading effect. In

table 5.3 the benefit of using higher order (8 X 8) antenna configuration over lower order (6 X 6) antenna configuration is shown in the form of SNR gain in dB for M-PSK over Rician channel.

5.1.2 M-QAM over different Fading channels

In this section the BER performance of MIMO-OFDM system is analyzed using M-QAM over different fading channels.

5.1.2.1 M-QAM over AWGN channel

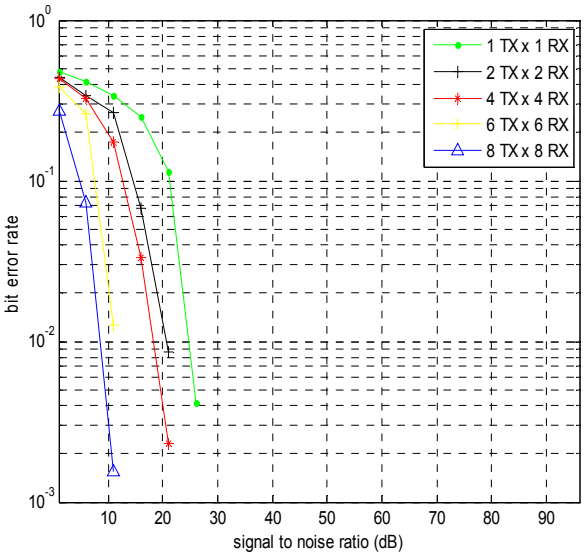

(a) 64-QAM

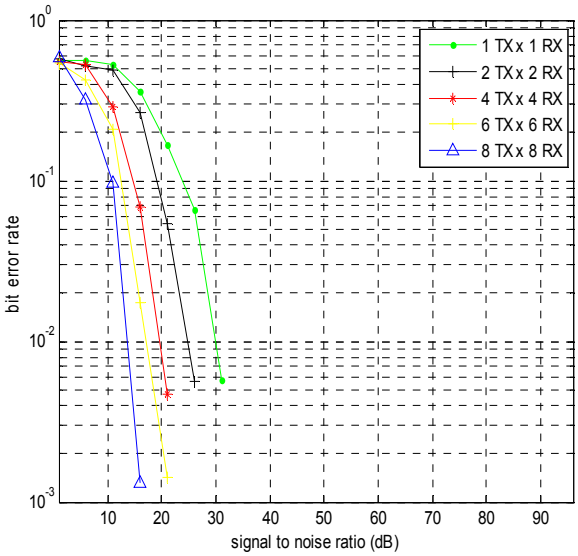

(b) 256-QAM

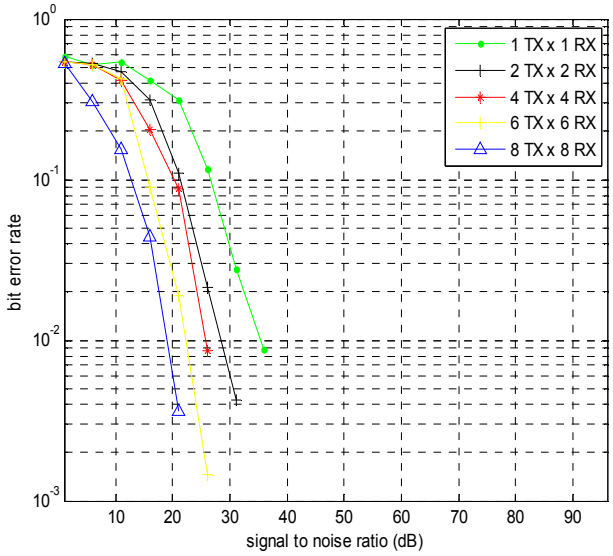

(c) 1024-QAM

Figure 5.4: SNR vs BER plots for M-QAM over AWGN channel a) 64-QAM b) 256-QAM c) 1024-QAM

For MIMO-OFDM system SNR vs BER plots using M-QAM over AWGN channel employing different antenna configurations are shown in Figure 5.4 (a) – (c). The graphs gives the clear idea that in MIMO-OFDM system as we goes on increasing the no. of Transmitting and Receiving antennas the BER keeps on decreasing due to space diversity and the proposed system provide better BER performance as compared to the other antenna configurations.

Table 5.4: SNR improvement for M-QAM in AWGN channel by using 8 X 8 antenna configuration over 6 X 6 antenna configuration

Different Modulations	SNR improvement for AWGN channel (dB)
64-QAM	2.7 dB
256-QAM	3.5 dB
1024-QAM	3.25dB

The prevalence of using higher order (8 X 8) antenna configuration over lower order (6 X 6) antenna configuration is shown in the form of SNR gain in dB for M-QAM over AWGN channel in table 5.4. As, we goes on to higher order antenna configuration the BER will keeps on decreasing

5.1.2.2 M-QAM over Rayleigh channel

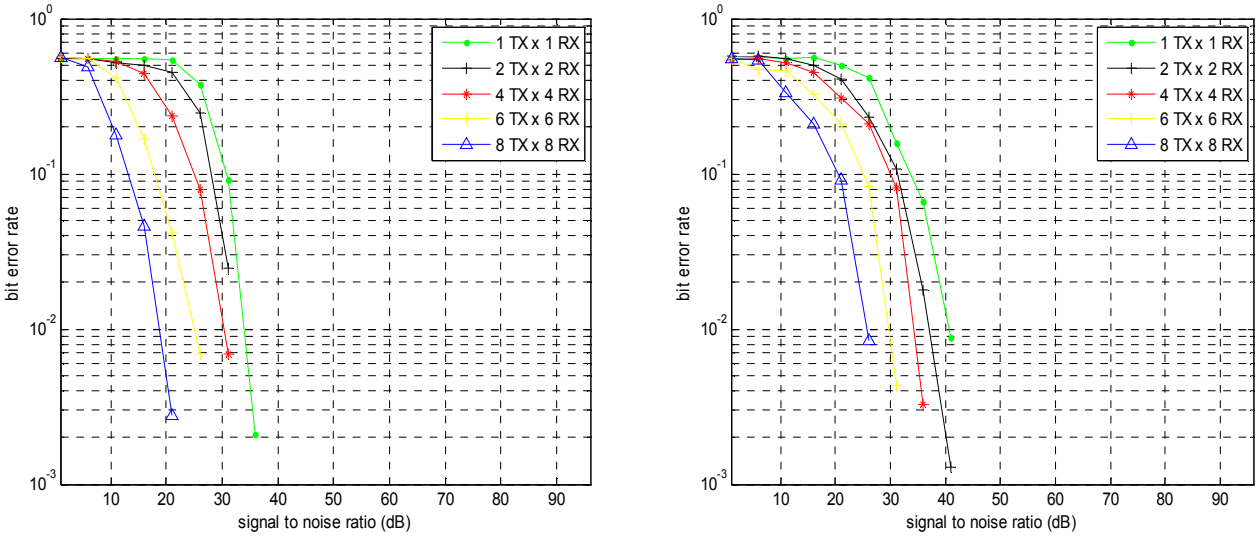

(a) 64-QAM **(b)** 256-QAM

Figure 5.5: SNR vs BER plots for M-QAM over Rayleigh channel a) 64-QAM b) 256-QAM c) 1024-QAM

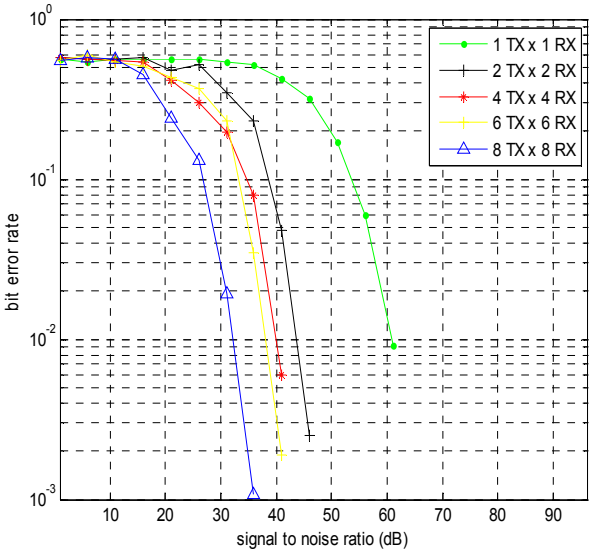

(c) 1024-QAM

Figure 5.5: SNR vs BER plots for M-QAM over Rayleigh channel a) 64-QAM b) 256-QAM c) 1024-QAM

SNR vs BER plots for M-QAM over Rayleigh channel for MIMO-OFDM system employing different antenna configurations have been presented in Figure 5.5 (a) – (c). Here the graphs indicates that in MIMO-OFDM system the BER keeps on decreasing due to space diversity, when we increases the no. of Transmitting and Receiving antennas and the proposed system provide better BER performance as compared to the other antenna configurations. Here the BER is higher than the BER for MIMO-OFDM with M-QAM in AWGN channel.

Table 5.5: SNR improvement for M-QAM in Rayleigh channel by using 8 X 8 antenna configuration over 6 X 6 antenna configuration

Different Modulations	SNR improvement for Rayleigh channel (dB)
64-QAM	5 dB
256-QAM	3.8 dB
1024-QAM	2.5 dB

The utility of using higher order (8 X 8) antenna configuration over lower order (6 X 6) antenna configuration is shown in the form of SNR gain in dB for M-QAM over Rayleigh channel in table 5.5. As, we goes on to higher order antenna configuration the BER will keeps on

decreasing. The SNR gain varies from one modulation level to another due to random noise and fading effect.

5.1.2.3 M-QAM over Rician channel

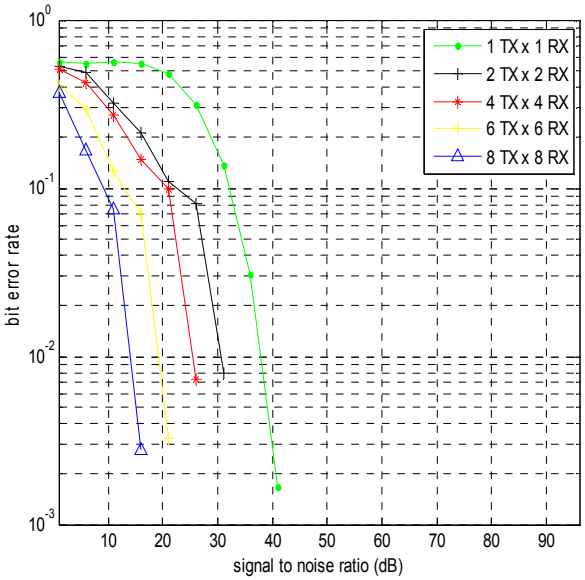

(a) 64-QAM

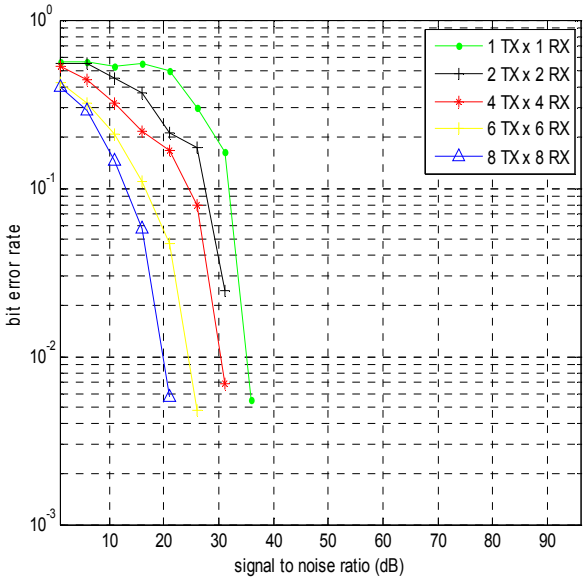

(b) 256-QAM

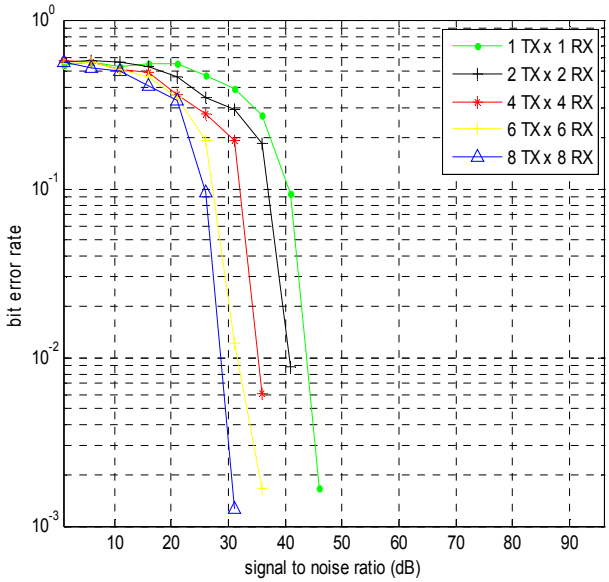

(c) 1024-QAM

Figure 5.6: SNR vs BER plots for M-QAM over Rician channel a) 64-QAM b) 256-QAM c) 1024-QAM

The performance in the form of SNR vs BER plots for M-QAM over Rician channel for MIMO-OFDM system employing different antenna configurations have been presented in Figure 5.6 (a) – (c). The graphs clearly point out the dependency of the MIMO-OFDM system on the no. of Transmitters and Recievers. Here the BER keeps on decreasing due to space diversity as we goes on increasing the no. of Transmitting and Receiving antennas and the proposed system provide better BER performance as compared to the other antenna configurations. Here the BER is less than the M-PSK modulated signal, because of the spacing of the constellation points, but it is higher than the BER for MIMO-OFDM with M-QAM in AWGN channel.

Table 5.6: SNR improvement for M-QAM in Rician channel by using 8 X 8 antenna configuration over 6 X 6 antenna configuration

Different Modulations	SNR improvement for Rician channel (dB)
64-QAM	5 dB
256-QAM	4.7 dB
1024-QAM	2.9 dB

As, we goes on to higher order antenna configuration the BER will keeps on decreasing. The SNR gain varies from one modulation level to another due to random noise and fading effect. In table 5.6 the convenience of using higher order (8 X 8) antenna configuration over lower order (6 X 6) antenna configuration is shown in the form of SNR gain in dB for M-PSK over Rician channel.

5.2 Spectral Efficiency Analysis of MIMO-OFDM system

Spectral efficiency is defined as the number of bits per second per hertz (b/s/Hz). There are only three techniques are available in literature. On the basis of these techniques there are various models in each. These are modulation techniques, coding techniques and spectrum shaping techniques. In theory, the number of modulation levels proportional relation with the spectral efficiency. But an increase in modulation result the higher precision is required at the demodulator to detect the phase and frequency. Which require the higher S/N ratio for same BER. Another way to achieve spectral efficiency is the FEC coding

In this section Spectral Efficiency analysis of MIMO-OFDM system using QOSTBC code structure is done for higher order Modulations over different fading channels. First, the analysis of MIMO-OFDM system using M-PSK is presented over different fading channels and then same procedure is done for M-QAM. The fading chanels used for this purpose are AWGN, Rayleigh and Rician channels.

5.2.1 M-PSK over different Fading channels

In this section the Spectral Efficiency performance of MIMO-OFDM system is analyzed using M-PSK over different fading channels. Fading channels used here are AWGN, Rayleigh and Rician Fading channels. The results are provided in the formof SNR vs BER plots for different antenna configurations like 1 X 1,2 X 2, 4 X 4, 6 X 6 and 8 X 8.

5.2.1.1 M-PSK over AWGN channel

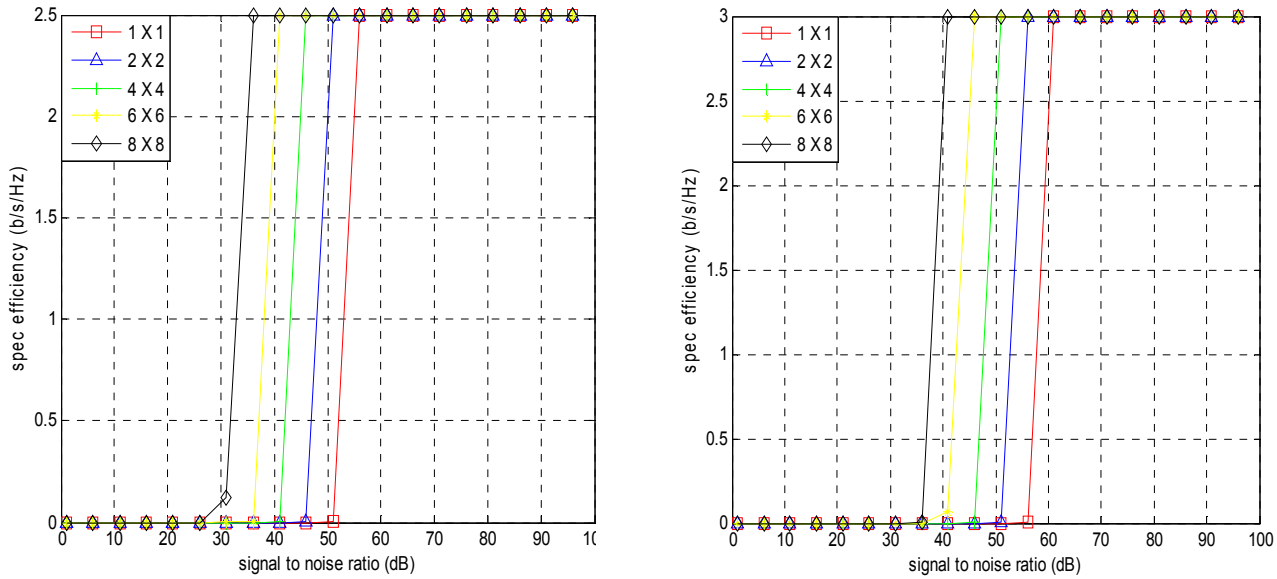

(a) 32-PSK **(b)** 64-PSK

Figure 5.7: Spectral Efficiency plots for M-PSK over AWGN channel a) 32-PSK b) 64-PSK c) 128-PSK d) 256-PSK e) 512-PSK f) 1024-PSK

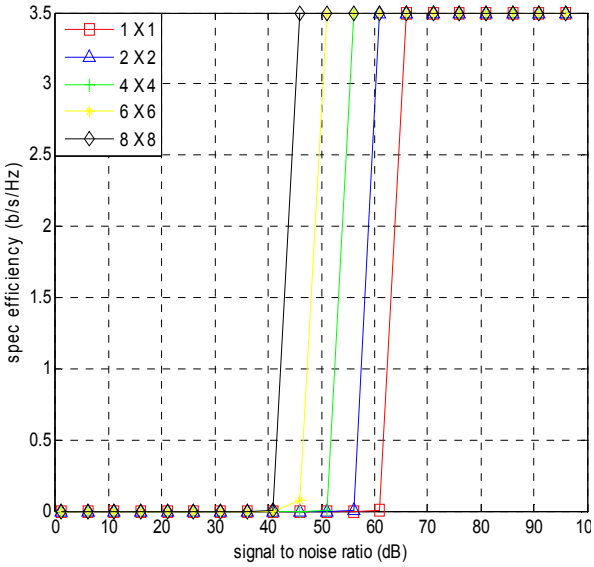

(c) 128-PSK

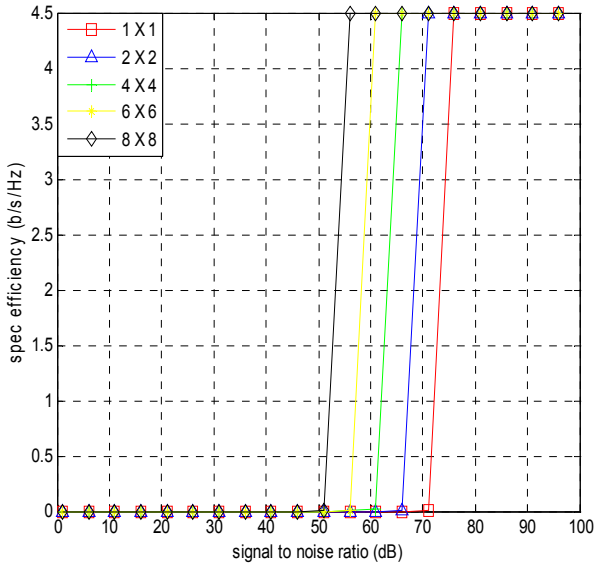

(e) 512-PSK

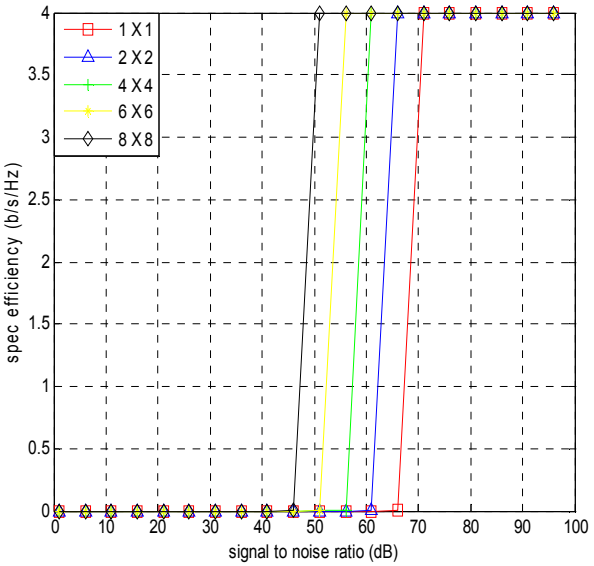

(d) 256-PSK

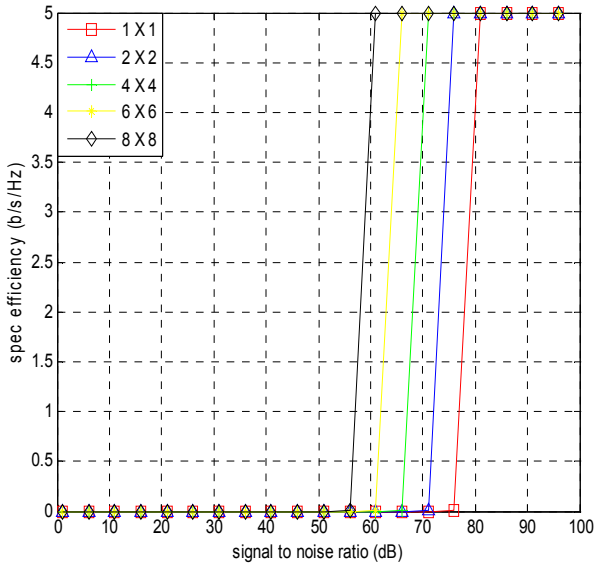

(f) 1024-PSK

Figure 5.7: Spectral Efficiency plots for M-PSK over AWGN channel a) 32-PSK b) 64-PSK c) 128-PSK d) 256-PSK e) 512-PSK f) 1024-PSK

Spectral efficiency plots for M-PSK over AWGN channel for MIMO-OFDM system employing different antenna configurations have been presented in Figure 5.7 (a) – (f). Here the graph depicts that in MIMO-OFDM system as we goes on increasing the no. of Transmitting and Receiving antennas the Spectral efficiency keeps on increasing due to space diversity and the proposed system provide better performance as compared to the other antenna configurations.

5.2.1.2 M-PSK over Rayleigh channel

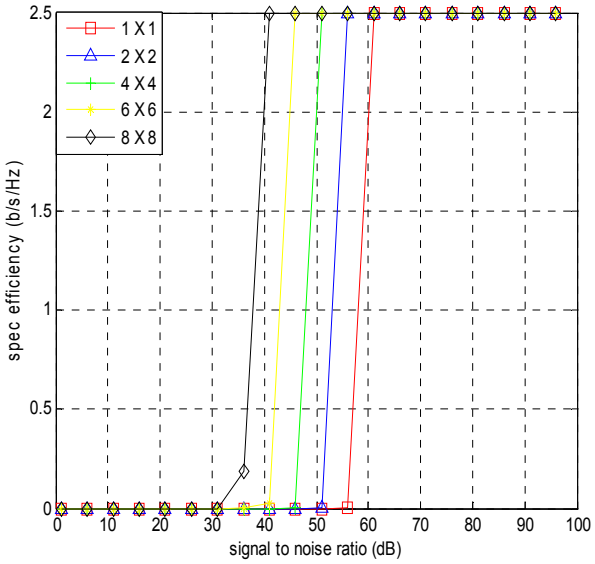

(a) 32-PSK

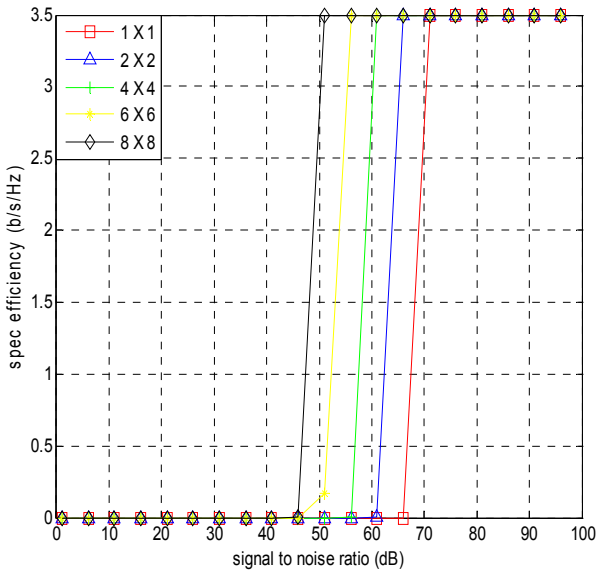

(c) 128-PSK

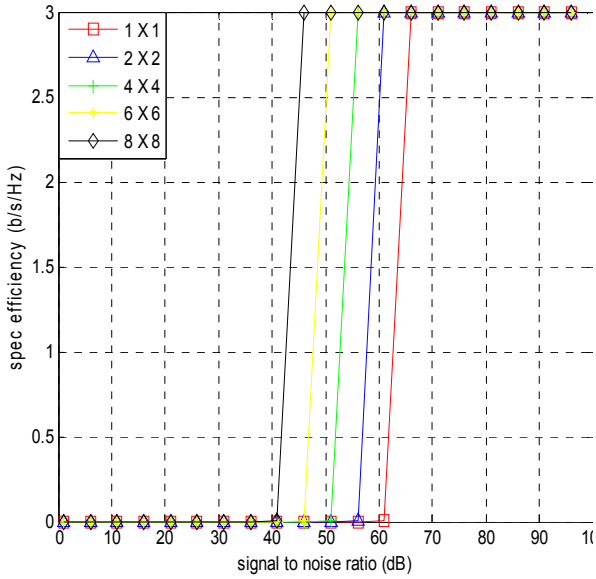

(b) 64-PSK

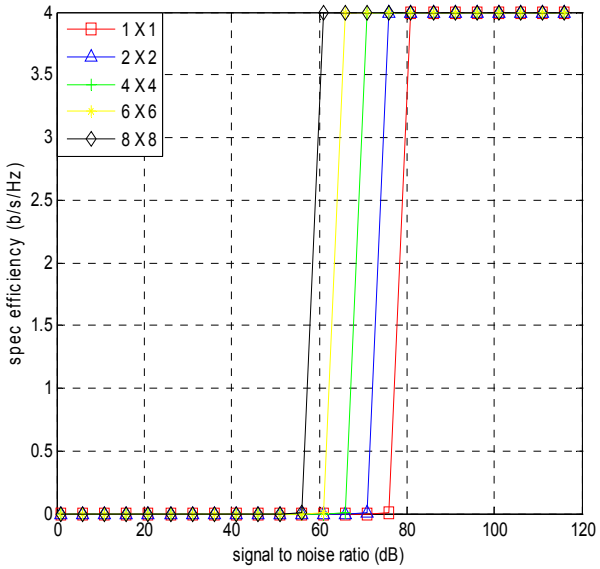

(d) 256-PSK

Figure 5.8: Spectral Efficiency plots for M-PSK over Rayleigh channel a) 32-PSK b) 64-PSK c) 128-PSK d) 256-PSK e) 512-PSK f) 1024-PSK

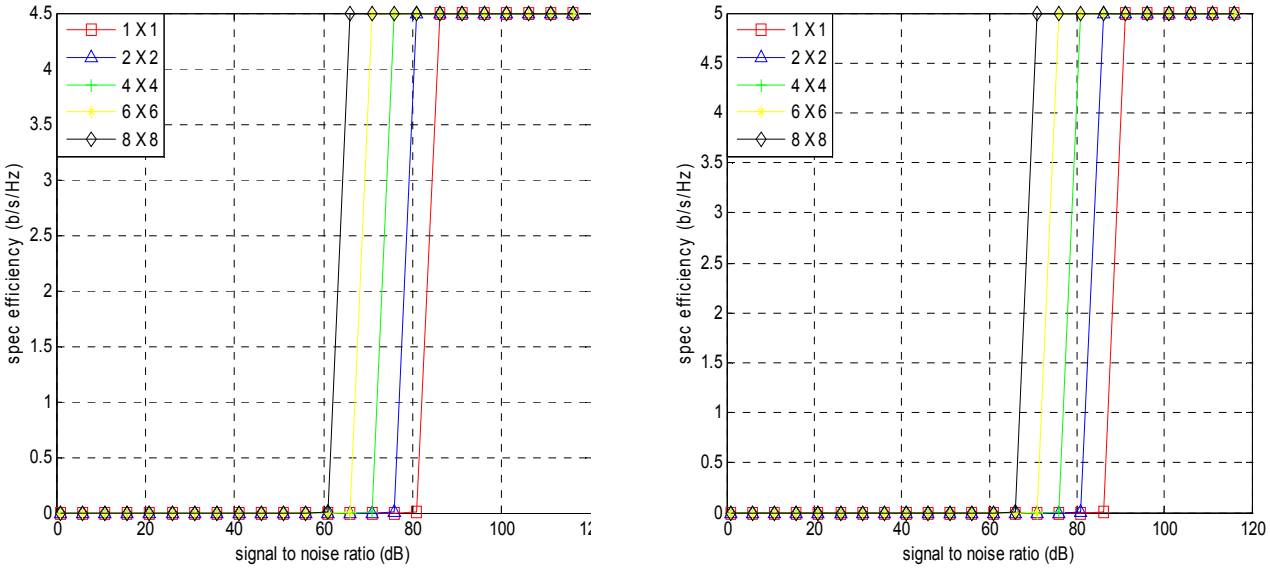

(e) 512-PSK **(f)** 1024-PSK

Figure 5.8: Spectral Efficiency plots for M-PSK over Rayleigh channel a) 32-PSK b) 64-PSK c) 128-PSK d) 256-PSK e) 512-PSK f) 1024-PSK

In figure 5.8 (a) – (f) spectral efficiency plots for M-PSK over Rayleigh channel for MIMO-OFDM system employing different antenna configurations have been presented. It can be concluded from the graphs that in MIMO-OFDM system as we goes on increasing the no. of Transmitting and Receiving antennas the spectral efficiency keeps on increasing due to space diversity and the proposed system provide better performance as compared to the other antenna configurations.

5.2.1.3 M-PSK over Rician channel

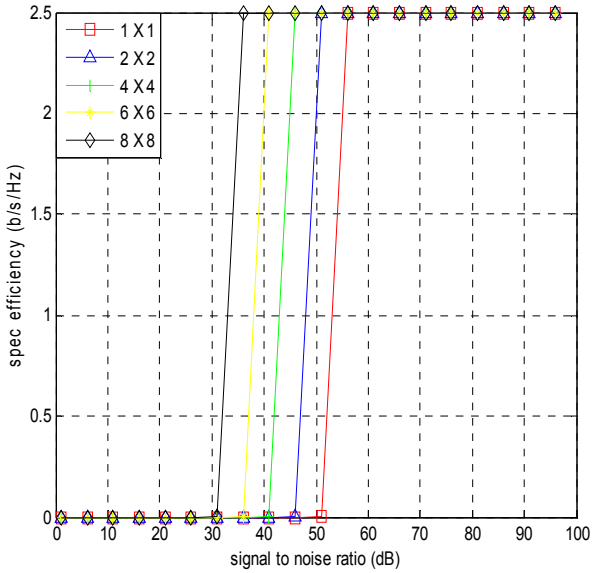

(a) 32-PSK

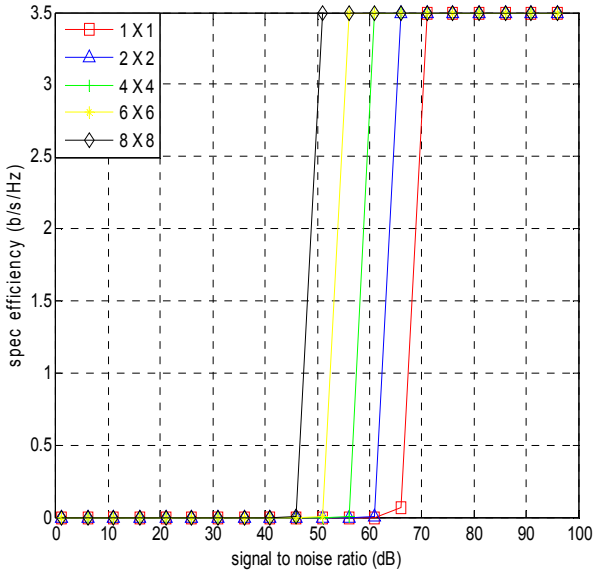

(c) 128-PSK

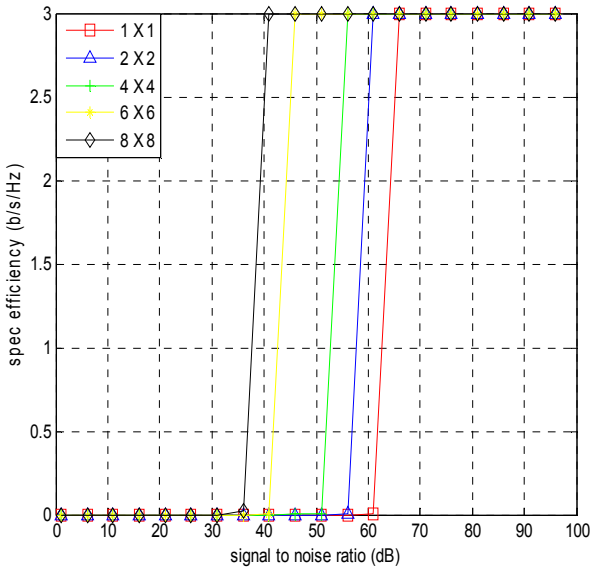

(b) 64-PSK

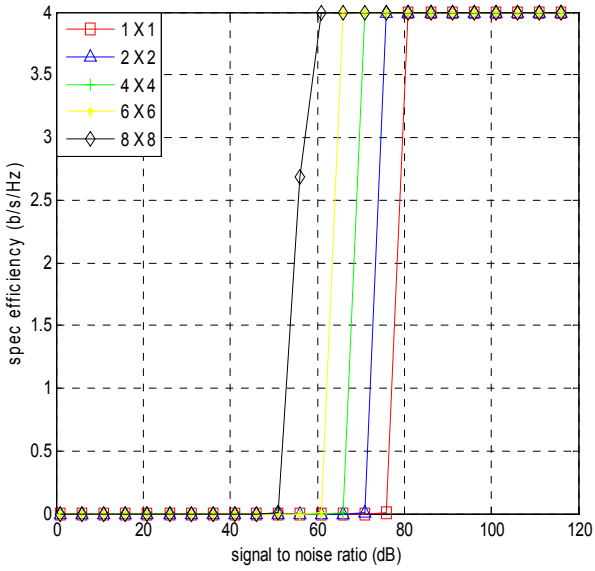

(d) 256-PSK

Figure 5.9: Spectral Efficiency plots for M-PSK over Rician channel a) 32-PSK b) 64-PSK c) 128-PSK d) 256-PSK e) 512-PSK f) 1024-PSK

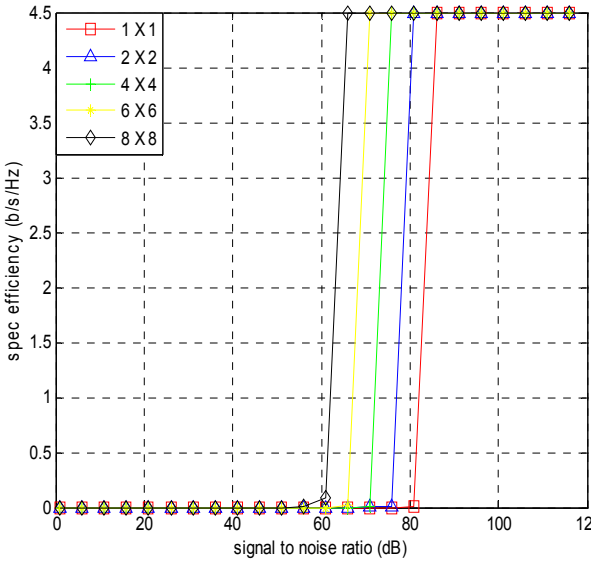

(e) 512-PSK

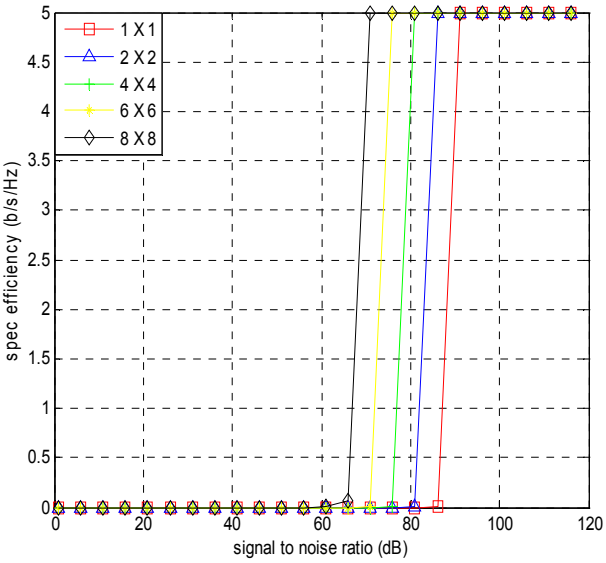

(e) 1024-PSK

Figure 5.9: Spectral Efficiency plots for M-PSK over Rician channel a) 32-PSK b) 64-PSK c) 128-PSK d) 256-PSK e) 512-PSK f) 1024-PSK

For MIMO-OFDM system Spectral Efficiency plots using M-PSK over Rician channel employing different antenna configurations are shown in Figure 5.9 (a) – (f). The graphs gives the clear idea that in MIMO-OFDM system as we goes on increasing the no. of Transmitting and Receiving antennas the Spectral Efficiency keeps on increasing due to space diversity and the proposed system provide better BER performance as compared to the other antenna configurations.

5.2.2 M-QAM over different Fading channels

In this section the Spectral Efficiency performance of MIMO-OFDM system is analyzed using M-QAM over different fading channels. Fading channels used here are AWGN, Rayleigh and Rician Fading channels. The results are provided in the formof SNR vs BER plots for different antenna configurations like 1 X 1,2 X 2, 4 X 4, 6 X 6 and 8 X 8.

5.2.2.1 M-QAM over AWGN channel

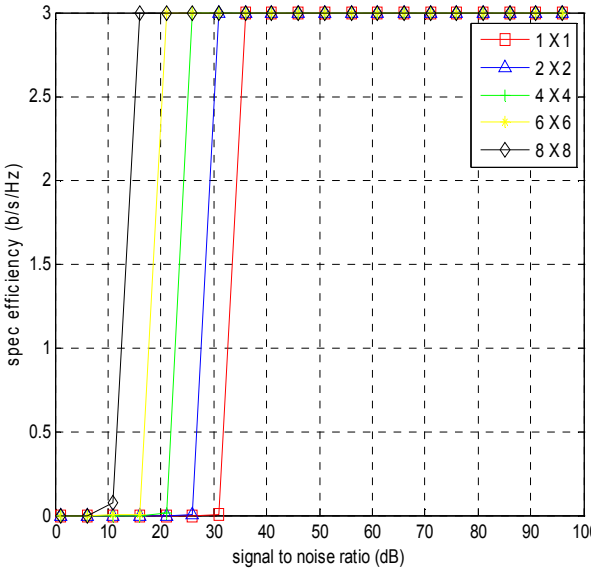

(a) 64-QAM

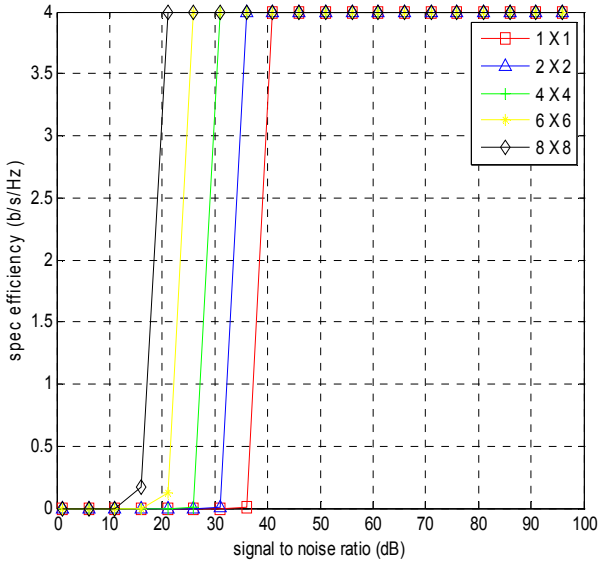

(b) 256-QAM

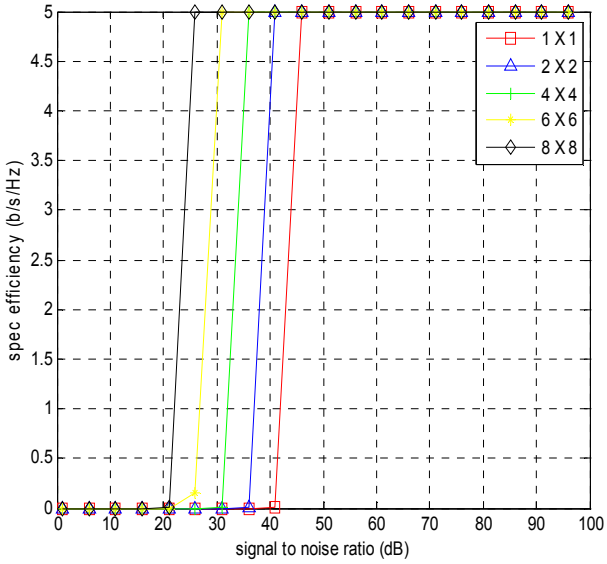

(c) 1024-QAM

Figure 5.10: Spectral Efficiency plots for M-QAM over AWGN channel a) 64-QAM b) 256-QAM c) 1024-QAM

The performance in the form of Spectral Efficiency plots for M-QAM over AWGN channel for MIMO-OFDM system employing different antenna configurations have been presented in Figure 5.10 (a) – (c). The graphs clearly point out the dependency of the MIMO-OFDM system on the no. of Transmitting and Receiving antennas. Here the Spectral Efficiency keeps on increasing

due to space diversity as we goes on increasing the no. of Transmitters and Receivers and the proposed system provide better BER performance as compared to the other antenna configurations.

5.2.2.2 M-QAM over Rayleigh channel

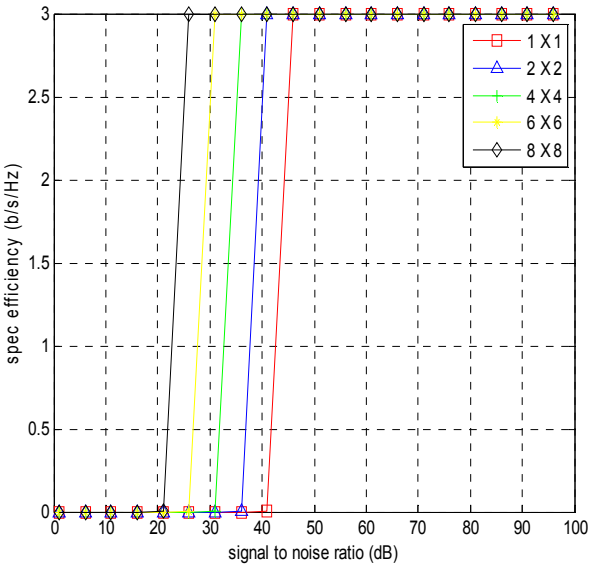

(a) 64-QAM

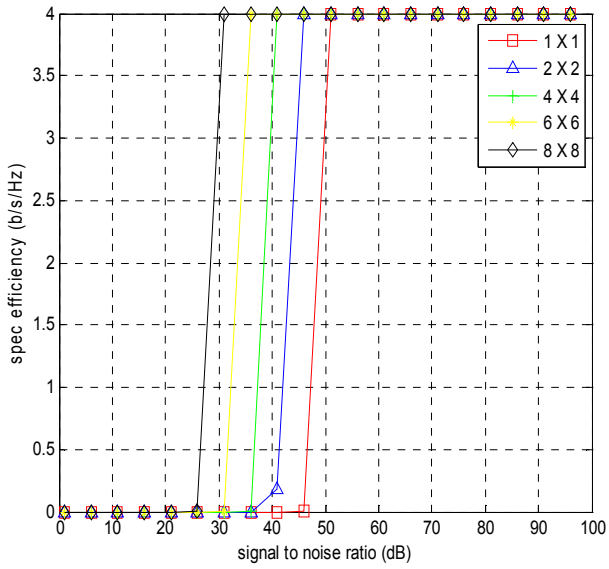

(b) 256-QAM

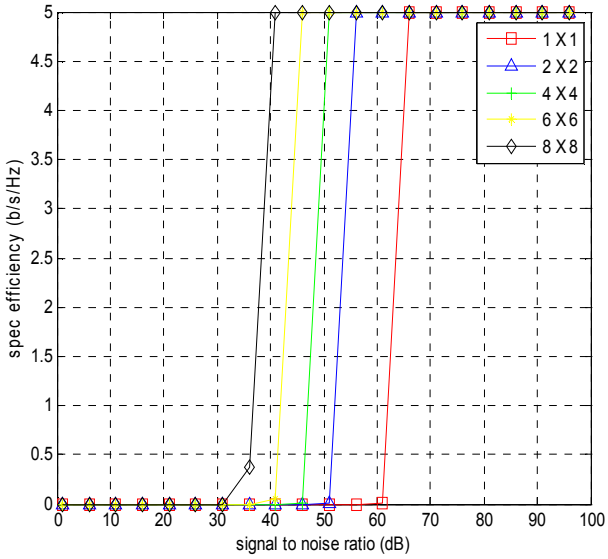

(c) 1024-QAM

Figure 5.11: Spectral Efficiency plots for M-QAM over Rayleigh channel a) 64-QAM b) 256-QAM c) 1024-QAM

Spectral Efficiency plots for M-QAM over Rayleigh channel for MIMO-OFDM system employing different antenna configurations have been presented in Figure 5.11 (a) – (c). Here the graphs indicates that in MIMO-OFDM system the Spectral Efficiency keeps on increasing due to space diversity, when we increases the no. of Transmitting and Receiving antennas and the proposed system provide better BER performance as compared to the other antenna configurations.

5.2.2.3 M-QAM over Rician channel

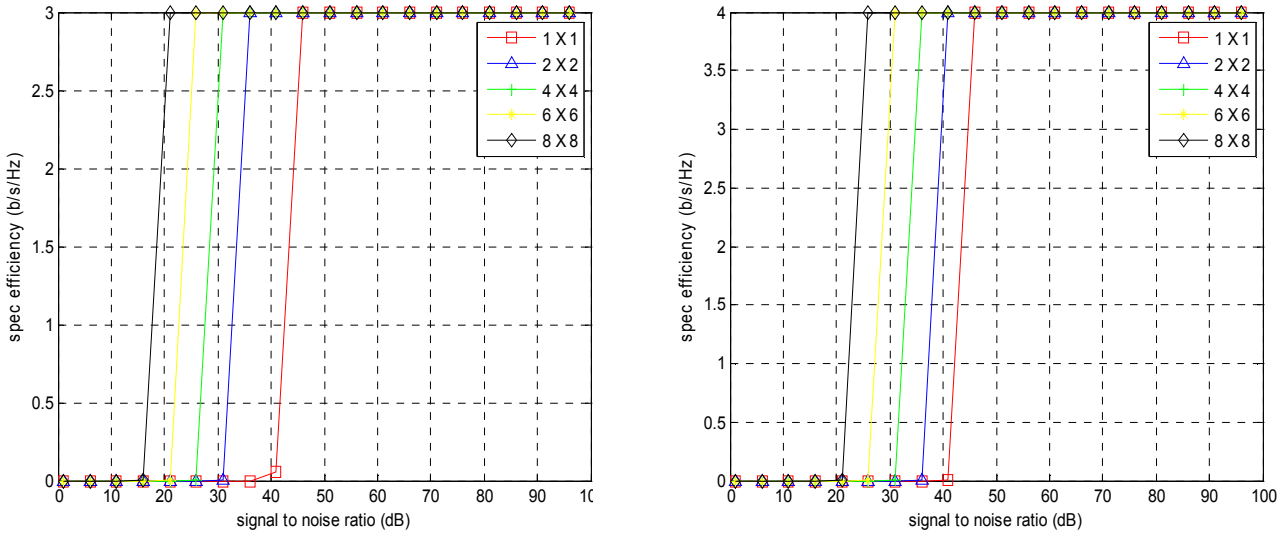

(a) 64-QAM **(b)** 256-QAM

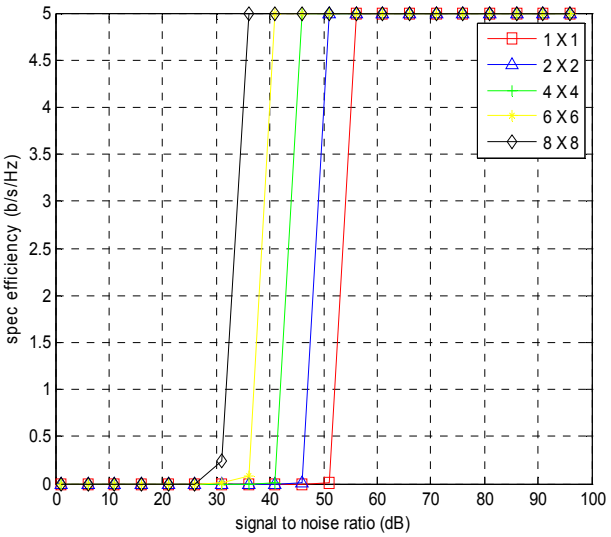

(d) 1024-QAM

Figure 5.12: Spectral Efficiency plots for M-QAM over Rician channel a) 64-QAM b) 256-QAM c) 1024-QAM

In Figure 5.12 (a) - (c) Spectral Efficiency plots for M-QAM over Rician channel for MIMO-OFDM system employing different antenna configurations are shown. It can be concluded from the graphs that in MIMO-OFDM system as we goes on increasing the no. of Transmitting and Receiving antennas the Spectral Efficiency keeps on increasing due to space diversity and the proposed system provide better Spectral Efficiency performance as compared to the other antenna configurations.

5.3 Analysis of MIMO-OFDM System with Standard WiMAX Protocol

The MIMO-OFDM system with WiMAX PROTOCOL is implemented according to the table 4.1. Then, the data output of the down link is transmitted using the alamouti space time coding using 2 transmitting antennas. At, the receiver side the input data is detected using the Zero Forcing Algorithm. The analysis is done on the basis of SNR vs BER graph for AWGN and Rayleigh channels.

5.3.1 BER Analysis for AWGN channel

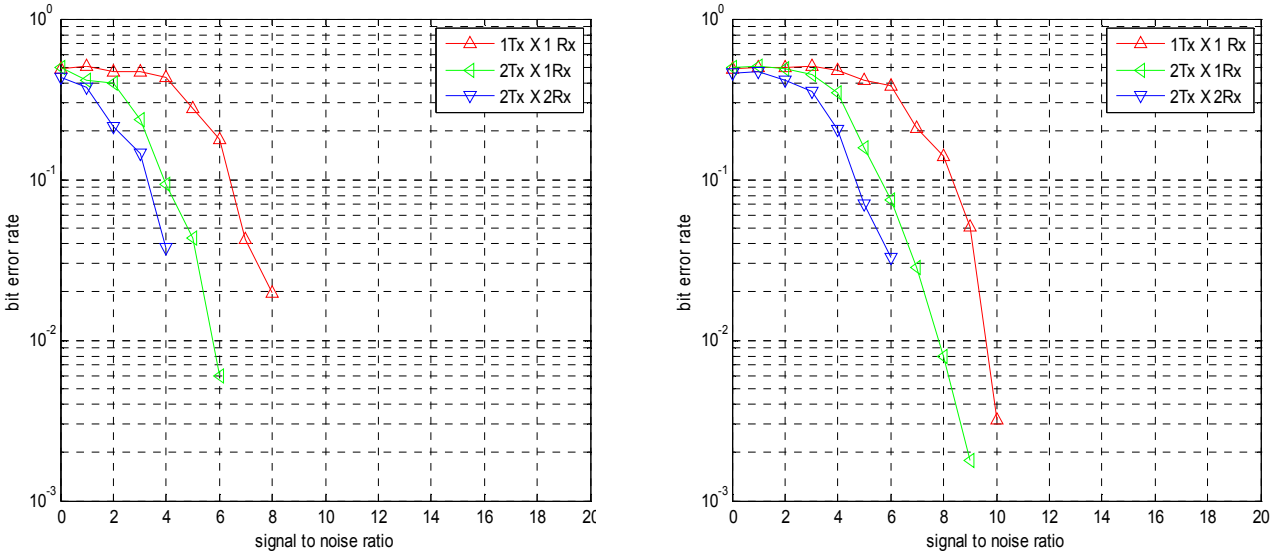

(a) 1/2 code rate **(b)** 3/4 code rate

Figure 5.13: SNR vs BER plots for QPSK with different code rate for AWGN channel employing MIMO-OFDM in WiMAX Physical Layer a) 1/2 code rate b) 3/4 code rate

Figure 5.13 (a) - (b) clearly shows the dependency of BER on the no. of transmitting and receiving antennas. As we goes on increasing the no. of transmitting and receiving antennas the BER will also keeps on decreasing due to space diversity. Table 5.7 shows the comparison between QPSK with code rate of 1/2 and QPSK with code rate of 3/4 over AWGN channel on the bases of SNR values for different antenna configuration. It clear from the table that as we goes on increasing the no. of antennas BER will keeps on decreasing and will become zero at higher SNR values.

Table 5.7: Comparison of QPSK with different code rates over AWGN channel using different antenna configurations

QPSK with different code rate oven AWGN channel	SNR value for 1 X 1 Antennas where BER is Zero	SNR value for 2 X 1 Antennas where BER is Zero	SNR value for 2 X 2 Antennas where BER is Zero
1/2 code rate	8	6	4
3/4 code rate	10	8	6

5.3.2 BER Analysis for Rayleigh channel

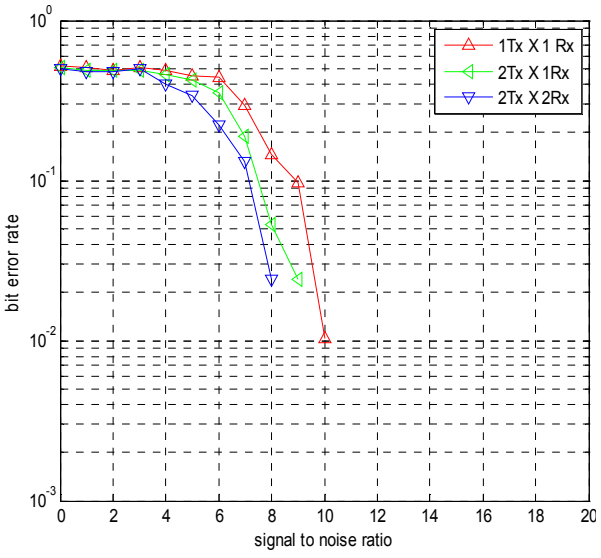

a) 1/2 code rate

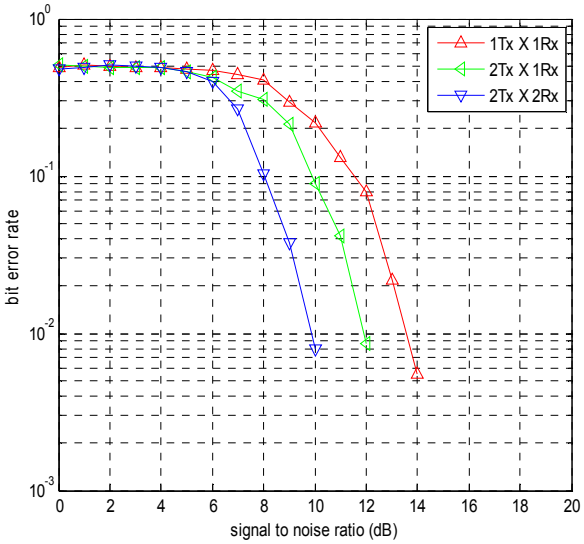

b) 3/4 code rate

Figure 5.14: SNR vs BER plots for QPSK with different code rate for Rayleigh channel employing MIMO-OFDM in WiMAX Physical Layer a) 1/2 code rate b) 3/4 code rate

The effect of increasing the on the no. of transmitting and receiving antennas on the BER is shown on Figure 5.14 (a) – (b) for QPSK over Rayleigh channel. As we goes on increasing the no. of transmitting and receiving antennas the BER will also keeps on decreasing due o space diversity. Table 5.8 shows the comparison between QPSK with code rate of 1/2 and QPSK with code rate of 3/4 over Rayleigh channel on the bases of SNR values for different antenna configuration. It clear from the table that as we goes on increasing the no. of antennas BER will keeps on decreasing and will become zero at higher SNR values.

Table 5.8: Comparison of QPSK with different code rates over Rayleigh channel using different antenna configurations

QPSK with different code rate oven Rayleigh channel	SNR value for 1 X 1 Antennas where BER is Zero	SNR value for 2 X 1 Antennas where BER is Zero	SNR value for 2 X 2 Antennas where BER is Zero
1/2 code rate	10	9.6	8
3/4 code rate	14	12	10

5.3.3 Spectral Efficiency Analysis for AWGN channel

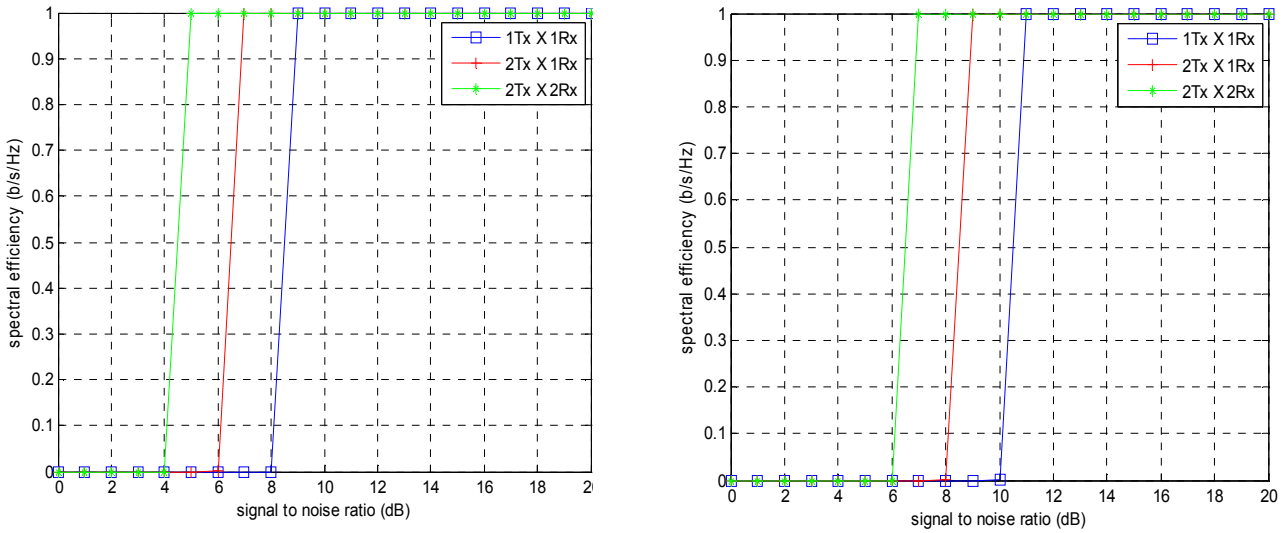

a) 1/2 code

b) 3/4 code rate

Figure 5.15: Spectral Efficiency plots for QPSK with different code rate for AWGN channel employing MIMO-OFDM in WiMAX Physical Layer a) 1/2 code rate b) 3/4 code rate

Figure 5.15 (a) – (b) clearly shows the dependency of Spectral Efficiency on the no. of transmitting and receiving antennas. As we goes on increasing the no. of transmitting and receiving antennas the Spectral Efficiency will also keeps on increasing due to space diversity.

5.3.4 Spectral Efficiency Analysis for Rayleigh channel

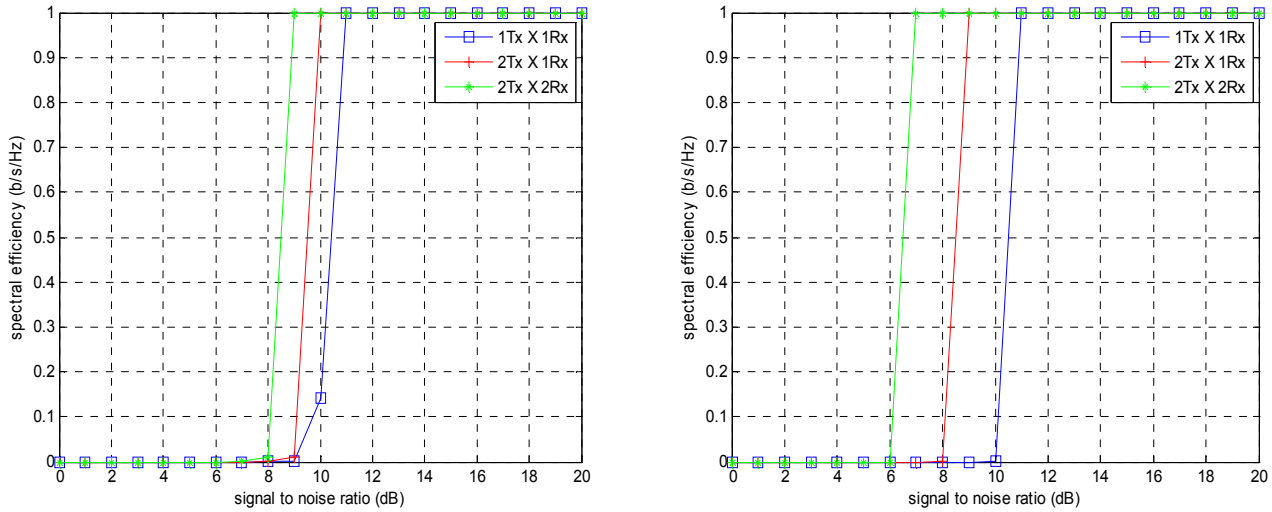

a) 1/2 code rate **b)** 3/4 code rate

Figure 5.16: Spectral Efficiency plots for QPSK with different code rate for Rayleigh channel employing MIMO-OFDM in WiMAX Physical Layer a) 1/2 code rate b) 3/4 code rate

The effect of increasing the on the no. of transmitting and receiving antennas on the Spectral Efficiency is shown on Figure 5.16 a) – b) for QPSK over Rayleigh channel. As we goes on increasing the no. of transmitting and receiving antennas the Spectral Efficiency will also keeps on increasing due o space diversity.

CHAPTER 6: CONCLUSION & FUTURE SCOPE

6.1 Conclusion

In the present work, an idea about the performance of the MIMO-OFDM systems at higher modulation levels and for different antenna configurations is presented. Performance of MIMO-OFDM system is analyzed under different fading channels. MIMO-OFDM system can be implemented using higher order modulations to achieve large data capacity. But there is a problem of BER (bit error rate) which increases as the order of the modulation increases. Because on increasing the order of modulation the decision region for the demodulator in the constellation diagram also decreases, as a result of this the demodulator will produce erroneous results at its output. The channel will distort the signal more severely at lower values of SNR (signal to noise ratio). These distortions will cause the shifting of the constellation points of the signal and this will cause the demodulator to produce the degraded results at its output. But as SNR is increased the effect of the distortions introduced by the channel will also goes on decreasing, as a result of this the BER will also decreases. In this way large data capacity can be achieved over the existing channels by using higher order modulations, the only thing that should be kept in mind is the extent to which we can increase the values of the SNR. Higher the SNR higher will be the data capacity.

The motive of using high order antenna configuration (8 X 8) is to increase the space diversity, which will further decrease the BER at given SNR as compared to lower order Antenna configurations namely 1 X 1, 2 X 2, 4 X 4 and 6 X 6. By doing so, even higher data capacity at any given SNR can be achieved. The proposed MIMO-OFDM system with 8 X 8 antenna configuration provides better SNR gain of 3-5 dB due to increased space diversity as compared to the MIMO-OFDM system with 6 X 6 antenna configuration at a BER of 10^{-2}.

On the basis of above parameters Spectral efficiency analysis is the second goal of the present work. Results shows that on increasing the no. of transmitting antennas and receiving antennas there is an improvement in the spectral efficiency also.

MIMO-OFDM system is also implemented with WiMAX Protocol using Alamouti 2 X N_R Space Time Coding. The system is tested under AWGN and Rayleigh channel environments.

The BER will decrease on increasing the no. of Transmitters or Receivers due to space diversity. There is a gain of approximately 2 dB by increasing the no. of transmitters or receivers. Same procedure is done for analyzing the spectral efficiency of the MIMO-OFDM system implemented with WiMAX Protocol. The results have shown that there is an improvement in spectral efficiency as the no. of transmitting and receiving antennas increases.

6.2 Future Scope

Further this work can be extended to increase the performance of the MIMO-OFDM system by using the other channel encoder types and other variants of the convolutional encoder (2/3, 3/4). Also there is a chance to implement the MIMO-OFDM system by using different Modulation types. The space diversity can also be increased by using more no. of transmitting and receiving antennas i.e. 12 X 12, 16 X 16 etc.

REFERENCES

[1] L. J. Cimini, "Analysis and simulation of a digital mobile channel using orthogonal frequency division multiplexing", IEEE Transaction on Communications, Vol. 33, Issue 7, pp. 665–675, July 1985.

[2] Part 11: Wireless LAN Medium Access Control (MAC) and Physical Layer (PHY) Specifications: High-Speed Physical Layer in the 5 GHz Band, IEEE Standard 802.11a-1999.

[3] Roger B. Marks, Ken Stanwood and Chang IEEE Standard for Local and Metropolitan Area Networks Part16: Air Interface for Fixed Broadband Wireless Access Systems", *IEEE 802.16-2004*, 1 October, 2004

[4] S. Alamouti, "A simple transmit diversity technique for wireless communications", IEEE Journal on Selected Areas of Communication, Vol. 16, pp. 1451–1458, Oct. 1998.

[5] V. Tarokh, H. Jafarkhani and A. R. Calderbank, "Space–time block codes from orthogonal designs", IEEE Transactions on Information Theory, Vol. 45, pp. 1456–1467, July 1999.

[6] G. Ganesan and P. Stoica. 2001. "Space-time block codes: a maximum SNR approach", IEEE Transactions on Information Theory, Vol. 47, Issue 4, May 2001, pp. 1650–1656.

[7] P. W. Wolniansky, G. J. Foschini, G. D. Golden and R. A. Valenzuela, "V-Blast: An architecture for realizing very high data rates over the rich-scattering channel", International Symposium on Signals, Systems and Electronics, pp. 295–300, 1998.

[8] J. Ha, A. N. Mody, J. H. Sung, J. Barry, S. Mclaughlin and G. L. Stuber, "LDPC coded OFDM with Alamouti/SVD diversity technique," IEEE Journal on Wireless Personal Communication, Vol. 23, Issue 1, pp. 183–194, Oct. 2002.

[9] M. Jiang and L. Hanzo, "Multiuser MIMO-OFDM for next generation wireless systems," In Proceedings of IEEE, Vol.95, Issue 7, pp.1430-1469, July 2007.

[10] C. C. Tu and B. Champagne, "Subspace Blind MIMO-OFDM Channel Estimation with Short Averaging Periods: Performance Analysis," IEEE Conference on Wireless Communications and Networking, pp. 24–29, April 2008.

[11] A. Tarighat and A. H. Sayed, "MIMO OFDM receivers for systems with IQ imbalances," IEEE Transactions on Signal Processing, Vol. 53, Issue 9, pp. 3583–3596, September 2005.

[12] R. Y. Mesleh, H. Haas, S. Sinanovic, C. W. Ahn and S. Yun, "Spatial modulation", IEEE Transaction on Vehicular Technology, Vol. 57, Issue 4, pp. 2228-2241, July 2008.

[13] P. S. Mundra , T. L. Singal and R. Kapur, "The Choice of A Digital Modulation ,Schemes in A Mobile Radio System", IEEE Vehicular Technology Conference, Issue 5, pp 1-4,1993.

[14] W. A. C. Fernando, R.M.A.P. Rajatheva and K. M. Ahmed, "Performance of Coded OFDM with Higher Modulation Schemes", International Conference on Communication Technology, Vol. 2, pp 1-5, 1998.

[15] A. Mraz and L. Pap, "General Performance Analysis of M-PSK and M-QAM Wireless Communications Applied to OFDMA Interference", IEEE Wireless Telecommunication symposium, Issue 4, pp 1-7, 2010.

[16] Y. Li, J. H. Winters and N. R. Sollenberger, "MIMO-OFDM for Wireless Communications: Signal Detection With Enhanced Channel Estimation", IEEE Transaction on Communications, Vol. 50, Issue 9, pp 1471-1477, 2009.

[17] S. Moghe and R. Upadhyay, "Comparison of SISO and MIMO Techniques in 802.11n Wireless Local Area Network", International Conference on Emerging Trends in Electronic and Photonic Devices & Systems, pp 245-246, 2009.

[18] Y. Wu and R. Calderbank, "Code Diversity in Multiple Antenna Wireless Communication", IEEE Journal of Selected Topics in Signal Processing, Vol. 3, Issue 6, pp 928-937, 2009.

[19] M. S. Al-Janabi, C. C. Tsimenidis, B. S. Sharif and S. Y. Le Goff, "Bit and Power Allocation Strategy for AMC-based MIMO-OFDMA WiMAX Systems", IEEE 6th International Conference on Wireless and Mobile Computing, Networking and Communications, pp 575-579, 2010.

[20] F. Delestre and Y. Sun, "A Channel Estimation Method for MIMO-OFDM Mobile WiMax Systems", International Symposium on Wireless Communication systems, pp 956-960, 2010.

[21] S. Ajey, B.Srivalli and G.V.Rangaraj, "On Performance of MIMO-OFDM Based LTE Systems", International Conference on Wireless Communications and Sensor Computing, pp 1-5, 2010.

[22] M. M. Avval, C. Snow and L. Lampe, "Error-Rate Analysis for Bit-Loaded Coded MIMO-OFDM", IEEE Transaction on Vehicular Technology, Vol. 59, Issue 5, pp 2340-2351, 2010.

[23] D. Molteni, M. Nicoli, and U. Spagnolini, "Performance of MIMO-OFDMA Systems in Correlated Fading Channels and Non-Stationary Interference", IEEE Transaction on Wireless Communication, Vol. 10, Issue 5, pp 1-15, 2011.

[24] J. Huang, J. Zhang, Z. Liu, J. Li and X. Li, "Transmit Beamforming for MIMO-OFDM Systems with Limited Feedback", IEEE Vehicular Technology Conference, pp 1-5, 2008.

[25] F. J. L. Martinez, E. M. Naya, J. F. Paris and A. J. Goldsmith, "BER Analysis for MIMO-OFDM Beamforming with MRC under Channel Prediction and Interpolation Errors", IEEE Global Telecommunication Conference, pp 1-7, 2009.

[26] K. Yi, W. Li, Y. Sun, and D. Zhu, "Low Complexity Beamfoming Algorithm for Multiuser MIMO Systems", International Conference on Wireless Communications and Signal Processing, pp 1-5, 2009.

[27] Q. Tao, C. Luo and P. Li, "Transmit Beamforming for Quasi-Orthogonal Space–time coded system in Rayleigh Fading Environments", International Conference on Wireless Communications, Networking and Mobile Computing, pp 1-4, 2009.

[28] X. Sun , L. J. Cimini , L. J. Greenstein and D. S. Chan, "ICI/ISI Aware Beamforming for MIMO-OFDM Wireless System", 43rd Annual Conference on Information Sciences and Systems, pp 103-107, 2009.

[29] S. Rahima and N. Hamdi, "A Variance Based Scheduling Strategy for Multi-user MIMO-OFDM System with Generalized Beamforming (GBF)", IEEE Mediterranean Electro technical Conference, pp 1259-1262, 2010.

[30] V. Tarokh, N. Seshadri and A. R. Calderbank, "Space–Time Codes for High Data Rate Wireless Communication: Performance Criterion and Code Construction", IEEE Transactions on Information Theory, Vol. 44, Issue 2, pp 744-765, 1998.

[31] R. S. Blum, Y. Li, J. H. Winters, and Q. Yan, "Improved Space–Time Coding for MIMO-OFDM Wireless Communications", IEEE Transaction on Communications, Vol. 49, Issue 11, pp 1873-1878, 2001.

[32] S. Suthaharan, A. Nallanathan and B. Kannan, "Space-Time Coded MIMO-OFDM for High Capacity and High Data-Rate Wireless Communication Over Frequency Selective Fading Channels", International workshop on Mobile and Wireless Communications, pp 424-428, 2002

[33] A. K. M. N. lslam, S. P. Majumder, "Performance Analysis of a MIMO-OFDM Wireless Link with STBC in the Presence of Fading and Timing Jitter", 12th International Conference on Computer and Information Technology, pp 105-110, 2009.

[34] Y. Huang, B. Pei, and H. Zhang, "System Performance Research and Analysis of MIMO-OFDM Based on Space-Time Block Codes", International Conference on Intelligent Control and Information Processing, pp 414-417, 2010.

[35] H. Jafarkhani, "A Quasi-Orthogonal Space–Time Block Code", IEEE Transaction on Communications, Vol. 49, Issue 1, pp 42-45, 2001

[36] N. Sharma and C. B. Papadias, "Improved Quasi-Orthogonal Codes through Constellation Rotation", IEEE Transaction on Communications, Vol. 51, Issue 3, pp 332-335, 2003.

[37] J. Hou, M. H. Lee and J. Y. Park, "Matrices Analysis of Quasi-Orthogonal Space- Time Block Codes", IEEE Communications Letters, Vol. 7, No. 8, pp 385-387, 2003.

[38] W. Su and X. G. Xia, "Signal Constellations for Quasi-Orthogonal Space–Time Block Codes With Full Diversity", IEEE Transactions on Information Theory, Vol. 50, Issue 10, pp 2331-2347, 2004.

[39] B. Badic, P. Fuxjaeger and H. Weinrichter, "Performance of quasi-orthogonal space-time code with antenna selection", Electronics Letters , Vol. 40, Issue 20, pp 1282-1284, 2004.

[40] L. Liu and H. Jafarkhani, "Application of Quasi-Orthogonal Space-Time Block Codes in Beamforming", IEEE Transactions on Signal Processing, Vol. 53, Issue 1, pp 54-63, 2005.

[41] C. Toker, S. Lambotharan and J. A. Chambers, "Closed-Loop Quasi-Orthogonal STBCs and Their Performance in Multipath Fading Environments and When Combined With Turbo Codes", IEEE Transaction on Wireless Communications, Vol. 3, Issue 6, pp 1890-1896, 2004.

[42] H. Jafarkhani and N. Hassanpour, "Super-Quasi-Orthogonal Space–Time Trellis Codes for Four Transmit Antennas", IEEE Transaction on Wireless Communications, Vol. 4, Issue 1, pp 215-227, 2005.

[43] J. K. Milleth, K. Giridhar, and D. Jalihal, "Closed-Loop Transmit Diversity Schemes for Five and Six Transmit Antennas", IEEE Transactions on Signal Processing, Vol. 12, Issue 2, pp 130-133, 2005.

[44] X. B. Liang, "A Complex Orthogonal Space-Time Block Code for 8 Transmit Antennas", IEEE Communication Letters, Vol. 9, Issue 2, pp 115-117, 2005.

[45] X. Wu, C. Jia-nian and Y. Rui, "Design and Analysis of Low Complexity Quasi orthogonal Space-time Block Code", IEEE Conference on Industrial Electronics and Applications, pp 3848-3852, 2009.

[46] J. S. Jeong, S. B. Park, C. B. Jo, E. J. Yoo and Y. S. Byun, "Quasi-Orthogonal Space-Time Block Codes based on Single Symbol Decoding for Four Transmit Antennas", International Conference on Advanced Communication Technology, pp 1742-1745, 2009.

[47] S. Cho and S. Kim, "Computationally efficient QO-STBC OFDM Transmitters", International Conference on Wireless Communications Networking and Mobile Computing, pp 1-4, 2010.

[48] M. B. Breinholt, M. D. Zoltowski and T. A. Thomas, "Space-Time Equalization and Interference Cancellation for MIMO OFDM", 36th Asilomar conference on Signals, Systems and Computers, Vol. 2, pp 1688-1693, 2003.

[49] X. Zhang , Y. Su and G. Tao, "Signal Detection Technology Research of MIMO-OFDM System", 3rd International Congress on Image and Signal Processing, pp 3031-3034, 2010.

[50] Z. wang and S. Zhang, "Group Iterative Linear ZF Receiver for MIMOOFDM Systems", Second International Conference on Networks Security, Wireless Communications and Trusted Computing, pp 248-251, 2010.

[51] P. V. Bien, W. Sheng, X. Ma and H. Wang, "Improved Decoder Schemes for QOSTBCs Based on Single-Symbol Decoding", International Conference on Advanced Technologies for Communications, pp 7-10, 2010.

[52] A. R. S. Bahai, B. R. Saltzberg, M. Ergen, *Multi-carrier Digital Communication Theory and Applications of OFDM* by Springer Science & Business Media, 2004.

[53] A. Yiwleak and C. Pirak, "Intercarrier Interference Cancellation Using Complex Conjugate Technique for Alamouti-Coded MIMO-OFDM Systems" International conference on Electrical Engineering/Electronics Computer Telecommunications and Information Technology, pp-1168-1172, 2010.

[54] B. P. Lathi, *Modern Digital and Analog Communication Systems* by CBS College Publishing, 1983

[55] W. Y., Zou and Y. Wu, "COFDM: An Overview", IEEE Transactions on Broadcasting, Vol. 41, Issue 1, pp 1-8, 1995.

[56] F. H. Gregorio, "802.11a - OFDM PHY: Coding AND Interleaving", Helsinki University of Technology (Signal Processing Laboratory), Vol. 4, Issue 8, pp. 1-6, 2006.

[57] S. B. Weinstein and P. M. Ebert, "Data Transmission by Frequency-Division Multiplexing Using the Discrete Fourier Transform", IEEE Transactions on Communications Technology, Vol. 19**,** Issue 10**,** pp 628-634, 1971.

[58] A. Sadat and W. B**.** Mikhael, "Fast Fourier Transform for High Speed OFDM Wireless Multimedia System", 44th IEEE Midwest symposium on circuits and systems, Vol. 2, pp 938-942, 2001.

[59] A. Vahlin and N. Holte, "Use of guard interval in OFDM in multipath channels", Electronics Letter, Vol. 30, Issue 24, pp 2015-2016, 1996.

[60] W. Henkel, G. Taubock, P. Odling, P. O. Borjesson and N. Petersson, "The Cyclic Prefix of OFDM/DMT – An Analysis", International Zurich Seminar on Broadband Communications, Issue 2, pp 1-3, 2002.

[61] E. Casas and C. Leung, "Performance of OFDM/FM scheme for data transmission over fading mobile radio channels", 36th IEEE Vehicular Technology Conference, Vol. 36, Issue 5, pp 103-108, 1986.

[62]S. Kaiser, "On the performance of different detection techniques for OFDM-CDMA in fading channels", IEEE Global Telecommunication Conference, Vol. 3, Issue 11, pp 2059-2063, 1995.

[63 H. B. Voelcker, "Phase-shift keying in fading channels" , In IEEE Proceeding on Electronics and Communication Engineering, Vol. 107, Issue 31, pp 31-38, 1960.

[64] A. V. Zelst and T. C. W. Schenk, "Implementation of a MIMO OFDM-Based Wireless LAN System," IEEE Transaction on Signal Processing, Vol. 52, Issue 2, pp 483-494, February 2004.

[65] C. E. Shanon, " A mathematical theory of communication", Bell System Technology Journal., vol. 27, pp. 379-423 (Part one), pp. 623-656 (Part two), Oct. 1948.

[66] A. Paulraj, R. Nabar, and D. Gore, *Introduction to Space–Time Wireless Communications*, by Cambridge University Press, Cambridge, UK, 2003.

[67] D. A. Gore and A. J. Paulraj, "MIMO antenna subset selection with space–time coding", IEEE Transaction on Signal Processing, Vol. 50, Issue 10, pp. 2580–2588, October 2002.

[68] A. Boariu and D.M. Ionescu "A class of nonorthogonal rate-one space time block codes with controlled interference," IEEE Transactions on Wireless Communications, Vol. 2, Issue 2, pp. 270–395, March 2003.

[69] L. He and H. Ge, "Fast maximum likelihood decoding of quasi-orthogonal codes", Asilomar Conference Signals, Systems, Computer, Vol. 1, pp. 1022–1026, Nov. 2003.

[70] C. K. Sung, J. Kim, and I. Lee, "Quasi-orthogonal STBC with iterative decoding in bit interleaved coded modulation", IEEE conference on Vehicular Technology, Vol. 2, pp. 1323–1327, September 2004.

[71] C. Yuen, Y. L. Guan, and T. T. Tjhung, "Quasi-orthogonal STBC with minimum decoding complexity" IEEE Transaction on Wireless Communication, Vol. 4, Issue 5, pp. 2089–2094, September 2005.

[72] H. Sari, "Characteristics and Compensation of Multipath Propagation in Broadband Wireless Access System", European Conference on Propagation and Syetms, pp15-18 March 2005

[73] V. Erceg, K.V.S. Hari, M.S. Smith and D.S. Baum "Channel Models for Fixed Wireless Applications", IEEE 802.16.3 Task Group Contributions, Febuary 2001

[74] M. N. Khan and S. Ghuari, "The WiMAX 802.16e Physical Layer Model", International Conference on Wireless, Mobile and Multimedia Networks, pp 117-120, 2007.

[75] S. P. Alex and L. M. A. Jalloul, "Performance Evaluation of MIMO in IEEE802.16e/WiMAX", IEEE Journal of Selected Topics in Signal Processing, Vol. 2, No. 2, pp 181-190, April 2008.

LIST OF PUBLICATIONS

[1] L. Kansal, A. Kansal and K. Singh, "Performance Analysis of MIMO-OFDM System Using QOSTBC Code Structure For M-QAM", Canadian Journal On Signal Processing Vol. 2, No. 2, pp 4-15, May 2011.

[2] L. Kansal, A. Kansal and K. Singh, "Performance Analysis of MIMO-OFDM System Using QOSTBC Code Structure For M-PSK", Signal Processnig: An Intrenational Journal, Volume 5, Issue 2, 2011, Accepted for Publication.

[3] L. Kansal, A. Kansal and K. Singh, "Performance of Alamouti Space Time Coding in Fading Channels For IEEE 802.16e Protocol", International Journal Of Scientific & Engineering Research, Volume 2, Issue 5, May -2011, Accepted for Publication.

[4] L. Kansal, A. Kansal and K. Singh, "Analysis Of Different High Level Modulation Techniques For OFDM System", International Journal Of VLSI and Signal Processing Applications, Vol. 1, Issue 2 , pp 102-107, May 2011.